Scientific Excellence • Resource Protection & Conservation • Benefits for Canadians
Excellence scientifique • Protection et conservation des ressources • Bénéfices aux Canadiens

Intercomparison of Current Measurements from the Georges Bank Frontal Study

J.W. Loder, R.G. Pettipas, and D.J. Belliveau

Physical and Chemical Sciences Branch
Scotia-Fundy Region
Department of Fisheries and Oceans

Bedford Institute of Oceanography
P.O. Box 1006
Dartmouth, Nova Scotia
Canada B2Y 4A2

August 1990

Canadian Technical Report of Hydrography and Ocean Sciences No. 127

Fisheries and Oceans Pêches et Océans

Canada

Canadian Technical Report of Hydrography and Ocean Sciences

Technical reports contain scientific and technical information that contributes to existing knowledge but which is not normally appropriate for primary literature. The subject matter is related generally to programs and interests of the Ocean Science and Surveys (OSS) sector of the Department of Fisheries and Oceans.

Technical reports may be cited as full publications. The correct citation appears above the abstract of each report. Each report is abstracted in *Aquatic Sciences and Fisheries Abstracts* and indexed in the Department's annual index to scientific and technical publications.

Technical reports are produced regionally but are numbered nationally. Requests for individual reports will be filled by the issuing establishment listed on the front cover and title page. Out of stock reports will be supplied for a fee by commercial agents.

Regional and headquarters establishments of Ocean Science and Surveys ceased publication of their various report series as of December 1981. A complete listing of these publications is published in the *Canadian Journal of Fisheries and Aquatic Sciences*, Volume 39: Index to Publications 1982. The current series, which begins with report number 1, was initiated in January 1982.

Rapport technique canadien sur l'hydrographie et les sciences océaniques

Les rapports techniques contiennent des renseignements scientifiques et techniques qui constituent une contribution aux connaissances actuelles, mais qui ne sont pas normalement appropriés pour la publication dans un journal scientifique. Le sujet est généralement lié aux programmes et intérêts du service des Sciences et levés océaniques (SLO) du ministère des Pêches et des Océans.

Les rapports techniques peuvent être cités comme des publications complètes. Le titre exact paraît au-dessus du résumé de chaque rapport. Les rapports techniques sont résumés dans la revue *Résumés des sciences aquatiques et halieutiques*, et ils sont classés dans l'index annuel des publications scientifiques et techniques du Ministère.

Les rapports techniques sont produits à l'échelon régional, mais numérotés à l'échelon national. Les demandes de rapports seront satisfaites par l'établissement auteur dont le nom figure sur la couverture et la page du titre. Les rapports épuisés seront fournis contre rétribution par des agents commerciaux.

Les établissements des Sciences et levés océaniques dans les régions et à l'administration centrale ont cessé de publier leurs diverses séries de rapports en décembre 1981. Une liste complète de ces publications figure dans le volume 39, Index des publications 1982 du *Journal canadien des sciences halieutiques et aquatiques*. La série actuelle a commencé avec la publication du rapport numéro 1 en janvier 1982.

Canadian Technical Report of

Hydrography and Ocean Sciences No. 127

August 1990

INTERCOMPARISON OF CURRENT MEASUREMENTS FROM THE GEORGES BANK FRONTAL STUDY

by

John W. Loder[1], Roger G. Pettipas[2] and Donald J. Belliveau[1]

[1]Physical and Chemical Sciences Branch
Department of Fisheries and Oceans
Bedford Institute of Oceanography
P.O. Box 1006
Dartmouth, N.S.
Canada B2Y 4A2

[2]Department of Oceanography
Dalhousie University
Halifax, N.S.
Canada B3H 4J1

ACKNOWLEDGEMENTS

The Georges Bank Frontal Study was principally funded by the Federal Panel on Energy, Research and Development (PERD), and the Physical and Chemical Sciences Branch (PCS) of the Department of Fisheries and Oceans (DFO) of Canada. Additional support was provided by the Biological Sciences Branch of DFO, and the Natural Sciences and Engineering Research Council of Canada through a grant to J. Grant of Dalhousie University.

A large number of individuals at the Bedford Institute of Oceanography contributed to the successful execution of the current measurement component of the field study. Special thanks are due to: Neil Oakey who served as chief scientist on the two principal cruises, Ken Drinkwater who conducted the 1989 field program, and Ed Horne as the other co-principal investigator; Jim Hamilton who designed the moorings and collaborated in the investigation of mooring motion; Bert Hartling and the other members of the PCS Current Meter Shop for numerous discussions on instruments and moorings; John Whitman who provided advice on the Ametek Straza current profiler and checked the Georges Bank data for indications of reliability; and the members of the PCS Data Shop, particularly Helen Hayden, for patience in the processing of a large and partially-degraded data set. We also thank all of the scientific staff and the ship's officers and crew of Dawson cruises 88017, 88023 and 88036 for their valuable contributions to the study.

Finally, we are grateful to Joel Gast and Lee Gordon of RD Instruments for helpful advice.

Cat. No. Fs 97-18/127E. ISSN 0711-6764

Correct citation for this publication:

Loder, J.W., R.G. Pettipas and D.J. Belliveau. 1990. Intercomparison of current measurements from the Georges Bank Frontal Study. Can. Tech. Rep. Hydrogr. Ocean Sci. No. 127: vi + 75 pp.

ABSTRACT

Loder, J.W., R.G. Pettipas and D.J. Belliveau. 1990. Intercomparison of current measurements from the Georges Bank Frontal Study. Can. Tech. Rep. Hydrogr. Ocean Sci. No. 127: vi + 75 pp.

Current measurements taken with four different instruments during the 1988-89 Georges Bank Frontal Study are intercompared. The observational data set includes measurements from: Aanderaa (paddle-wheel version) current meters (RCMs) on nine different moorings at six different sites, a bottom-mounted (RDI) acoustic Doppler current profiler (ADCP) at one of the sites, two InterOcean S4 electromagnetic current meters on one of the RCM moorings, and a ship-mounted (Ametek Straza) ADCP during sixteen anchor stations at the mooring sites. These anchor stations had durations of 6 to 32 hours. Statistical, tidal and regression analyses, and various graphical presentations are used in the intercomparison.

At the four "Bank" sites where little horizontal structure in the current field was expected, the direction estimates from the four measurement techniques were generally in excellent agreement; however, there were significant discrepancies in rate. In particular, the RCMs at mid-depth underestimated rate by about 20% at speeds greater than 0.8 m/s, and those at 10 m above bottom underestimated rate by about the same amount at all speeds, but with less consistency among moorings. An S4 meter deployed at mid-depth also yielded degraded current measurements for some flow speeds above 0.7 m/s. In the upper 20 m (and below the region of RDI sidelobe reflection from the surface), the RDI rates were reduced by about 10% compared to the others, the RCM rates were high relative to those of the Ametek and S4, and there were intermittent discrepancies between the Ametek and the others. In addition, there were discrepancies in the mean currents averaged over the tidal period in a number of cases, with magnitudes typically 25-50% of the mean-current magnitude.

The possible sources of these discrepancies are briefly examined. The leading candidate for the RCM underestimation is shielding of the paddle-wheel rotors associated with mooring-line vibration caused by vortex shedding from spherical buoyancy packages. This vibration also appears to have been the origin of the S4 degradation, although the specific mechanism is unclear. It appears that the near-surface degradation of the RDI arose from poor Doppler tracking during periods of low backscatter intensity and high vertical shear. This was exacerbated by the use of short pulses. Other probable factors contributing to the near-surface rate discrepancies were an RCM calibration problem and real spatial structure in the flow field, probably due to internal waves. Finally, a number of factors probably contributed to the mean-current discrepancies, particularly offsets in the RDI associated with frequency skewing of the acoustic pulses and mispositioning of the filters, and amplification of the mean-current relative errors by the various inaccuracies in the measurement of the strong fluctuating (tidal) currents.

RÉSUMÉ

Loder, J.W., R.G. Pettipas and D.J. Belliveau. 1990. Intercomparison of current measurements from the Georges Bank Frontal Study. Can. Tech. Rep. Hydrogr. Ocean Sci. No. 127: vi + 75 pp.

Des mesures des courants ont été effectuées avec quatre instruments différents pendant l'Étude du talus frontal du banc de Georges en 1988-89. Les ensembles de données d'observation englobent des mesures effectuées avec: des courantomètres Aanderaa (type à roue à aubes) (RCM) en neuf points d'amarrage répartis en six emplacements différents, un profileur acoustique Doppler de courant (ADCP) installé sur le fond (RDI) en l'un des emplacements, deux courantomètres électromagnétiques InterOcean S4 sur l'un des amarrages pour RCM et un ADCP (Ametek Straza) installé sur un navire pendant 16 mouillages aux points d'amarrage. Ces mouillages ont été de durées varient de 6 à 32 heures. Des analyses statistiques, des marées et de régression ainsi que diverses présentations graphiques sont utilisées pour l'intercomparaison.

Aux quatres emplacements du "banc" où l'on s'attendait à ce que le champ de courant ne soit que faiblement structuré suivant l'horizontale, les quatre méthodes de mesure fournissaient des estimations de la direction qui concordaient généralement très bien; cependant il existait des écarts importants quant à la vitesse. En particulier, les RCM à la profondeur médiane sous-estimaient d'environ 20% les vitesses supérieures à 0,8 m/s, et ceux placés à 10 m au-dessus du fond sous-estimaient toutes les vitesses, environ par la même quantité, mais de manière moins uniforme d'un point d'amarage à l'autre. Un S4 installé à la profondeur médiane fournissait également des mesures dégradées du courant pour certaines vitesses d'écoulement supérieures à 0,7 m/s. Dans les 20 m supérieurs (et sous la région de réflexion par la surface des lobes latéraux du RDI), les vitesses obtenues au moyen du RDI étaient d'environ 10% inférieures aux autres, les vitesses mesurées avec les RCM étaient élevées comparativement à celles mesurées avec l'Ametek et les S4, et il existait des écarts intermittents entre l'Ametek et les autres appareils. De plus, il y avait dans un certain nombre de cas des écarts au niveau des courants moyens calculés pour la période tidale, les vitesses obtenues étant de manière caractéristique de 25 à 50% inférieures à la vitesse du courant moyen.

Les causes possibles de ces écarts sont brièvement examinées. La cause la plus plausible de la sous-estimation par les RCM tient au fait que la rotation des roues à aubes est entravée par l'effet d'écran associé à la vibration des câbles d'amarrage due aux tourbillons engendrés par les jeux de flotteurs sphériques. Cette vibration semble également à l'origine de la dégradation des mesures effectuées avec les S4, bien que le mécanisme spécifique ne soit pas clairement compris. Il semble que la dégradation des mesures effectuées près de la surface avec le RDI découle d'une mauvaise poursuite Doppler pendant les périodes de faible intensité de la rétrodiffusion et de cisaillement important suivant la verticale. Ce problème était aggravé par l'utilisation de courtes impulsions. Parmi les autres facteurs probables des écarts de vitesse obtenus près de la surface, mentionnons un problème d'étalonnage des RCM et la présence d'une structure spatiale réelle dans le champ

d'écoulement, probablement attribuable à des ondes internes. Finalement, un certain nombre de facteurs expliquaient probablement les écarts observés au niveau du courant moyen, en particulier des décalages des mesures effectuées avec les RDI associées à une distortion en fréquence des impulsions acoustiques et à un mauvais positionnement des filtres ainsi que l'amplification des erreurs relatives sur le courant moyen attribuable à diverses imprécisions de la mesure des forts courants (de marée) variables.

TABLE OF CONTENTS

1. INTRODUCTION

During the periods June - October 1988 and July 1989, the Department of Fisheries and Oceans at the Bedford Institute of Oceanography (BIO) conducted a field study of currents and mixing at a tidal front on Georges Bank. As part of this study, current measurements were obtained from moored instruments at six sites (Fig. 1, Table 1) and from a ship-mounted (Ametek Straza) acoustic Doppler current profiler (ADCP) operated nearly continuously during two principal survey periods. The moored instruments were Aanderaa (paddle-wheel version) current meters (henceforth RCMs) deployed at three to five depths at each site, a bottom-mounted (RD Instruments) ADCP deployed at one of the sites, and two InterOcean S4 electromagnetic current meters deployed on one of the RCM moorings. The Ametek measurements included current profiles in the vicinity of the mooring sites while the research vessel was at anchor obtaining repeated turbulence profiles.

This report presents the results of an intercomparison of currents measured with the four different types of instrumentation. The intercomparison was initiated in part as a field test for the RDI ADCP, but largely as part of quality control on the RCM and Ametek data sets. Since the RCMs and the Ametek had been in routine use at BIO for several years, major discrepancies were not expected; consequently, the measurement programs involving these instruments were designed more on the basis of scientific objectives than as an intercomparison of measurement techniques. Nevertheless, the study has yielded the most extensive data set to date at BIO for the intercomparison of acoustic and mechanical current measurements, together with some significant (and disappointing) results. Consequently, this first report from the Georges Bank Frontal Study focuses on the quantitative consistency of the current measurements with each other and with numerical tidal model predictions. Results of other analyses on the edited data from the moored component of the study will be presented in a follow-up report.

In Section 2 the instrumentation, measurement program and data analysis procedures are briefly described. Section 3 presents the results of the intercomparison for the mooring site at which all four types of measurement were made. The results for the other sites are presented in Section 4, and for the comparison with tidal model predictions in Section 5. The report concludes with a discussion of possibilities for the origin of various discrepancies in Section 6, and a summary in Section 7.

2. METHODOLOGY

a. Instrumentation

The RCMs were modified versions RCM5, RCM7 or RCM8 (Table 2), all with paddle-wheel rotors designed to reduce overspeeding in the surface wave zone (e.g. Saunders 1980). The instruments were self-recording with the RCM5s (Aanderaa Instruments 1979) using a magnetic tape and the RCM7s and RCM8s (Aanderaa Instruments 1987) solid-state memory. The RCM5s recorded instantaneous values of current direction, temperature, conductivity (optionally) and pressure (optionally) at the end of each 30-min recording interval, and rate (current speed) averaged over the interval. The RCM7s and RCM8s, whose recording intervals were set to 2, 5 or 30 min (Table 2), also recorded instantaneous values of temperature, conductivity and pressure at the end of each interval, but used vector

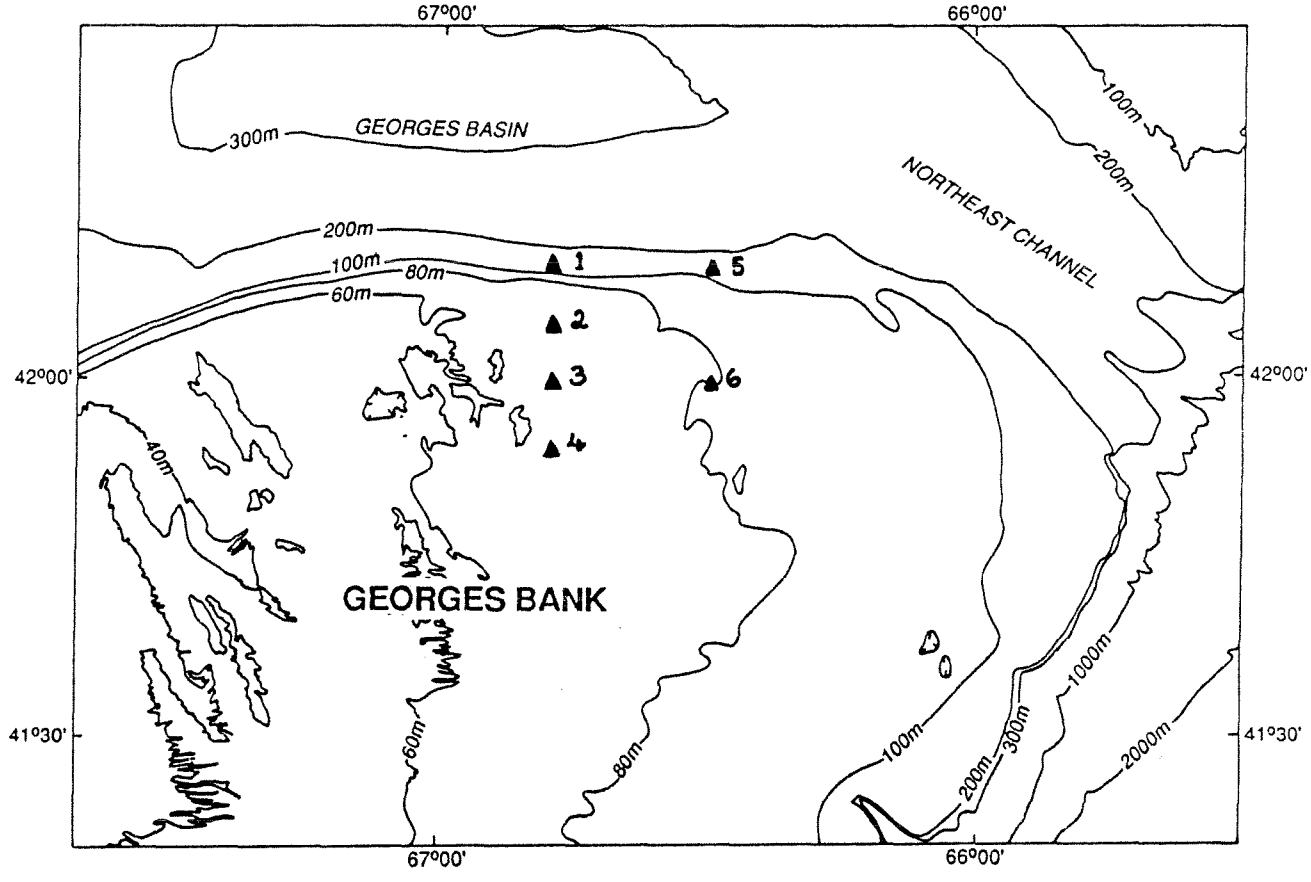

Figure 1. Location map for the mooring sites on Georges Bank. Depths are in meters.

Table 1. Summary of positions, water depths, and deployment and recovery times (UTC) and dates (day/month) for current meter moorings in the Georges Bank Frontal Study. BIO No. refers to the BIO Consecutive Mooring Number. The sites are shown in Figure 1.

BIO No.	Site	Depth (m)	Position Lat (N)	Position Long (W)	Deployment Time/Date	Recovery Time/Date	Remarks
1988							
889	1	155	42°10.0′	66°47.9′	1532/26/06	1755/14/10	
891	2	67	42°04.8′	66°48.1′	1921/27/06	1451/11/07	
893	3	67	41°59.8′	66°47.9′	1838/25/06	2018/11/07	
895	4	63	41°53.7′	66°47.8′	1610/27/06	1328/14/10	
896	5	148	42°09.1′	66°29.7′	1043/27/06	1630/09/07	
897	6	83	41°58.6′	66°30.2′	1326/27/06	2048/09/07	
912	2	67	42°04.8′	66°48.1′	1655/11/07	1247/30/09	Replaced 891
913	3	67	41°59.8′	66°48.0′	2159/11/07	1433/15/10	Replaced 893
919	2	66	42°04.7′	66°47.9′	1552/30/09	1902/15/10	Replaced 912
920	3	68	41°59.6′	66°47.9′	1113/01/06	1633/13/07	RDI mooring
1989							
955	3	70	41°59.9′	66°48.0′	2255/13/07	1323/30/07	S4s added

Table 2. Summary of instrument depths (below mean surface), types, sensors, recording intervals and data return periods (hr UTC/dy/mo) for moored current measurements during the Georges Bank Frontal Study. See Table 1 for positions and water depths. For Sensors: R = Rate; D = Direction; T = Temperature; C = Conductivity; P = Pressure; U,V = Velocity Components; O = Instrument Orientation; and Ti = Tilt.

BIO No.	Depth (m)	Instrument Type	Instrument No.	Sensors	Interval (min)	Current Data Return Period	Remarks
1988							
889	21	RCM5	822	R,D,T,C,P	30	1600/26/6-1630/14/10	
"	43	RCM5	1286	R,D,T,C,P	30	1530/26/6-1730/14/10	
"	67	RCM7	9142	R,D,T,C	30	NIL	Faulty rotor counter
"	90	RCM5	5573	R,D,T	30	1530/26/6-0600/11/7	Rotor problem
"	145	RCM7	9078	R,D,T,C	30	1530/26/6-1730/14/10	
891	11	RCM5	3298	R,D,T,C,P	30	1930/27/6-1430/11/7	
"	35	RCM5	5571	R,D,T,C,P	30	1930/27/6-1430/11/7	
"	57	RCM5	4271	R,D,T,C	30	1930/27/6-1430/11/7	
"	64	RCM5	828	R,D,T	30	1930/27/6-1430/11/7	
893	12	RCM5	6400	R,D,T,C,P	30	1830/25/6-2000/11/7	
"	34	RCM5	6410	R,D,T,C,P	30	1830/25/6-2000/11/7	
"	57	RCM5	4421	R,D,T,C	30	1830/25/6-2000/11/7	
"	64	RCM5	1944	R,D,T	30	1830/25/6-2000/11/7	
895	11	RCM5	7123	R,D,T,C,P	30	1630/27/6-1300/14/10	
"	34	RCM5	5568	R,D,T	30	1630/27/6-1300/14/10	
"	53	RCM5	2664	R,D,T	30	1630/27/6-1300/14/10	
"	60	RCM5	4195	R,D,T	30	NIL	All R missing
896	10	RCM5	7525	R,D,T,C,P	30	1100/27/6-1530/9/7	Many bad R
"	39	RCM5	6411	R,D,T	30	1100/27/6-1600/9/7	
"	71	RCM5	8695	R,D,T,C,P	30	1100/27/6-1600/9/7	
"	102	RCM5	7134	R,D,T	30	1100/27/6-1600/9/7	
"	138	RCM7	9145	R,D,T,C	30	1100/27/6-1600/9/7	
897	10	RCM5	8696	R,D,T,C,P	30	1330/27/6-2000/9/7	
"	41	RCM5	8697	R,D,T,C,P	30	1330/27/6-2000/9/7	
"	73	RCM7	9071	R,D,T,C	30	1330/27/6-2000/9/7	

Table 2. (continued)

BIO No.	Depth (m)	Instrument Type	No.	Sensors	Interval (min)	Current Data Return Period	Remarks
1988							
912	11	RCM5	8695	R,D,T,C,P	30	1700/11/7-0730/29/8	Instr broke loose
"	35	RCM5	8696	R,D,T,C,P	30	1700/11/7-1230/30/9	
"	57	RCM5	8697	R,D,T,C,P	30	1700/11/7-1230/30/9	
"	64	RCM5	7134	R,D,T	30	1700/11/7-1230/30/9	
913	12	RCM5	7525	R,D,T,C,P	30	2200/11/7-1400/20/8	Most R deleted
"	34	RCM5	5571	R,D,T,C,P	30	2200/11/7-1430/15/10	
"	57	RCM5	4271	R,D,T,C	30	2200/11/7-0500/19/8	Most R deleted
"	64	RCM5	828	R,D,T	30	2200/11/7-1430/15/10	
919	10	RCM7	9071	R,D,T,C	2.5	NIL	Battery failure
"	34	RCM8	9355	R,D,T,C	2.5	1558/30/9-1730/15/10	
"	56	RCM7	9145	R,D,T,C	5	1600/30/9-1850/15/10	
"	63	RCM8	9328	R,D,T,C	5	1600/30/9-1900/15/10	
920	68	RDI		R,D	15	0315/2/6-1630/13/7	
1989							
955	13	RCM5	828	R,D,T,C	5	2255/13/7-1320/30/7	
"	14	S4	04410744	U,V,P T,C,O	2 60	2256/13/7-0425/29/7	
"	36	RCM5	4271	R,D,T,C	5	2255/13/7-1320/30/7	
"	37	S4	04430830	U,V,T,C,	2	2256/13/7-1323/30/7	
"	60	RCM5	5573	R,D,T,C	5	2255/13/7-1320/30/7	

averaging for currents: for the 2- and 5-min recording intervals, instantaneous direction and averaged rate were sampled every 12 s, and then vector averaged to obtain the recording-interval averages; for the 30-min recording interval, instantaneous direction and averaged rate were sampled every 36 s and used in vector averaging. The manufacturer's quoted accuracies for current measurements with these instruments are: for direction, $\pm 5^{\circ}$ for rates from 0.05 to 1.0 m/s and $\pm 7.5^{\circ}$ for rates from 0.025 to 0.05 m/s and from 1.0 to 2.0 m/s; and for rate, the greater of ± 0.01 m/s or $\pm 2\%$ of the actual rate, with a starting value of 0.02 m/s. Each of the instruments had its compass calibrated prior to deployment, while the manufacturer's calibration was used for rate.

The RCMs were deployed on single-leg subsurface moorings such as that shown in Figure 2 for mooring 893. Buoyancy was provided by a "Fairey" float (cylinder of length 2.3 m and diameter 0.5 m, with rounded nose and finned tail) at the top of each mooring and spherical "Viny" floats (diameter 0.34 m) positioned at least 2 m above intermediate-depth instruments. Mooring motion and tilt were estimated prior to deployment using a static model (Hamilton 1989), with vertical excursions of the Fairey floats predicted to be in the 5-10 m range. Post-deployment comparison of the predicted and observed pressures for mooring 893 (Hamilton 1989) showed good agreement, with maximum vertical excursions of 6 m for the RCMs and maximum mooring line tilts (at the instrument depths) of less than 30°. Since the RCMs were gimballed to allow a mooring line tilt (from the vertical) of up to 29° without any associated instrument tilt, and the compasses are stated to tolerate instrument tilts up to 12° (Aanderaa Instruments 1979, 1987), satisfactory instrument performance was expected.

The bottom-mounted ADCP (the RDI) was a 150-kHz RD-SC0150 unit supplied by RD Instruments Inc. The system simultaneously transmitted an acoustic pulse on four beams and computed three components of velocity and an error velocity from Doppler shifts of the backscattered sound from specified vertical bins (e.g. RD Instruments 1989). For the Georges Bank deployment, the acoustic beams were inclined at 20° to the vertical and the RDI was set to record 15-min (800-ping) (vector) averages of current velocity and backscatter intensity for 2.2-m bins, with the first bin centered 3.3 m above the transducer faces. The manufacturer's quoted accuracy for this configuration is ± 0.027 m/s for the horizontal velocity components, except in the upper 8% of the water column where side-lobe reflections from the sea surface are expected to degrade the estimates. The unit was moored in a newly-developed "trawl-resistant" mount (Dessureault and Belliveau 1987), which was designed to remain undisturbed in the presence of bottom-trawl fishing activity and which included a plastic cover over the transducer. The transducer faces were 0.4 m from the seafloor during the deployment, and tilt sensors indicated that the instrument's tilt was less than 2° on each axis. Preliminary results from the intercomparison suggested a compass offset of $5\text{-}10^{\circ}$, which was confirmed to be about 7° upon post-deployment calibration.

The ship-mounted ADCP (the Ametek) was a 300-kHz DCP-4400A/300 unit supplied by Ametek Straza. The system consists of a transducer mounted at 5 m below the sea surface through the hull of the research vessel CSS Dawson, with four acoustic beams inclined at 30° to the vertical. It can be operated in Profile, Bottom-track or Alternating modes and has data logging options of vector-averaged (in ship's co-ordinates) current

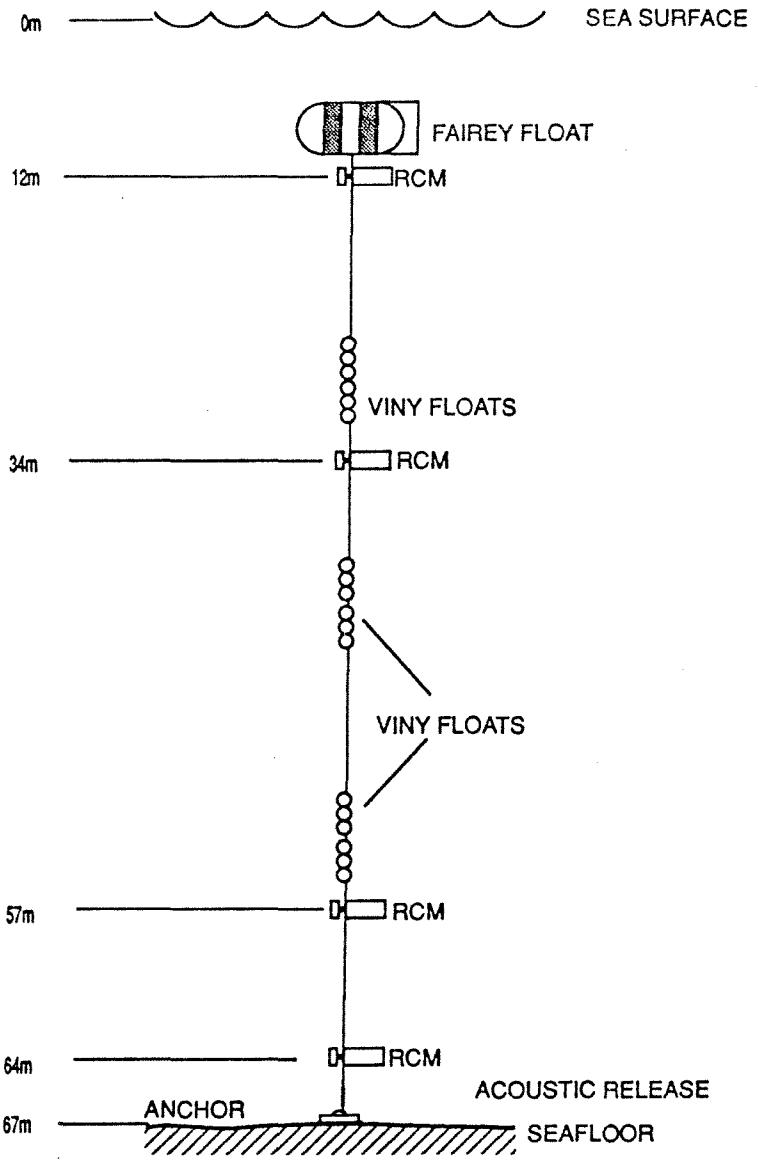

Figure 2. Design of a typical RCM mooring (893).

estimates on an HP-85 computer or individual-ping estimates on the main shipboard (MicroVAX) computer (see Cochrane 1985 for further details). During the Georges Bank surveys, the Ametek was generally operated at low power in Alternating mode, with absolute water velocity computed as relative water velocity minus bottom-track velocity, and averages over 200 pings (about 10 min) and 3.2-m vertical bins (Table 3) logged on HP-85 cassette tapes. With these settings, absolute water velocity estimates are available for bins centered on depths starting at about 8.8 m below the surface, and the expected standard errors (Cochrane 1985, Table 8; single-ping standard deviations divided by square root of number of pings) are 0.015 m/s for relative water velocity and 0.002 m/s for bottom-track velocity. With 1.6-m bins, the shallowest bin is centered near 8.0 m and the expected error for relative water velocity is 0.03 m/s. Analogous to the near-surface degradation of the RDI estimates, the Ametek velocities are expected to be degraded by side-lobe reflections from the bottom in the lower 15% of the interval between the transducer and seafloor. Previous field tests of the Dawson system (Cochrane 1985) have indicated that its bottom track speeds are overestimated by 2%, directions are accurate within 2°, and current speeds agree with moored current measurements within 10-20%. Comparisons between ADCP bottom tracking and LORAN-C navigation during the two principal Georges Bank surveys (J. Whitman, BIO, personal communication, 1989) indicate that the Ametek was overestimating bottom speed by about 1% and its transducer was misaligned by 0.5° clockwise. However, since the measurements presented here were taken while at anchor, the bottom-track errors should have a negligible effect on the absolute water velocity estimates.

The InterOcean S4 current meters are electromagnetic meters which measure velocity with two orthogonal sets of electrodes. The instruments sample every 0.5 s and, in the Georges Bank deployment, recorded the vector-averaged horizontal velocity for every second minute. Two S4 meters were included on mooring 955 in 1989, positioned about 0.5 m below the upper and mid-depth RCMs (otherwise, same mooring configuration as in Fig. 2). The upper S4 also recorded instantaneous pressure at 2-min intervals, and instantaneous temperature, conductivity and instrument orientation (compass reading) at 1-hr intervals. The mid-depth S4 additionally recorded instantaneous pressure, temperature, conductivity, orientation and instrument tilt at 2-min intervals. The latter S4 had the capability of internal correction of the measured velocity for a cosine-function reduction due to tilt, but this was not activated during the present deployment. The manufacturer's specifications (InterOcean 1987) for the S4 are: current range, 0-350 cm/s; current resolution, 0.2 cm/s; current accuracy, 2% ± 1 cm/s; direction resolution, 0.5°; and direction accuracy, 2°.

b. Field Measurement Program

The physical oceanographic component of the Georges Bank Frontal Study was executed on three dedicated cruises by the CSS Dawson and several Biological Sciences Branch cruises in 1988, and a single cruise in 1989. The periods of the dedicated cruises were: 88017 - 31 May to 3 June; 88023 - 23 June to 14 July; 88036 - 29 September to 17 October. The 1989 moored measurements were obtained during Lady Hammond cruise 89202.

In 1988, the moored instruments were deployed at four sites (#'s 1-4) on a primary sampling line (66°48'W) across the northern side of

Table 3. Summary of anchor stations (1988) for which RCM/Ametek intercomparison is carried out. Period (hr UTC/dy:mo) is that of Ametek data, and Position is ship's position at anchor. Depths are from the Ametek, and Bins are for Ametek vertical averaging. Comparison Depths are centre positions of Ametek bins from which data are compared against RCM data at nearby vertical level (see Table 2).

Stn	Cruise	Period Start - End	Position Lat (N)	Long (W)	Depths (m)	Bins (m)	Comparison Depths (m)
889A	88023	0433-1040/6:7	42°09.0′	66°48.0′	115-118	3.2	21,43,90
889B	88023	1757/6-0437/7:7	42°09.3′	66°47.9′	119-133	3.2	21,43,90
889C	88036	0443-1623/11:10	42°08.8′	66°47.7′	106-109	3.2	21,43
891A	88023	0553-1828/30:6	42°04.7′	66°46.6′	70-72	1.6	12,37,55
891B	88023	1321/5-0331/6:7	42°04.9′	66°46.7′	69-71	3.2	12,37,55
891C	88023	2348/10-1300/11:7	42°05.1′	66°46.3′	69-73	3.2	12,37,55
893A	88023	1705/28-1426/29:6	41°59.8′	66°46.7′	68-71	1.6/3.2	12,34,55
893B	88023	1434/4/7-0918/5:7	41°59.9′	66°46.4′	68-70	3.2	12,34,55
893C	88023	0018-1133/10:7	42°00.1′	66°46.9′	67-70	3.2	12,34,55
895A	88023	2054/3-1347/4:7	41°53.7′	66°46.9′	64-66	3.2	12,34,52
895B	88023	2332/7-2335/8:7	41°53.7′	66°46.4′	65-67	3.2	12,34,52
895C	88036	2333/1-1533/2:10	41°53.3′	66°46.4′	64-65	3.2	12,34,52
896A	88023	0141-1402/9:7	42°08.3′	66°29.4′	115-119	3.2	12,40,71,89
897A	88023	0703-1629/7:7	41°58.6′	66°29.0′	82-83	3.2	12,43,68
913A	88036	0030-1433/3:10	41°59.4′	66°46.1′	68-70	3.2	34
919A	88036	1600/4-0028/6:10	42°04.7′	66°46.6′	70-77	3.2	34,52

Georges Bank and two sites (#'s 5-6) on a secondary line (66°30'W) to the east (Fig. 1). Mooring positions and times, and water depths are summarized in Table 1 where each mooring is denoted by its BIO consecutive number. RCM moorings were maintained at sites 1 - 4 from late June to mid-October to observe long-term current and hydrographic variability across the front. Additional moorings on the secondary line during cruise 88023 provided information on along-isobath variability. Sites 2 - 4 on the Bank have similar depth/tidal-current regimes, as do sites 1 and 5 along the Bank edge. Site 6 on the Bank is at an intermediate depth. Each site was marked by at least three guard buoys deployed in an array about 0.5-0.8 km on a side (e.g. Fig. 3). RCMs were placed at nominal depths of 10 m above bottom and below surface, with additional instruments at intermediate depths and at 3 m above bottom at sites 2 - 4. Details on the instruments and returned data are summarized in Table 2. Particular instruments are henceforth denoted by mooring number and depth (in m) below the mean surface, e.g. (893-12); note that mooring motion and the tidal variation in water depth (less than 1 m) are not accounted for in this notation.

The RDI (mooring 920) was deployed at site 3 during cruise 88017 and recovered at the end of cruise 88023, giving 15 days of overlap with RCM mooring 893. The RDI location was approximately 0.5 km from mooring 893, and about 0.1 km from one of the guard buoys (although the relative positions are not precisely known). The scientific objective of the RDI deployment was to measure long-term current variability with increased vertical resolution.

During the two principal surveys (88023 and 88036), anchor stations were occupied about 1 - 2 km from the mooring sites, typically over a semidiurnal tidal period. These stations included repeated turbulence and CTD profiles, and continuous Ametek profiling intended to measure vertical shear and other current parameters with increased vertical and temporal resolution. The location and duration of these stations are summarized in Table 3, with the stations denoted by the corresponding RCM mooring number and a sequential letter. Three anchor stations were conducted near each of moorings 889, 891, 893 and 895, and one near moorings 896, 897, 913 and 919, with durations ranging from about 6 to 32 hr. Thus, concurrent Ametek data are available for subintervals of all the 1988 RCM moorings, with the exception of 912 which was deployed at the end of cruise 88023 and recovered at the start of 88036. Bottom depth estimates from the ship's sounder and the Ametek during the anchor stations indicate that the anchor site depths were within several meters of the RCM and RDI mooring site depths, with the exception of the Bank-edge sites (moorings 889 and 896) where the vessel was anchored on the shallow side of the RCM moorings for logistic reasons (anchor chain length).

In 1989, a single mooring with three RCMs was deployed for 17 days at site 3, to monitor the current regime during Lagrangian drifter tracking. The two S4s were added to the mooring for comparison with the RCMs, after analyses of the 1988 data indicated discrepancies between the RCM and ADCP measurements.

c. Data Processing

The processing of the RCM data followed the standard BIO procedure, with the direction assigned to each recording interval taken as the

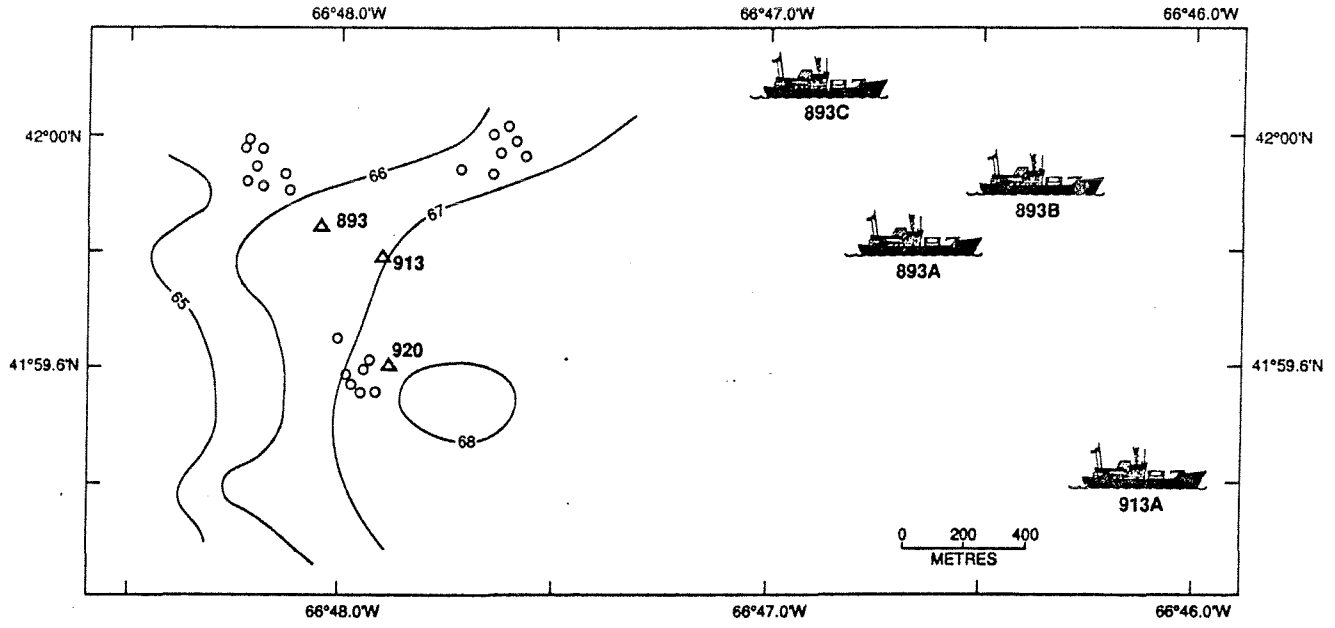

Figure 3. Mooring (Δ) and anchor station locations at site 3. The three clusters of small circles indicate the different estimated positions of the three guard buoys. The depth contours (m) are based on a pre-deployment survey of the immediate vicinity of the moorings using the ship's sounder.

average of the recorded values for that and the previous interval. For the RCM5s, the resulting direction value was thus the average of the instantaneous values from the start and end of the 30-min recording interval; in the presence of high-frequency current fluctuations, this value might be different from the (appropriate) direction of the vector-averaged velocity during the interval, but an alternative processing procedure cannot overcome this limitation of the sampling. On the other hand, for the RCM7s and RCM8s, the resulting direction value was an average of the vector-averaged velocity's directions during the present and previous recording intervals, thus introducing an erroneous phase lead of current direction relative to speed (and other variables). This inappropriate averaging of direction may partially offset the benefits of the RCM7/8s' vector-averaging capability, and clearly should be eliminated from the standard BIO procedure.

Following translation and direction averaging, time series plots of rate, direction, and u- (east true) and v- (north) components of velocity were visually inspected for suspect data. Portions of the rate records from instruments 889-90, 896-10, 913-11 and 913-57 were deleted due to obvious degradation (generally rotor-related), while the entire rate records from 889-67, 895-60 and 919-10 were missing or unreliable. Some of the direction records included apparent spikes (appearing in pairs due to the standard averaging procedure) where the direction deviated by more than 20° from the expected value based on its usual clockwise (tidal) progression. These were attributed to the instantaneous direction sampling in association with possible instrument swinging. A small number (2-20) of such direction values were deleted and replaced by interpolated values for records 895-11,-34,-53 and 912-35,-57; a larger number of such spikes in records 889-21,-43 were not removed. In the case of mooring 919 where the recording intervals were less than 30 min, the interval-averaged edited velocities were vector-averaged to obtain 30-min averages for use in the intercomparison. For mooring 955 (1989), intercomparison with the S4 measurements was done using the 5-min RCM averages.

The RDI yielded 15-min averages of the horizontal velocity components (east and north, approximately corresponding to the acoustic beam alignments), as well as of the vertical velocity, the error velocity and the backscatter intensity. Assuming a constant water depth of 68 m, velocity and backscatter estimates were available for 2.2-m bins centered at depths below the mean surface ranging from 1.4 m to 64.3 m. For the lower 7 bins, a 3-beam solution was used due to poor Doppler tracking in one of the beams, precluding calculation of the error velocity. A normal 4-beam solution was used for the remaining bins. The averaged vertical velocity magnitudes were as large as 0.06 m/s, which cannot be explained by barotropic tidal flow over the observed bottom slopes. The error velocities were as large as 0.12 m/s. The unexplainedly-large magnitudes of these velocities suggest possible degradation of the RDI data (see Belliveau and Loder 1990 for more details).

To illustrate the temporal and vertical structure of the 15-min RDI velocity data, Figure 4 shows (a) vertical profiles of the horizontal components for the first 12 time intervals (about 3 hr in total) during anchor station 893B, and (b) time series plots of these components at three vertical levels for the entire anchor period. On the basis of the expected near-surface degradation of the RDI velocities, the shallowest

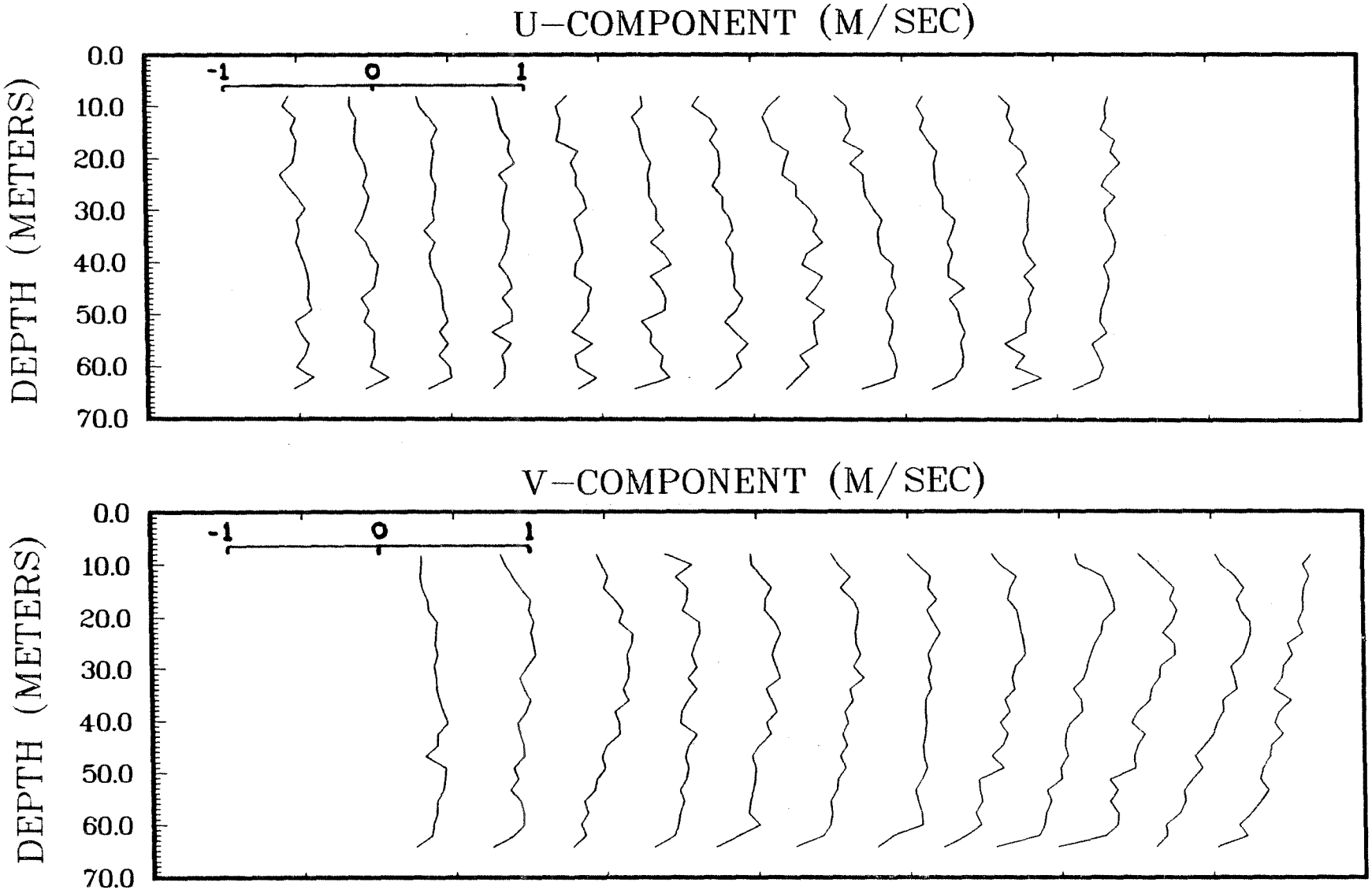

Figure 4a. Velocity profiles from the RDI for the first 12 time intervals (15 min each) in anchor station 893B. The velocity scale for the first profile is shown and each successive profile is offset by 0.45 m/s. The u- and v-components are respectively east and north.

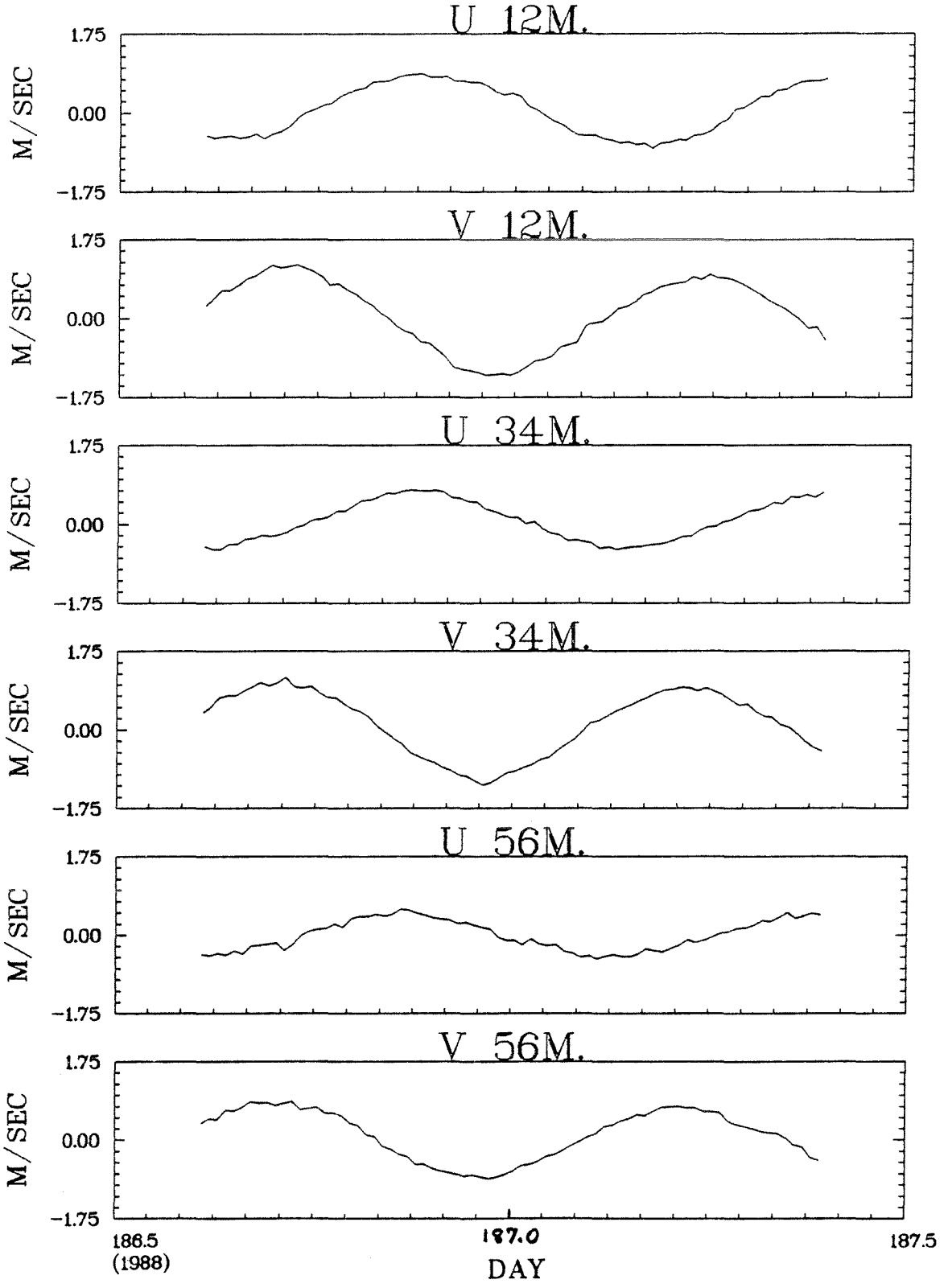

Figure 4b. Time series plots of the 15-min RDI velocity components at three vertical levels (12,34,56m) during anchor station 893B.

bin included in the profile plots is centered at 7.9 m. Some small-scale vertical structure is apparent in the profiles, but the velocity is dominated by a vertically-coherent variation over the periods shown. The time series plots indicate that this variation is the semidiurnal tidal current which is known to dominate the current regime on Georges Bank (e.g. Butman et al. 1982). For the intercomparison with the RCM and Ametek data, the RDI velocity estimates for the time-interval pairs corresponding to the RCM sampling intervals were vector-averaged to obtain 30-min velocity estimates.

The Ametek yielded velocity estimates for 3.2-m bins centered on depths starting at about 8.8 m below the surface, except for anchor station 891A and part of 893A when 1.6-m bins starting at 7.3-m depth were used. The recording interval was approximately 10 min (usually 200 pings), but variable. The temporal and vertical structure of the Ametek velocity data are illustrated in Figure 5 which shows (a) vertical profiles of the horizontal components for the first 18 time intervals during anchor station 893B, and (b) time series plots of these components for the entire anchor period at depths near those for which the RDI data are displayed in Figure 4b. These plots show similarities to those of the RDI data (Fig. 4), except for less small-scale vertical structure and a larger velocity reduction in the near-bottom region, presumably due to side-lobe degradation. Similar profile and time series plots of all the anchor-station Ametek data were visually inspected for obvious spikes, with a few profiles and several dozen other values being deleted. The profiles retained in the final data set were truncated in the sidelobe degradation region, taken to be below 55 m for those in Figure 5a. In addition, the Ametek data for a 9.5-hr period during anchor station 893A and for an 11-hr period at the start of station 919A were not included in the intercomparison due, respectively, to an apparent vertical offset (while using 1.6-m bins) and operation in Profiling mode (without bottom tracking). For the intercomparison with the RCM and RDI data, the Ametek data were decimated to the 30-min RCM sampling intervals, by taking unweighted vector averages of the Ametek estimates for all intervals centered within each RCM interval.

As an example of the resulting 30-min velocity estimates from the three different instruments used in 1988, Figure 6 shows time series plots of the u- and v-components at mid-depth during anchor station 893B. Substantial agreement is apparent but, as discussed in the following sections, there are significant quantitative differences.

The S4s yielded time series of 1-min averaged velocities at 2-min intervals. For the intercomparison with the RCM data, the S4 velocities were decimated to 5 min using unweighted vector averaging of samples centered in each 5-min interval. To determine the expected influence of tilt on the velocities measured by the 37-m S4, a cosine-function tilt correction was applied to the velocities (in instrument co-ordinates).

d. Intercomparison Analyses

The intercomparison included: time series plots such as shown in Figure 6; scatterplots of rate, direction and velocity components from one instrument against the same variable from another for the same depth and time period; first- and second-degree polynomial regressions between these variables; and comparison of means and standard deviations of rate and velocity components from different instruments for the same period

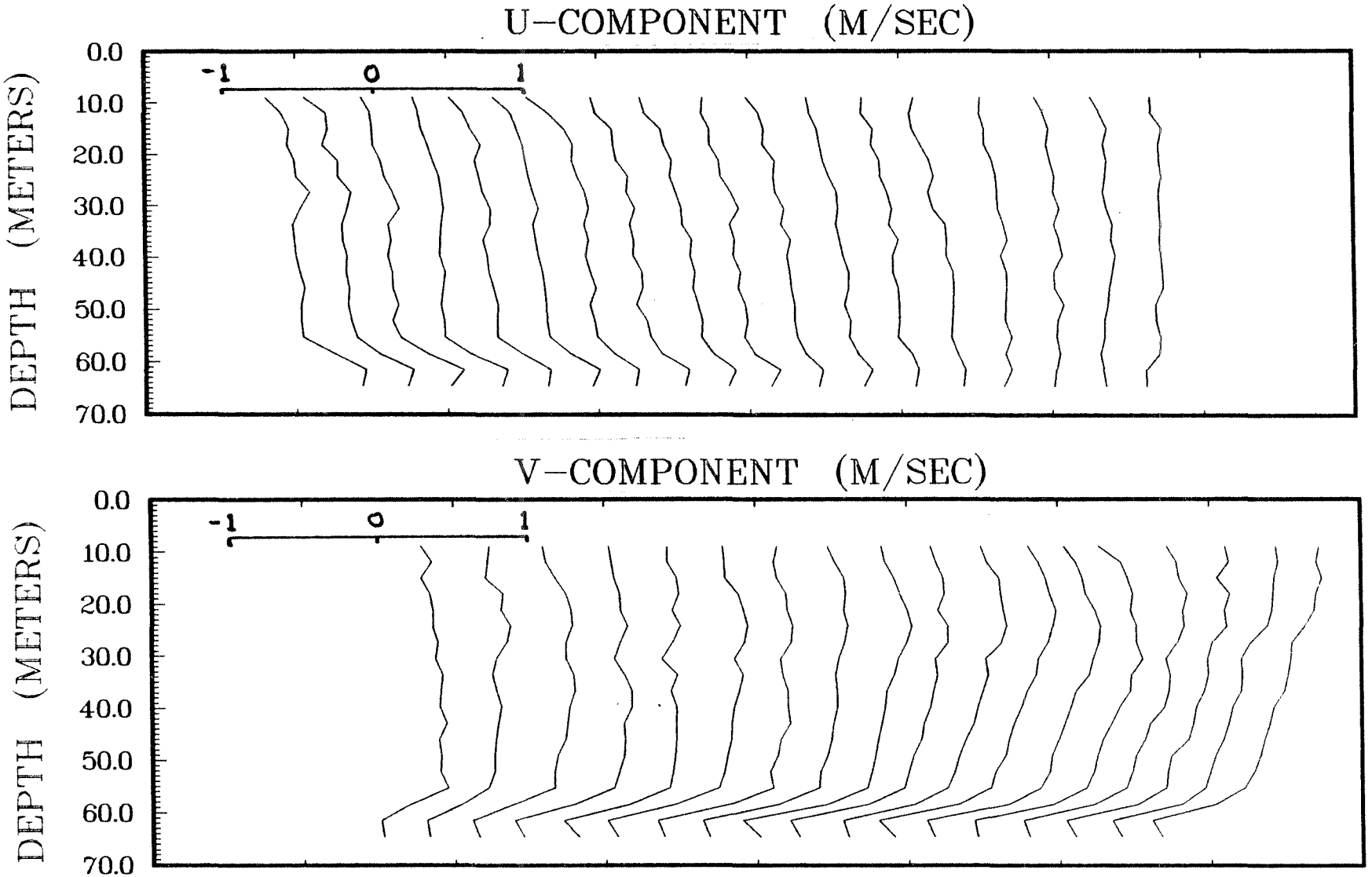

Figure 5a. Velocity profiles from the Ametek for the first 18 time intervals (≈ 10 min each) in anchor station 893B. The velocity scale for the first profile is shown and each successive profile is offset by 0.3 m/s.

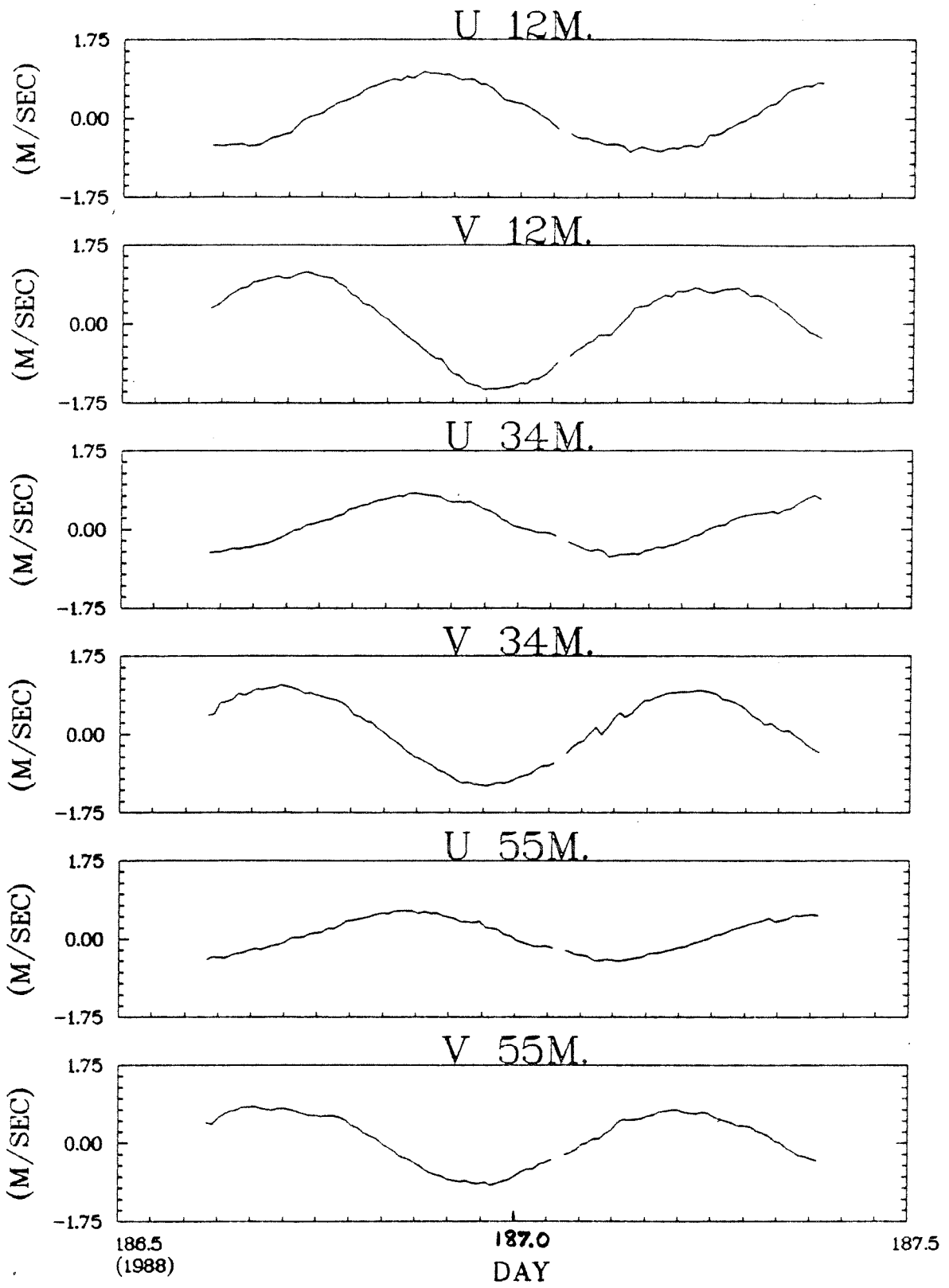

Figure 5b. Time series plots of the 10-min Ametek velocity components at three vertical levels (12,34,55m) during anchor station 893B.

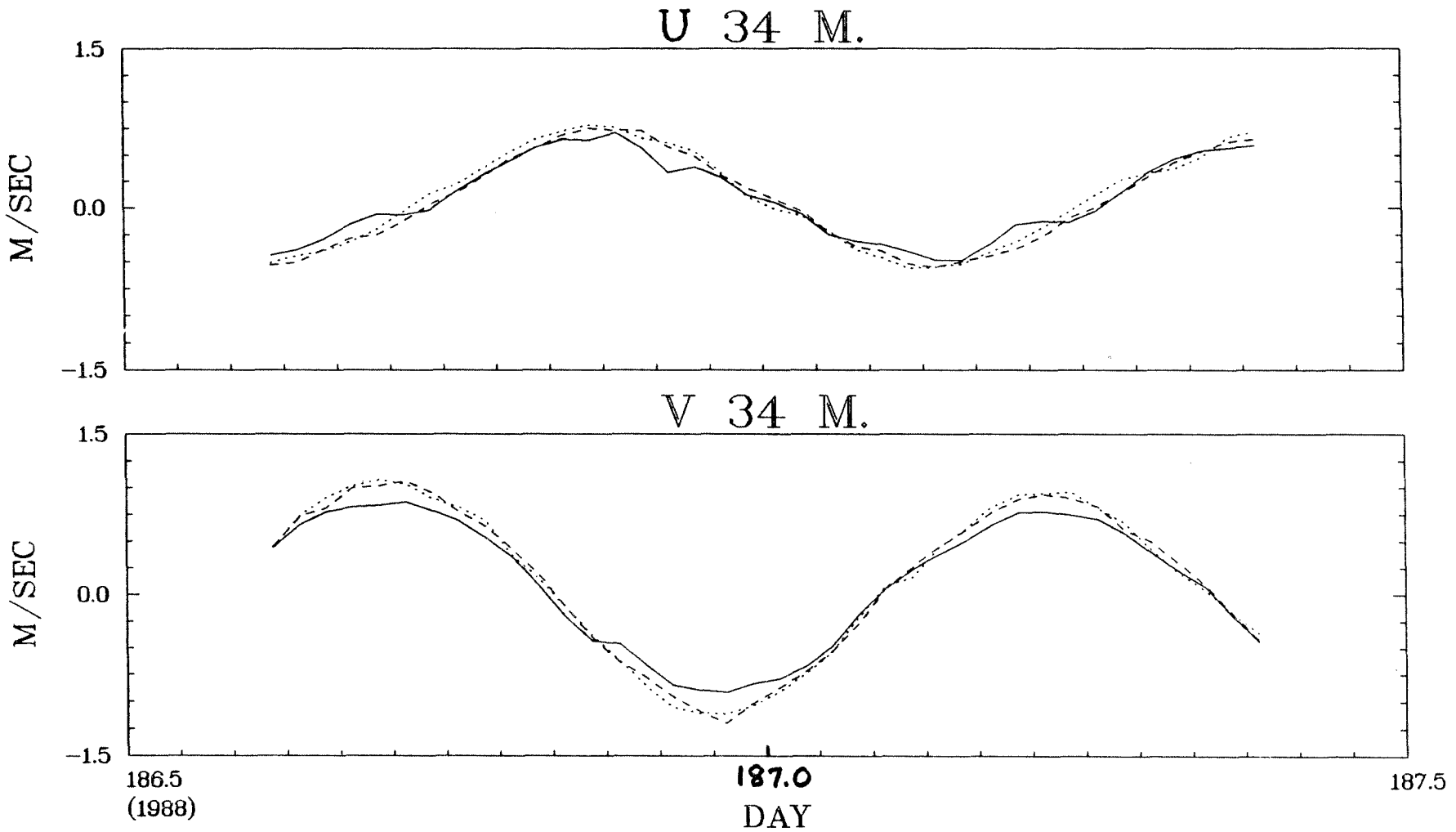

Figure 6. Time series plots of the 30-min RCM (——), RDI (---) and Ametek (...) velocity components at the 34-m level during anchor station 893B.

and position. In addition, taking advantage of the presence of a dominant semidiurnal tidal variation in the velocity field on Georges Bank, the results of harmonic tidal analysis of the different data sets were compared.

The regressions were computed using a standard BMDP software package (BMDP 1983). The linear regression results reported here include standard error estimates (s_o, s_1) for the intercept (a_o) and slope (a_1), as well as the squared correlation coefficient (r^2). In some cases, $\pm 360^\circ$ was added to a direction value before the regression computation.

The tidal analyses were obtained with the standard CMSYS program at BIO. For the anchor station time series, the analyses were performed for only a constant term (Z_0) and the M_2 constituent (period 12.4 hr). The 15- and 29-day analyses on the moored time series included the additional constituents customarily included for these record lengths. The reported phase lags are relative to the astronomical potential on the Greenwich meridian. The residual standard deviation (ν) between the observed data and the regression prediction was computed using a modified version of the BIO program (the Residual portion of the standard program was found to contain errors), as a measure of the residual variability in each time series. Uncertainty estimates on the M_2 amplitudes (probably underestimates due to the possibility of correlation among the residuals) were obtained following Godin (1972), who indicates that the error ΔA in a constituent's amplitude A is $[2\nu^2/(2N-1)]^{1/2}$ where N is the number of observations. The associated error in phase is $\sin^{-1}(\Delta A/A)$.

3. RCM/RDI/Ametek/S4 Intercomparison at Site 3

We first present intercomparison results for site 3 where current measurements were made with the four different instruments. The resulting data set includes: three anchor stations with Ametek data near RCM mooring 893 and the RDI mooring, 15 days of concurrent RCM and RDI data, one anchor station with Ametek data near mooring 913, and 15-16 days of concurrent RCM and S4 data. The depth was nearly uniform (67-70 m) at this frontal-zone site, and the surface-to-bottom density difference was generally less than 1 σ_t unit during moorings 893 and 955, and anchor station 913A, averaging about 0.5.

a. Anchor Stations at Mooring 893

STATISTICS AND TIDAL ANALYSIS

Figure 7 shows the means and standard deviations (square root of total variance) of the velocity components, estimated from the RCMs and two ADCPs, during anchor station 893B. This 19-hr station, during which wind speeds were less than 10 kts and seas/swells were light, has the largest data set involving all three instruments.

It can be seen (Fig. 7) that the RDI and Ametek standard deviations are in excellent agreement between the 20- and 55-m depth levels. Above 20 m, the RDI estimates are increasingly lower than the Ametek estimates as the surface is approached, reaching about 10% at 8-9 m. Below 55 m, the Ametek estimates are substantially reduced relative to those from the

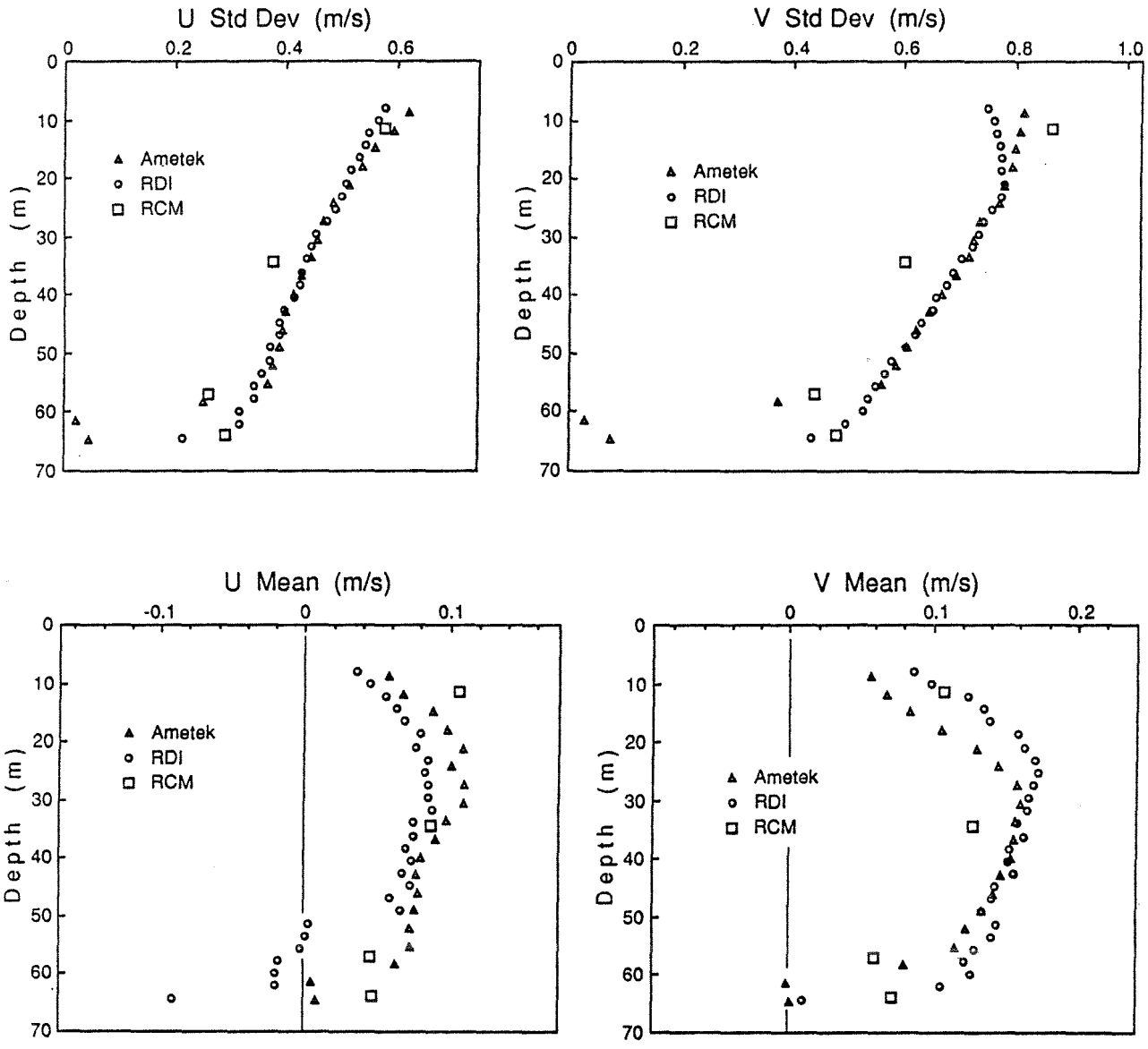

Figure 7. Standard deviations (square root of total variance) and means of the RCM, RDI and Ametek velocity components for various vertical levels during anchor station 893B. The u- and v-components are respectively east and north.

RDI. The latter is consistent with the expected near-bottom degradation of the Ametek estimates in the lower 9 m [15 % of (67-5) m], but the near-surface reduction in the RDI estimates has a greater vertical extent than expected for side-lobe reflection from the sea surface (8% of 68 m = 5.4 m). The standard deviations of the RCM estimates are 10-20% lower than those from the RDI and Ametek for the 34- and 57-m levels, in apparent good agreement with the RDI estimates for the 64-m level and with the RDI and Ametek estimates for the u-component at 12 m, and 7% higher than the Ametek estimates for the v-component at 12 m.

The means show further discrepancies. The vertical interval of good RDI/Ametek agreement is reduced, with the RDI estimates for the lower 7 bins offset relative to both the Ametek and RCM estimates, particularly for the u-component. This offset is apparently related to the 3-beam solution, since the deleted beam was oriented approximately east-west. The RDI mean velocity estimate for the lowest (64-m) bin is particularly suspect. In addition, there is a near-surface discrepancy between the RDI and Ametek means with a greater vertical extent than for the standard deviations. The RCM means show qualitative consistency with the acoustic estimates, but quantitative differences at some levels. (It should be noted that, since the length of this short anchor station was not an integer number of tidal cycles, these means are not representative of the so-called "residual current".)

Firmer statistical statements regarding the discrepancies in the estimates for station 893B can be made on the basis of the tidal analysis results (Fig. 8). The M_2 current amplitudes show similar vertical and instrumental patterns to the standard deviations in Figure 7 (as expected since the tidal current dominates the variability), except for u in the lowest RDI bin which is suspect. The residual standard deviations (ν) between the observed values and regression (tidal analysis) predictions are in the range 0.03-0.12 m/s for this station, with associated (probably lower-bound) amplitude errors (ΔA) in the range 0.01-0.03 m/s. Since the differences between the near-surface RDI and Ametek amplitudes are coherent across several vertical bins and are comparable to (if not larger than) the sum of the expected instrument and analysis errors, there is a suggestion of a significant degradation in one (or both) of the acoustic estimates of the time-varying component of velocity for depths above 20 m. The dynamically-unexpected fall-off in the RDI amplitudes above 20 m points to degradation in the RDI estimates as the leading candidate. Furthermore, the differences between the RCM amplitudes and the acoustic estimates for the 34- and 57-m levels clearly exceed the sum of the expected errors, while the differences in the v-component at 12 m are comparable to the combined errors. Since the RCM amplitudes show the dynamically-unexpected structure of being larger at 3 m than at 10 m above the seafloor, there is a suggestion of degradation in the RCM estimates at 34 and 57 m. In contrast to the current amplitudes, the differences among the different estimates of tidal current phase are less than 6° (except for the 64-m RDI and 58-m Ametek bins), and typically only a few degrees. Although the residual variance in the tidal analysis implies (lower-bound) phase errors of up to only 1.4°, the observed phase differences are substantially less than the 30-minute (15°) sampling interval so that the phase agreement between the different estimates is considered good. The constant terms (Z_0's) in the

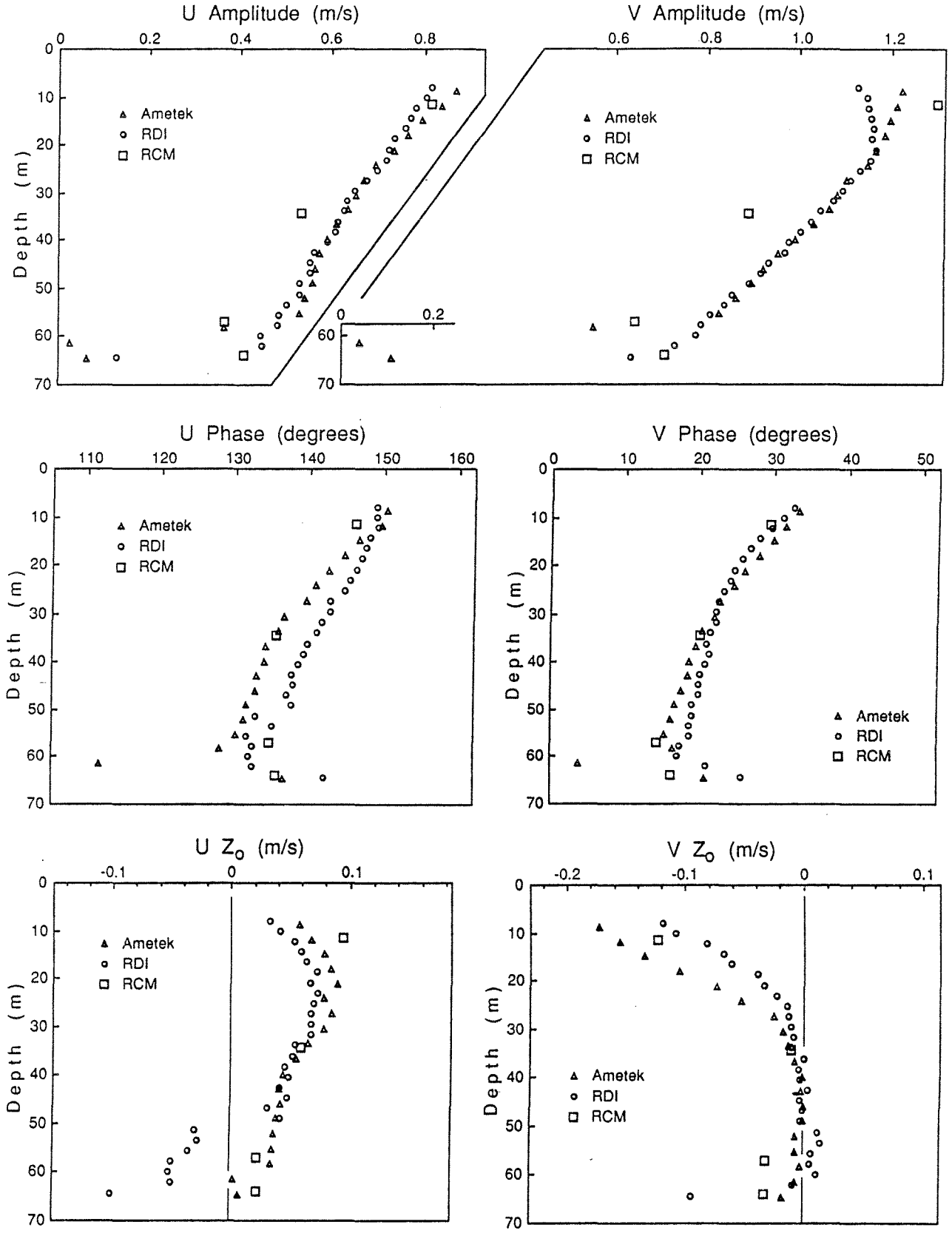

Figure 8. M_2 amplitudes and phases, and constant terms (Z_0's) for the RCM, RDI and Ametek velocity components at various vertical levels during anchor station 893B.

tidal analysis, which are indicative of the residual currents, have vertical and instrumental structures similar to those of the means in Figure 7. The magnitudes of the differences are generally comparable to the combined error estimates, suggesting real discrepancies among the different estimates of mean current.

The other two anchor stations at mooring 893 (A and C, Table 3) had durations of 21.5 and 11.5 hr respectively. However, the 9.5 hr of suspect Ametek data from station 893A resulted in a data gap which precluded tidal analysis. The standard deviations and means of the velocity components (Fig. 9) during the remainder of station 893A (wind speeds < 15 kts, light to moderate seas/swells) show substantial similarity in vertical and instrumental differences to those for station 893B (Fig. 7): in particular, relatively-low RCM standard deviations at 34 and 57 m and relatively-high values for v at 12 m, reduced RDI standard deviations for v in the upper 20 m, offsets in the RDI means for the lower 7 bins, and differences between the RDI and Ametek means for u in the upper 30 m. There are also some contrasts to 893B, e.g. in the differences in the RDI and Ametek means for v.

The tidal analysis results for station 893C, during which wind speeds were up to 20 kts and seas/swells were again light, are shown in Figure 10. Similar discrepancies to those at the other stations are apparent, with the exceptions of reduced reductions in the 34 and 57-m RCM amplitudes, agreement of the RCM and Ametek amplitudes at 12 m, possible degradation in the 55-m Ametek velocities, and more complicated vertical structure in the RDI/Ametek mean-current differences.

On the basis of these results (and supported by other results not shown), it is concluded that the velocity estimates for the lowest RDI bin (64 m) and for Ametek bins below 55 m at site 3 are degraded. These data are henceforth deleted from the analyses.

SCATTERPLOTS AND REGRESSIONS

Further information on the origin of the discrepancies among the velocity estimates is available from scatterplots and regressions between the different 30-min estimates of a particular variable. Figures 11 (RDI vs Ametek) and 12 (RCM vs Ametek) show such scatterplots for rate and direction at three different vertical levels for the combined data from the three anchor stations at mooring 893. Regression results are summarized in Tables 4 and 5. On the basis of the apparent self-consistency of the Ametek data shown above (as well as that which follows) and the availability of Ametek data at most moorings, the Ametek time series is taken as the independent variable in the scatterplots and regressions presented in this report. Although this can be interpreted as taking the Ametek data as the tentative "standard", the major points arising from the intercomparison are independent of this choice.

It can be seen from the scatterplots and regression results that the various direction estimates during the anchor stations at mooring 893 are in excellent agreement, all lying close to the 1:1 line. In contrast, the rate plots show greater scatter, as well as substantial deviations from the dashed 1:1 line, suggesting that the discrepancies identified in the tidal analyses and statistics originate with the rate, rather than

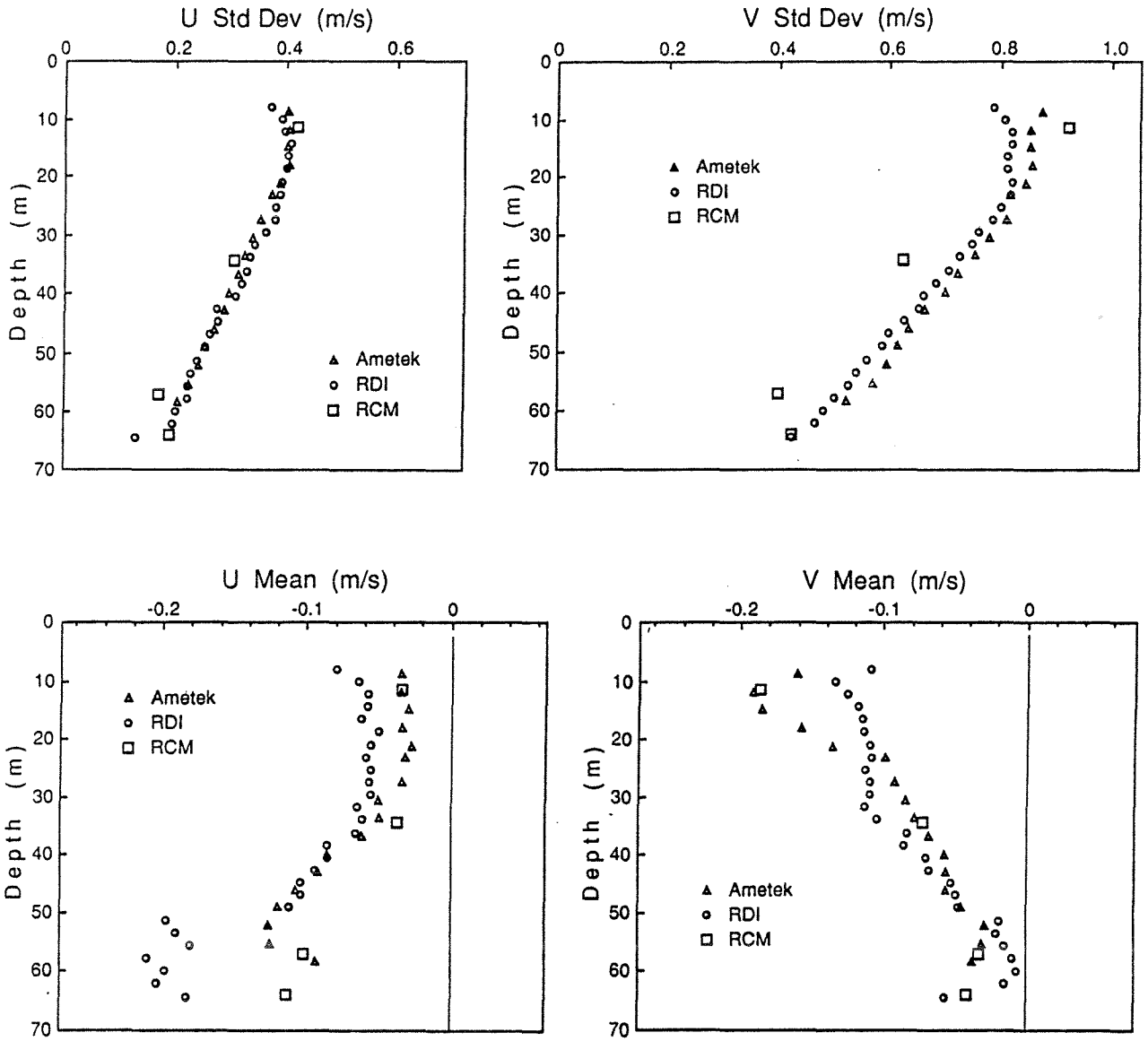

Figure 9. Standard deviations (square root of total variance) and means of the RCM, RDI and Ametek velocity components during anchor station 893A.

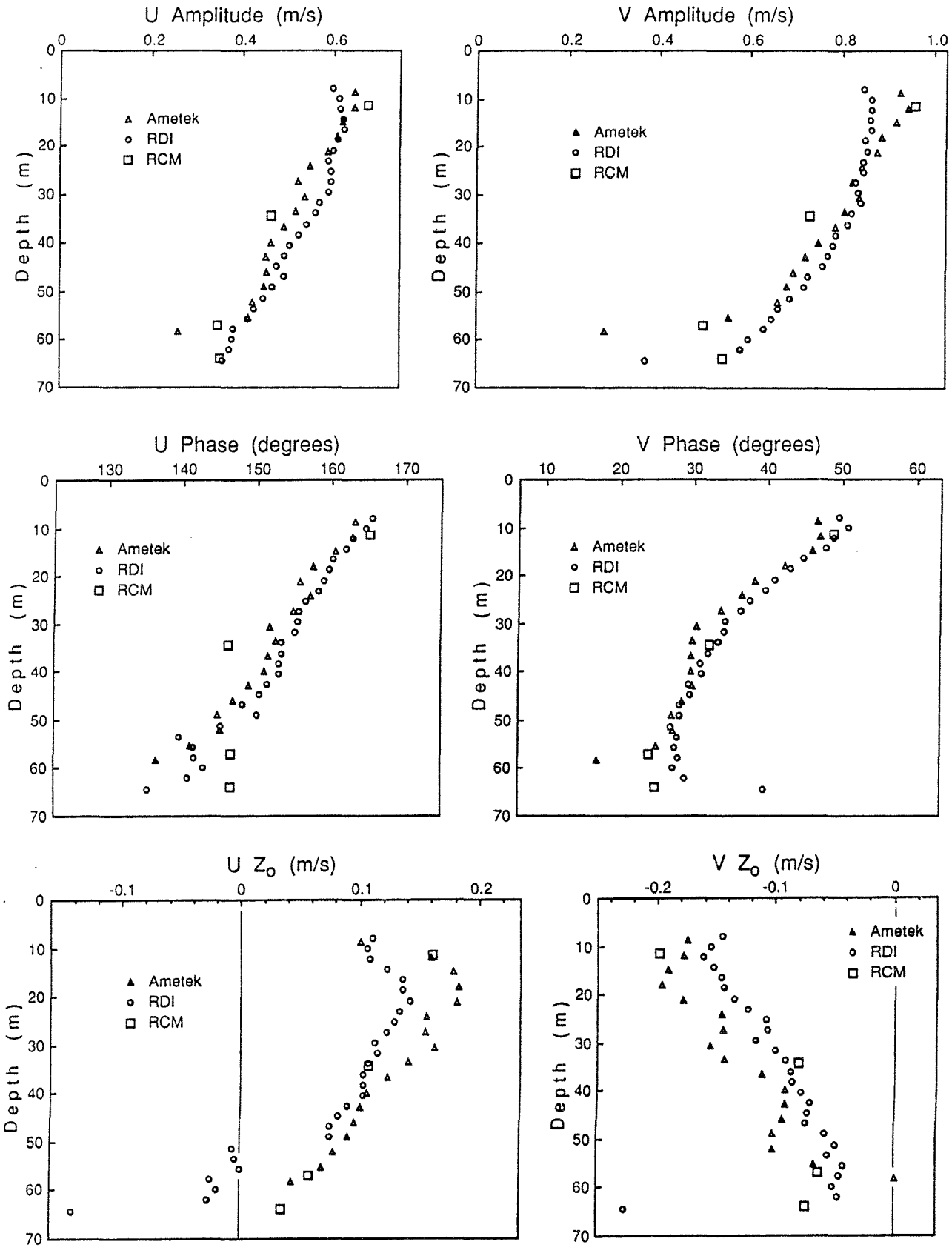

Figure 10. M_2 amplitudes and phases, and constant terms (Z_0's) for the RCM, RDI and Ametek velocity components during anchor station 893C.

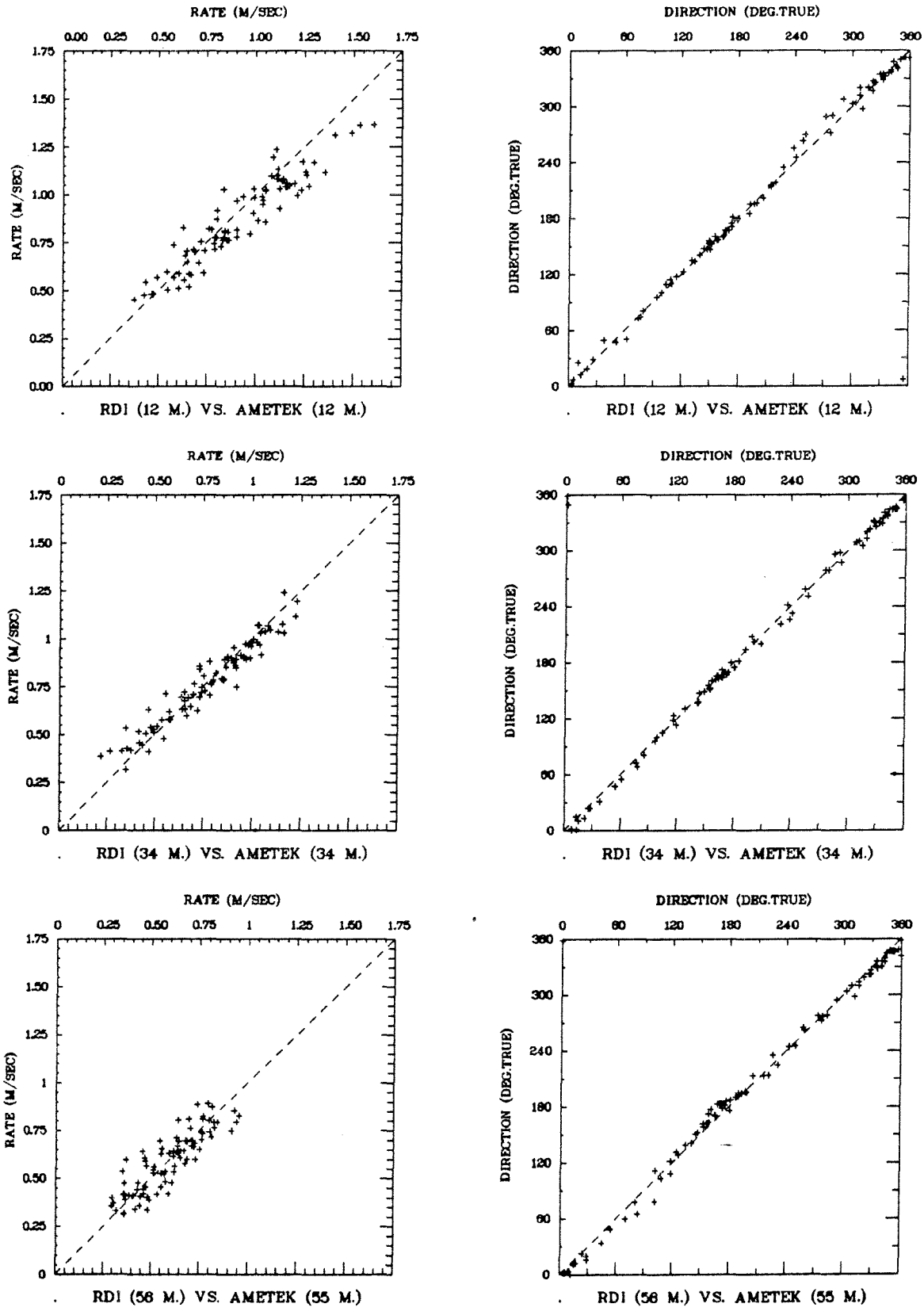

Figure 11. Rate and direction scatterplots for RDI (ordinate) versus Ametek (abscissa) data at three vertical levels during the three anchor stations at mooring 893. The dashed line is the 1:1 line.

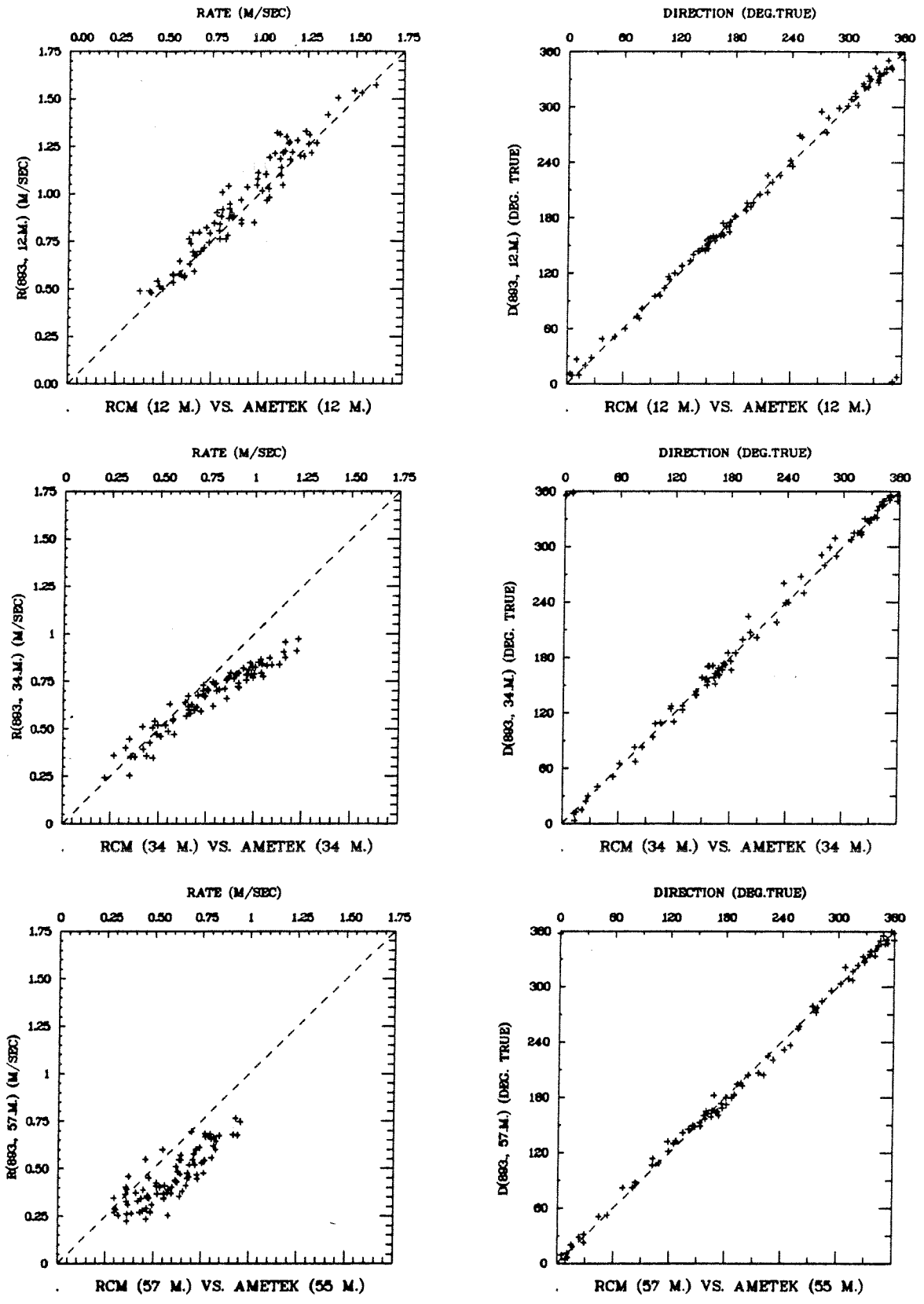

Figure 12. Rate and direction scatterplots for RCM (ordinate) versus Ametek (abscissa) data at three vertical levels during the three anchor stations at mooring 893. The dashed line is the 1:1 line.

Table 4. Summary of linear regression results for RATE at site 3. Results are presented for the mooring 893 anchor stations combined (893A+B+C), the 15-day RCM/RDI intercomparison (893/920), station 913A, and mooring 955 (RCM vs S4). The intercept (a_o), slope (a_1), their standard errors (s_o, s_1), the residual standard deviation (SD) between the observations and regression predictions, the squared correlation coefficient (r^2) and the number of observations (N) are given. The f ratio, high values of which indicate that a higher-degree regression polynomial is appropriate (BMDP 1983), is also given.

Depth Station	Dep/Ind Variable	$a_o \pm s_o$ (m/s)	$a_1 \pm s_1$	SD (m/s)	r^2	N	f Ratio
12-14 m							
893A+B+C	RDI12/AM12	.14 ±.03	.80 ±.03	.08	.88	86	1.0
"	RCM12/AM12	.05 ±.03	1.00 ±.03	.07	.94	86	.6
"	RCM12/RDI12	-.07 ±.03	1.19 ±.03	.07	.95	86	.6
893/920	RCM12/RDI12	-.04 ±.01	1.16 ±.01	.06	.95	771	1.5
955	RCM13/S4-14	-.03 ±.001	1.11 ±.001	.03	.99	4386	.3
34-37 m							
893A+B+C	RDI34/AM34	.13 ±.02	.83 ±.03	.06	.93	86	2.1
"	RCM34/AM34	.16 ±.02	.66 ±.02	.05	.92	86	11.2
"	RCM34/RDI34	.08 ±.02	.77 ±.02	.04	.94	86	46.8
893/920	RCM34/RDI34	.09 ±.01	.76 ±.01	.04	.95	771	167.1
913A	RCM34/AM34	.10 ±.04	.74 ±.05	.05	.89	28	1.1
955	RCM36/S4-37	-.16 ±.005	1.27 ±.01	.07	.87	4781	118.2
55-57 m							
893A+B+C	RDI56/AM55	.11 ±.03	.81 ±.05	.08	.73	86	.1
"	RCM57/AM55	.04 ±.03	.69 ±.05	.08	.71	86	7.6
"	RCM57/RDI56	-.01 ±.03	.78 ±.04	.06	.80	86	6.6
893/920	RCM57/RDI56	-.04 ±.01	.82 ±.02	.07	.78	771	25.3
62-64m							
893/920	RCM64/RDI62	.00 ±.01	.93 ±.02	.07	.79	771	.9

Table 5. Summary of linear regression results for DIRECTION at site 3. Results are presented for the mooring 893 anchor stations combined (893A+B+C), the 15-day RCM/RDI intercomparison (893/920), station 913A, and mooring 955 (RCM vs S4). The intercept (a_o), slope (a_1), their standard errors (s_o, s_1), the residual standard deviation (SD) between the observations and regression predictions, the squared correlation coefficient (r^2) and the number of observations (N) are given.

Depth Station	Dep/Ind Variable	$a_o \pm s_o$ (°)	$a_1 \pm s_1$	SD (°)	r^2	N
12-14 m						
893A+B+C	RDI12/AM12	1.8 ±1.4	.998 ±.01	6.1	.997	86
"	RCM12/AM12	2.9 ±1.5	.997 ±.01	6.5	.996	86
"	RCM12/RDI12	1.2 ±1.1	.998 ±.005	4.7	.998	86
893/920	RCM12/RDI12	0.9 ±0.4	.995 ±.002	5.2	.998	771
955	RCM13/S4-14	-2.0 ±0.1	1.004 ±.001	3.4	.999	4386
34-37 m						
893A+B+C	RDI34/AM34	-3.9 ±1.0	1.008 ±.005	4.7	.998	86
"	RCM34/AM34	-2.8 ±1.7	1.018 ±.008	7.6	.995	86
"	RCM34/RDI34	1.1 ±1.4	1.010 ±.006	6.1	.997	86
893/920	RCM34/RDI34	4.2 ±0.5	.993 ±.002	6.6	.996	771
913A	RCM34/AM34	-4.7 ±2.3	1.018 ±.01	5.9	.997	28
955	RCM36/S4-37	-2.1 ±0.2	1.008 ±.001	6.6	.996	4781
55-57 m						
893A+B+C	RDI56/AM55	-0.8 ±1.7	.999 ±.008	7.5	.995	86
"	RCM57/AM55	1.2 ±1.4	.992 ±.006	6.1	.997	86
"	RCM57/RDI56	2.9 ±2.1	.988 ±.009	9.4	.993	86
893/920	RCM57/RDI56	7.0 ±0.7	.974 ±.003	9.8	.991	771
62-64m						
893/920	RCM64/RDI62	4.6 ±0.8	.979 ±.004	10.6	.990	771

direction, measurements. For 12 m, the scatterplots indicate that the rate relations are nearly linear, with suggestions of low RDI values at high speeds and high RCM values at all speeds. The rate regressions indicate significant differences from the 1:1 line for all except RCM vs Ametek, with standard deviations about the predicted line of 0.07-0.08 m/s. For 34 m, the rate scatterplots indicate that the RDI/Ametek relation is also nearly linear (although with a slope significantly different than 1 according to the regression results), but there is a clear suggestion of a nonlinear relation between the RCM and Ametek (also between the RCM and RDI; not shown), with the RCM rates being relatively low for speeds exceeding 0.8 m/s. Finally, for 55-57 m, the plots show increased scatter with the RDI/Ametek rates encompassing the 1:1 line and appearing linear (although different from the 1:1 line according to the regression), and the RCM/Ametek rates generally falling below the line.

b. 15-Day RCM/RDI Intercomparison

STATISTICS AND TIDAL ANALYSIS

The 15+ days of concurrent RCM and RDI measurements at site 3 provide a much larger data set for the intercomparison of those velocity estimates. Figures 13 and 14 show, respectively, the standard deviations and means, and the tidal analysis results for a 15-day portion of these records. Since the standard deviations and tidal current amplitudes show similar patterns, and the same is true for the means and Z_0's, we will focus on the tidal analysis results (Fig. 14).

The RDI M_2-current amplitudes decrease as the seafloor is approached, in qualitative agreement with the expectation for tidal currents in a homogeneous fluid (e.g. Prandle 1982). The exception is a 5% fall-off in the v amplitude in upper 20 m, similar to that seen in the anchor station data but with reduced magnitude. The RCM amplitudes show a similar relation to the RDI amplitudes as for the anchor stations: 10-12% high at 12 m, 12-15% low at 34 m, 20-25% low at 57 m, and apparently good agreement at 64 m. The residual standard deviations between the observed currents and regression predictions are in the range 0.07-0.17 m/s for this analysis for both the RCM and RDI data, implying (lower-bound) amplitude errors of about 0.01 m/s. The instrument-to-instrument differences noted above exceed the sum of these errors and the expected instrument errors, suggesting degradation in one or both of the velocity estimates.

The phases show similar differences to the anchor stations estimates, with the differences well within the sampling interval. Two noteworthy features of the phase are a 4°-offset for the u-component in the lower 7 RDI bins (apparently associated with the 3-beam solution but, perhaps fortuitously, giving better agreement with the 57-m RCM estimate), and an increase in phase lag for both the RCM and RDI v-components very near the bottom (in contrast to the vertical structure elsewhere in the water column).

The residual currents over the 15-day period (i.e. the Z_0's) show qualitative consistency, except for the lower portion of the water column where the 3-beam solution is used. The RCM estimates suggest a general

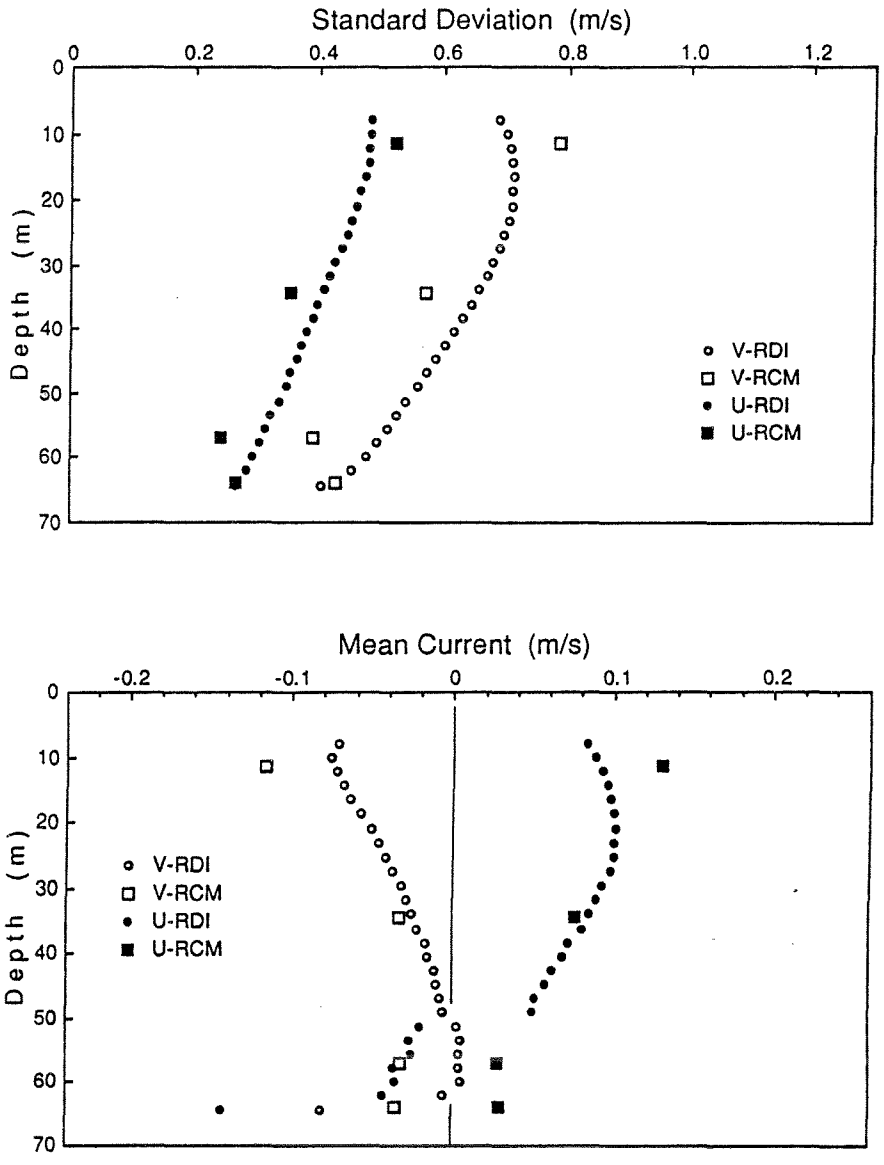

Figure 13. Standard deviations (square root of total variance) and means of the RCM and RDI velocity components during the 15-day intercomparison period for moorings 893 and 920.

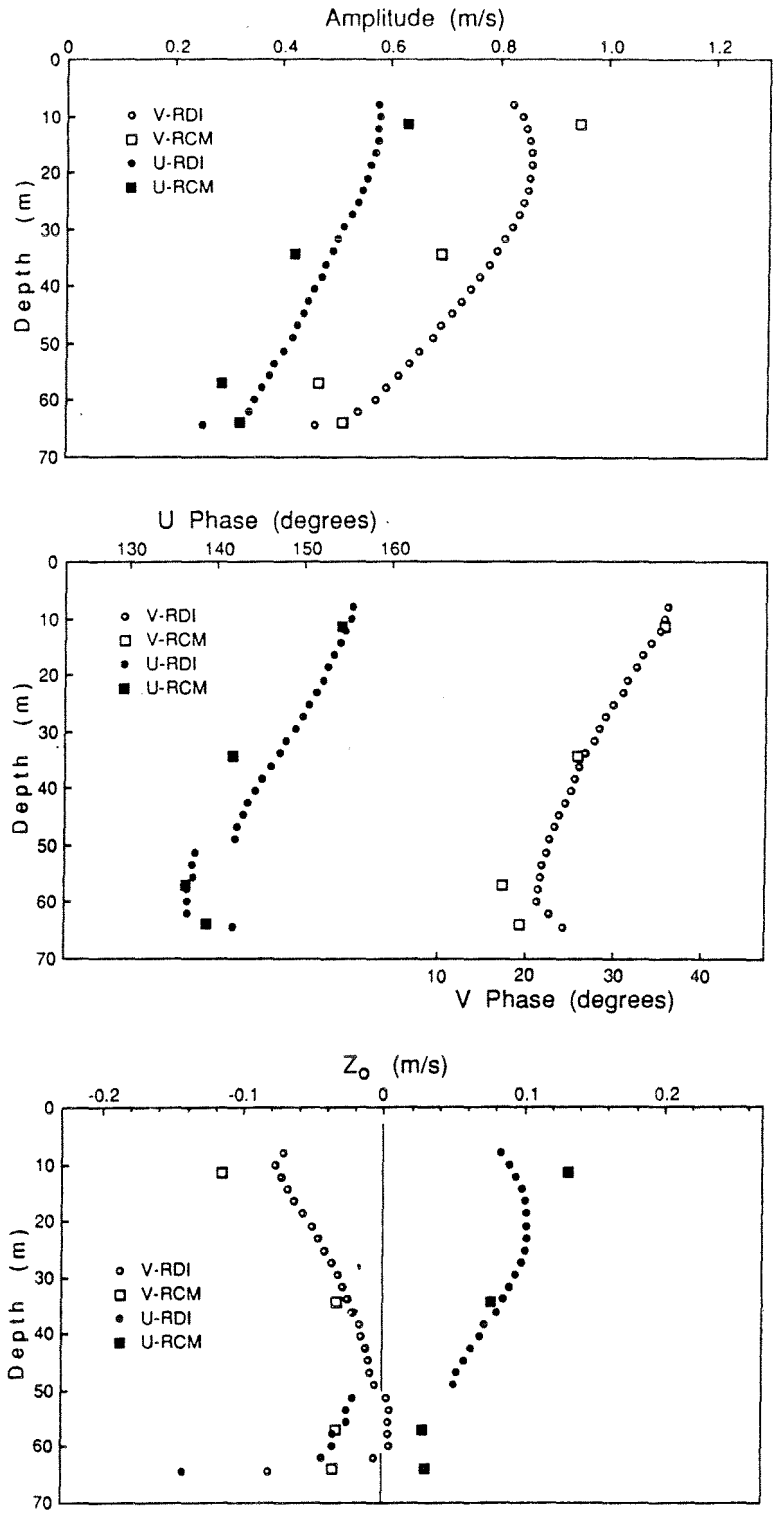

Figure 14. M_2 amplitudes and phases, and constant terms (Z_0's) for the RCM and RDI velocity components during the 15-day intercomparison of moorings 893 and 920.

southeastward mean flow at all depths, consistent with the known clockwise gyre on Georges Bank (e.g. Butman et al. 1987) and an on-Bank drift. This flow includes a baroclinic and weaker barotropic component. The RDI estimates in the upper half of the water column show the same features, but the lower 7 bins have offsets of about -0.07 m/s for u and +0.01 m/s for v resulting in sign changes for both components. Thus, there is a strong suggestion that the RDI estimates of the mean component of flow are unreliable for (at least) the lower 7 bins where the 3-beam solution was used.

SCATTERPLOTS AND REGRESSIONS

Figures 15 and 16 show scatterplots between the RCM and RDI variables for the four intercomparison levels. Since this is the largest data set of the intercomparison, plots are also shown for the velocity components to allow examination of the possible association of discrepancies with particular flow directions. The linear regression results for rate and direction are included in Tables 4 and 5.

The directions again lie close to the 1:1 line for all levels, with a particularly tight relation at 12 m. There is a slight increase in scatter at the other levels, and suggestions of a systematic direction-dependent deviation from the 1:1 line at the lower levels, indicating a possible phase difference between the instruments or mooring sites. The generally good agreement is confirmed by the direction regressions.

The rate scatterplots and regressions provide further support for the discrepancies discussed earlier. At 12 m, the RCM is relatively high by a fixed percentage (about 16%), consistent with the apparent degradation in the RDI estimates in the upper 20 m. At 34 m, there is a nonlinear relation with the RCM relatively low at all speeds, but particularly so at speeds exceeding 0.8 m/s. At 57 m, the relation appears more linear with the RCM rates low by about 18%, while the agreement at 62-64 m is as good as could be expected given the different vertical levels in a high shear zone.

The component scatterplots for 12 m show some suggestion of greater RCM/RDI differences in the east (+u) and south (-v) quadrants, and similarly in the north (+v) and south quadrants for 34 m. However, this may be simply a reflection of the higher speeds in these directions. On the other hand, the 57-m data show similar deviations in all quadrants. The u-component at 62-64 m shows a uniform offset towards the negative RDI axis, consistent with the offsets apparent in the lower 7 RDI bins in Figures 13 and 14.

c. Anchor Station at Mooring 913: RCM vs Ametek

The final RCM/Ametek intercomparison data set for site 3 is from a 14-hr anchor station at mooring 913 (913A, Table 3). This mooring replaced mooring 893 at the end of cruise 88023, with the same design (Fig. 2). Unfortunately, the 12- and 57-m RCMs did not return usable rate estimates for the anchor station period, so that intercomparison with the Ametek is only possible for the 34-m level. Wind speeds were 12-25 kts and sea/swells were light to moderate during the anchor

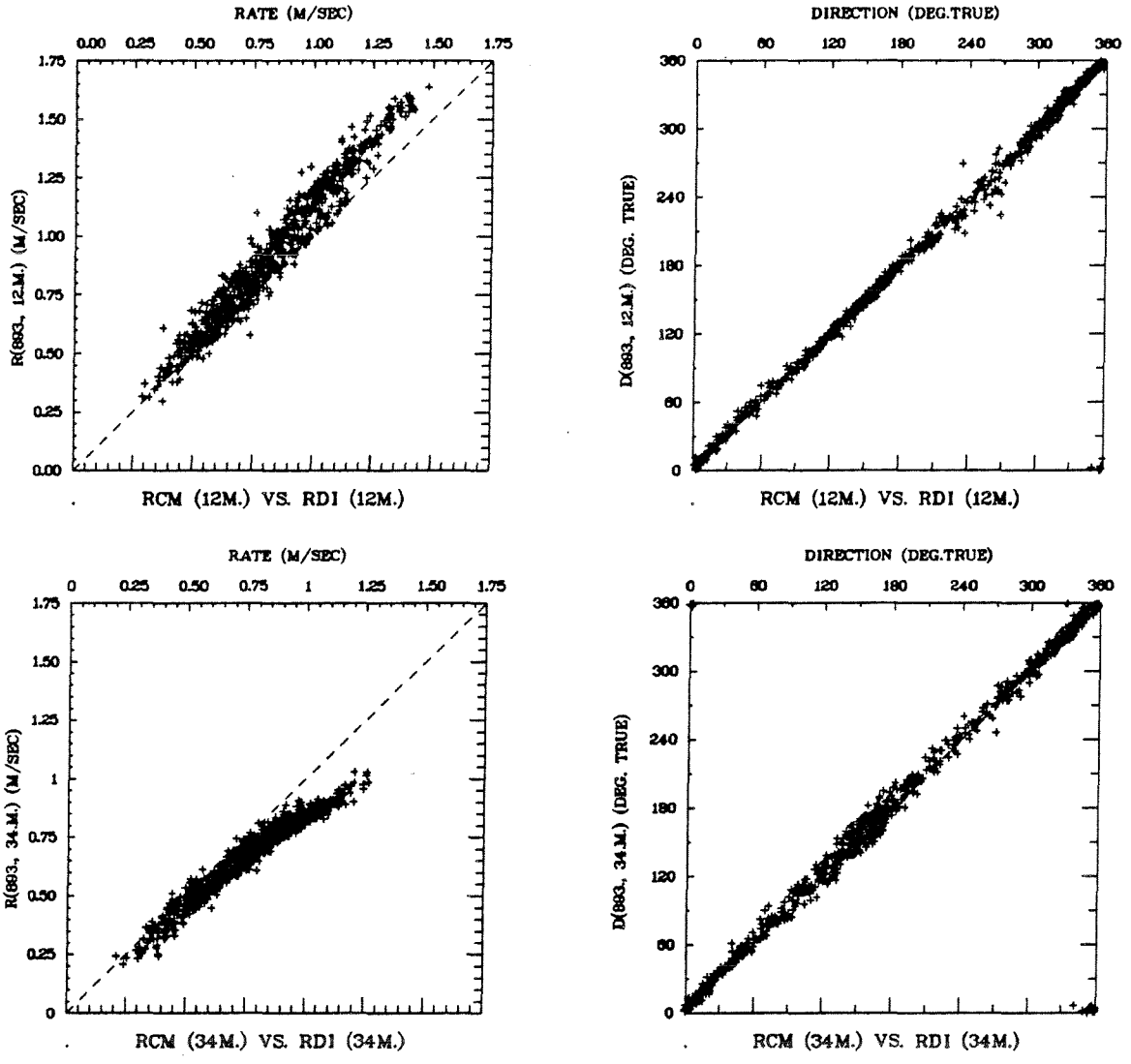

Figure 15a. Rate and direction scatterplots for RCM (ordinate) versus RDI (abscissa) data at 12 and 34 m during the 15-day intercomparison of moorings 893 and 920. The dashed line is the 1:1 line.

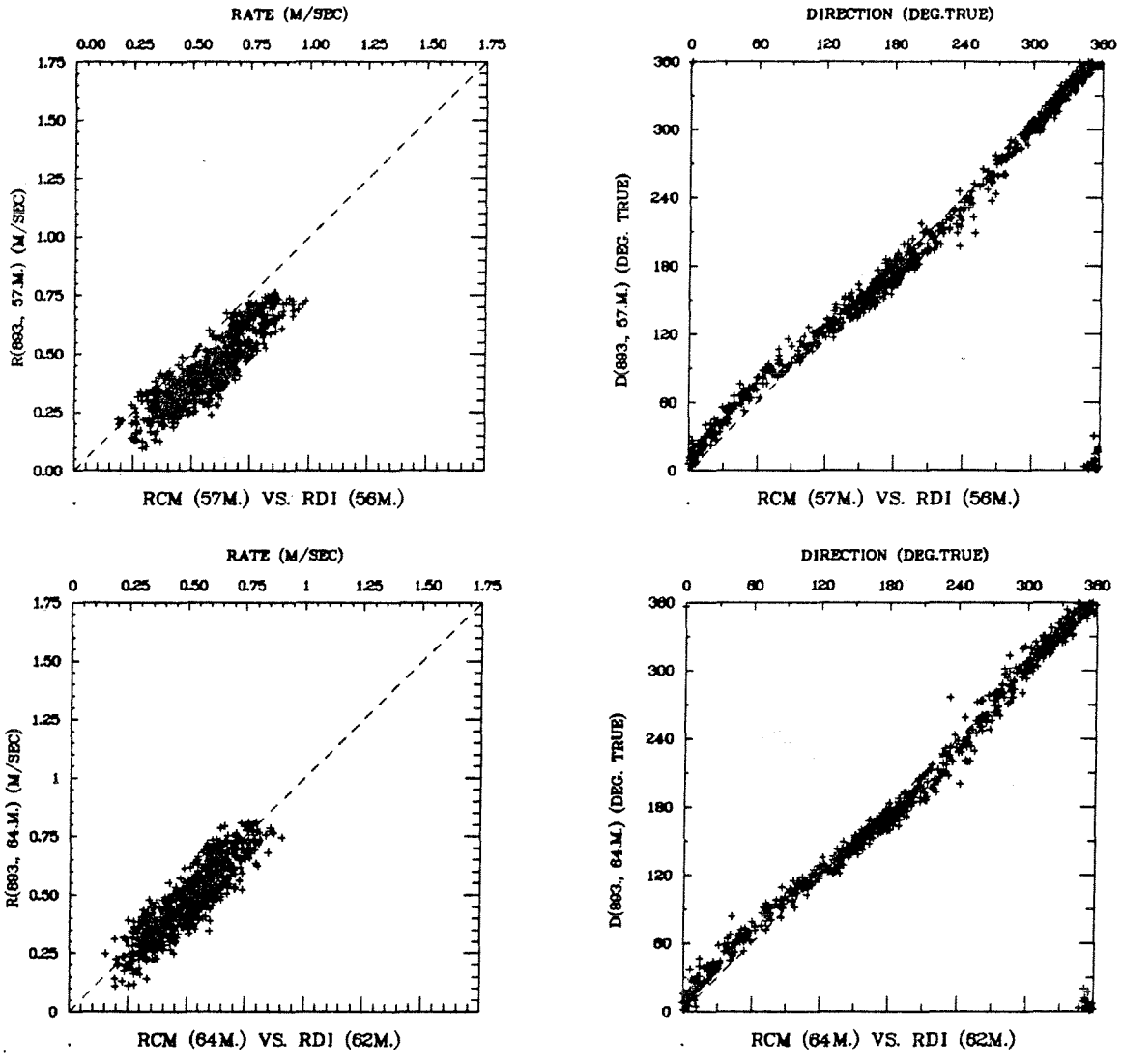

Figure 15b. Rate and direction scatterplots for RCM versus RDI data at 56-57 and 62-64 m during the 15-day intercomparison of moorings 893 and 920.

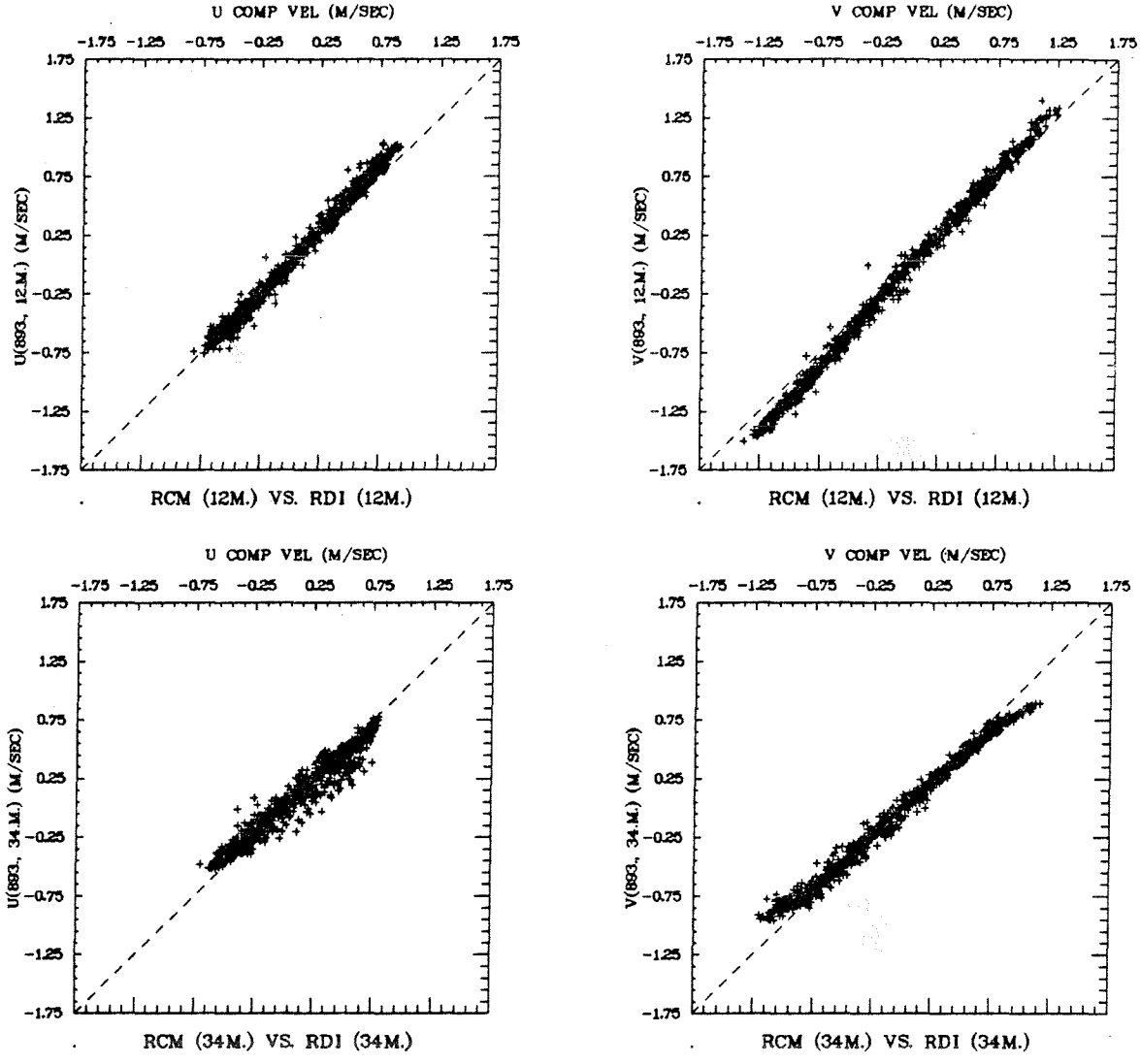

Figure 16a. U- and v-component scatterplots for RCM (ordinate) versus RDI (abscissa) data at 12 and 34 m during the 15-day intercomparison of moorings 893 and 920.

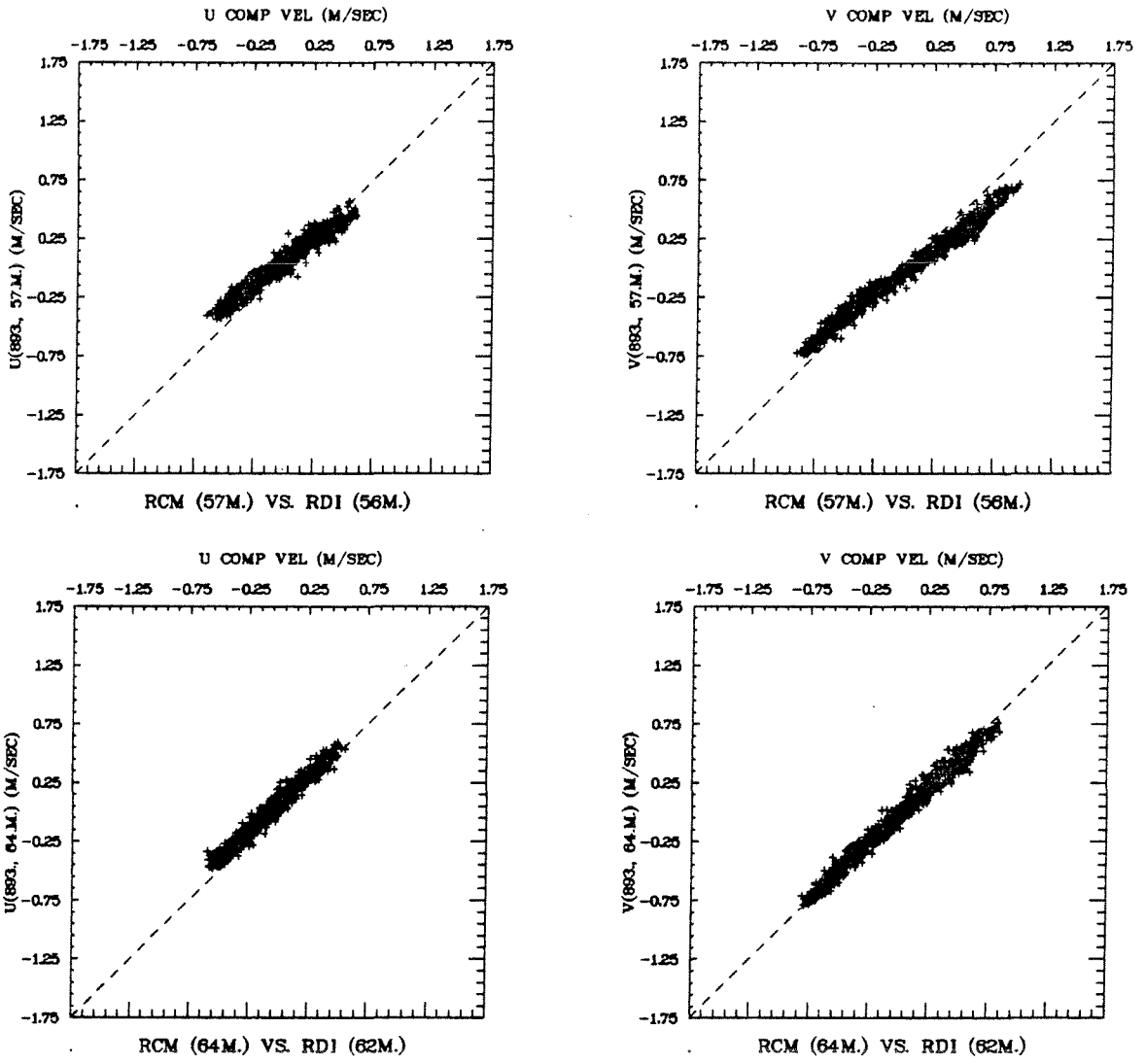

Figure 16b. U- and v-component scatterplots for RCM versus RDI data at 56-57 and 62-64 m during the 15-day intercomparison of moorings 893 and 920.

station.

The scatterplots for rate and direction are shown in Figure 17, and the corresponding linear regression results included in Tables 4 and 5. Good direction agreement and relatively-low RCM rates, particularly at speeds exceeding 0.6 m/s, are apparent. The regression line is not significantly different from that for the RCM vs RDI data in the 15-day comparison, and only marginally different from the RCM vs Ametek data for the mooring 893 stations.

d. Mooring 955: RCM vs S4

The 1989 deployment of RCMs and S4s on the same mooring (955) provides a large data set for the comparison of RCM and electromagnetic current measurements. The M_2 current amplitudes (not shown) from the RCM measurements have a similar (normalized) vertical structure to those from mooring 893, suggesting similar RCM performance for the two different moorings. The vertical structure of the M_2 current amplitude from the S4 measurements is similar to that from the RCMs, but this is misleading as shown in the rate and direction scatterplots for RCM versus S4 (Fig. 18). The direction plots again show good agreement, albeit with some suggestion of increased scatter at mid-depth (also see regression results in Table 5). The rate plot for the upper level is similar to the RCM/Ametek rate plot for that level in mooring 893 (Fig. 12), with relatively-high RCM rates (also see Table 4). On the other hand, the mid-depth rate plot suggests two loci of points: one near the 1:1 line for all speeds (up to 0.95 m/s), and the other deviating from the 1:1 line for (RCM) speeds above 0.6 m/s with no S4 values above 0.95 m/s in spite of RCM values up to 1.1 m/s. The general features of this plot are not changed upon correction of the S4 rates for a cosine-function tilt degradation. As discussed further in Section 6, the measurements from the 37-m S4 are clearly degraded during certain strong flow regimes, thus limiting their value in determining the accuracy of the RCM measurements.

4. RCM/Ametek Intercomparisons at Other Sites

We next present the intercomparison results for the other sites, starting with the Bank sites (#'s 2,4,6) which have nearly-uniform depths (locally), and concluding with the Bank-edge sites (#'s 1,5).

a. Site 2 (Moorings 891, 919)

We start with site 2 which has the same depth (66-67 m) as site 3, but somewhat increased stratification (average surface-to-bottom density differences in the range 0.5-2.0 σ_t units during the anchor stations). The data set includes three anchor stations at mooring 891 (cruise 88023) and one at mooring 919 (cruise 88036).

MOORING 891

The results for mooring 891 are illustrated by the tidal analysis results shown in Figure 19 for station 891B, during which wind speeds were less than 8 kts and seas/swells light. The amplitude results are similar to those for site 3, with: the RCM values greater at 3 m above the seafloor than at 10 m, the Ametek values in the 58-m bin apparently degraded (as expected), and the RCM values at the mid-depth and 57 m

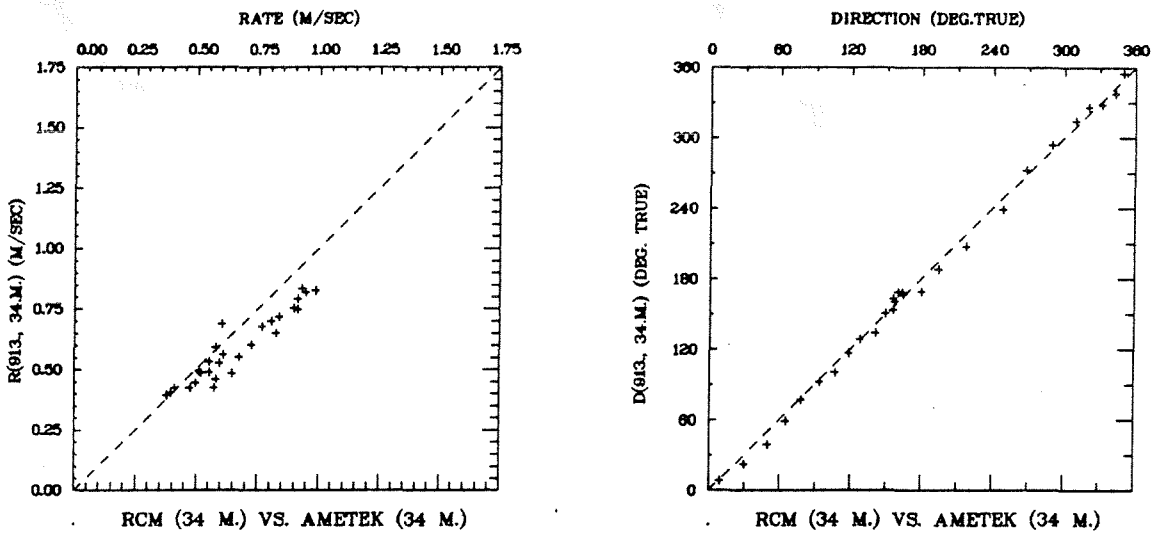

Figure 17. Rate and direction scatterplots for RCM (ordinate) versus Ametek (abscissa) data at the 34-m level during anchor station 913A. The dashed line is the 1:1 line.

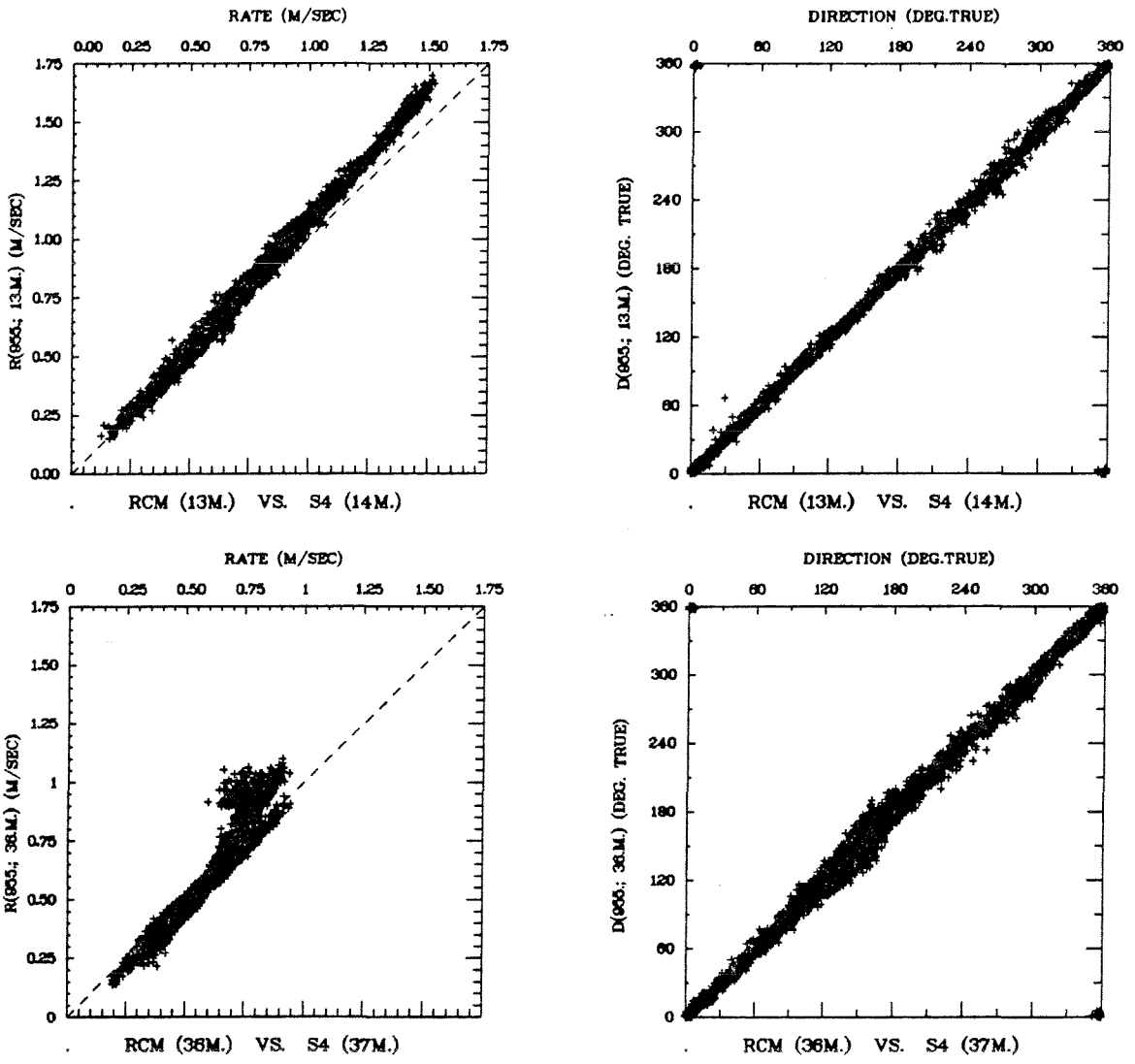

Figure 18. Rate and direction scatterplots for RCM (ordinate) versus S4 (abscissa) data at the upper and mid-depth levels from mooring 955.

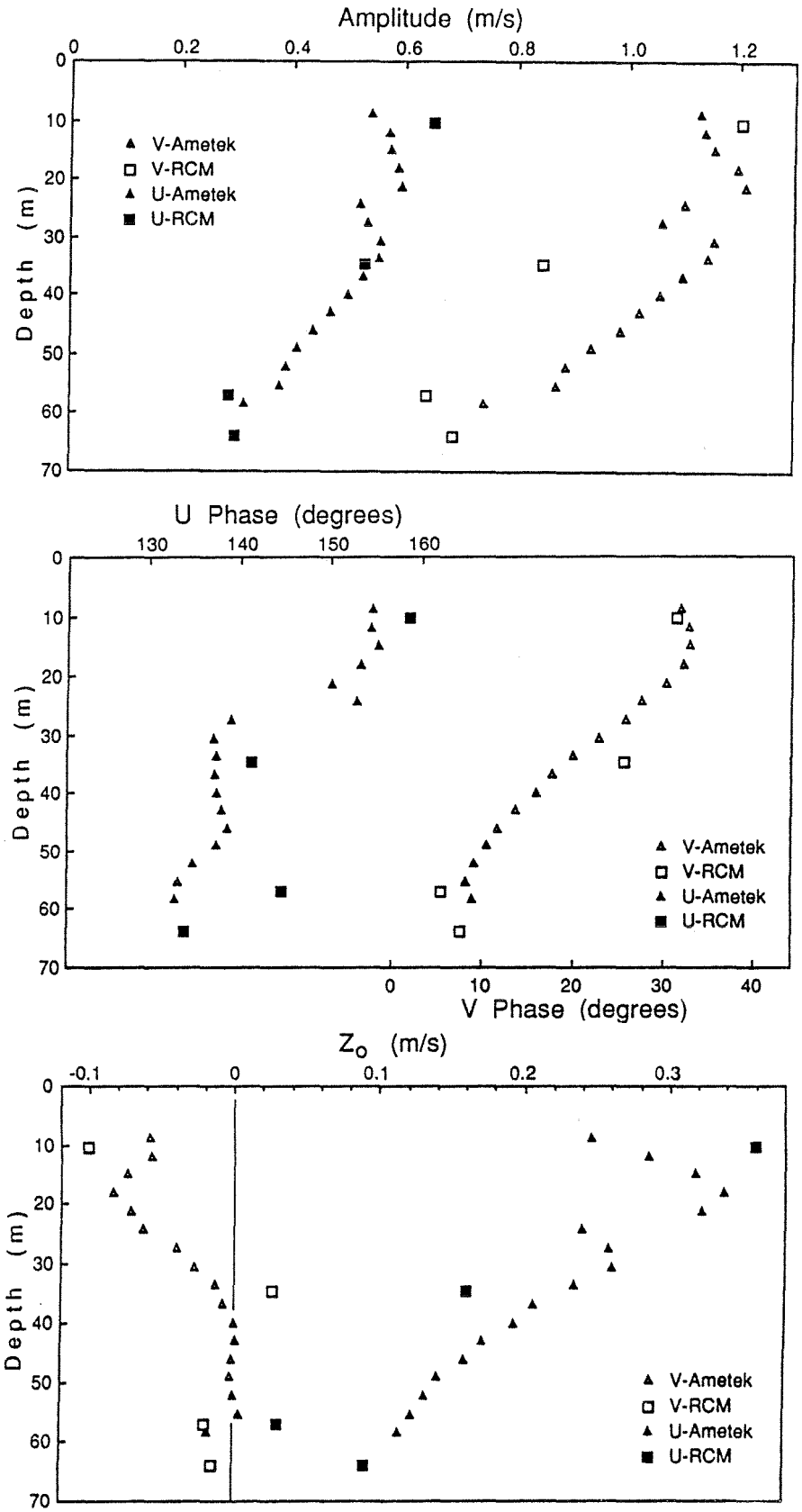

Figure 19. M_2 amplitudes and phases, and constant terms (Z_0's) for the RCM and Ametek velocity components during anchor station 891B.

levels significantly reduced relative to those from the Ametek. There is increased vertical structure in the Ametek amplitudes between 20 and 30 m, as well as in the u-component's phase and constant term (Z_0); since the pycnocline was approximately at this level, this structure may signify an internal tide contribution. The differences between RCM and Ametek phase are generally well within the sampling interval, with the exception of the u-component at 57 m which has a phase difference corresponding to 20 minutes. There is qualitative agreement between the different estimates of residual current, with the exception of the 57-m level where the RCM estimate for the u-component is low. A noteworthy feature of the Ametek data is a 30% decrease in the residual-current estimates and a 10% decrease in the M_2 amplitude in the near-surface region.

The rate and direction scatterplots for the three stations (combined) at mooring 891 are shown in Figure 20, with the corresponding regression results in Tables 6 and 7. (Wind speeds were less than 8 kts and in the range 8-15 kts at stations 891A and 891C respectively, and seas/swells were light.) There is again substantial similarity to the results for site 3 (e.g. Fig. 12, Tables 4 and 5), with the direction in good agreement, the rates in best agreement at the 12-m level, and the RCM rates at mid-depth and 57 m low compared to the Ametek estimates, particularly for Ametek rates above 0.8 m/s at 35 m.

MOORING 919

The final anchor station at site 2 was near mooring 919 which used vector-averaging RCMs with a 2-5 min recording interval (Table 2). The ship was anchored from 0500 UTC on 4 October to 0028 UTC on 6 October, including an interval (approximately 1430 UTC on 4 Oct to 1918 UTC on 5 Oct) when deck operations were suspended due to weather conditions. Since the Ametek was operated in Profiling mode (without bottom tracking) during the first 11 hours of this period, the anchor station is taken to start at 1600 UTC on the 4th (Table 3). Wind speeds were in excess of 25 knots up to about 1200 UTC on the 5th, and seas/swells (per ship's bridge log) were moderate to heavy throughout.

The tidal analysis results for this station are displayed in Figure 21. The Ametek profiles indicate reduced vertical structure in M_2-amplitude, phase and residual current compared to the mooring 891 stations. The RCM amplitude at mid-depth shows improved agreement with the Ametek estimate, while the 57-m RCM amplitude remains relatively low (the 12-m RCM did not return usable data). The phases are in good (within 15 min) agreement, and the residual currents show some qualitative similarity but substantial quantitative differences.

The rate and direction scatterplots for this station are shown in Figure 22, and the regression results in Tables 6 and 7. Increased direction scatter about the 1:1 line is apparent, although there still is generally good agreement. Rate at mid-depth differs from that at the other moorings at sites 2 and 3, here centered near the 1:1 line but with increased scatter. This may be a manifestation of increased random variability in either the RCM or Ametek measurements during storm conditions, or of a reduced systematic difference between the RCM and

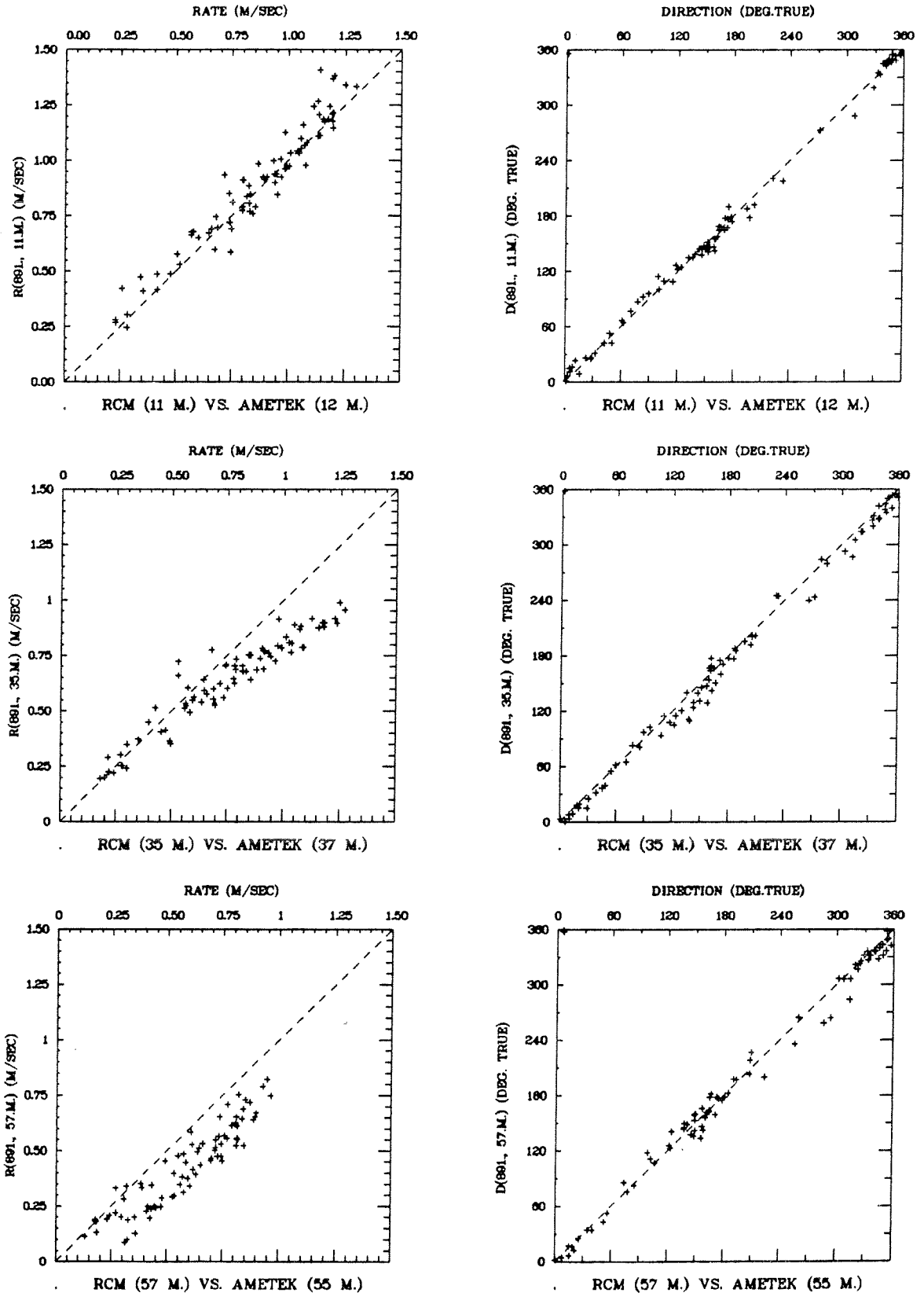

Figure 20. Rate and direction scatterplots for RCM (ordinate) versus Ametek (abscissa) data at three vertical levels during the three anchor stations at mooring 891.

Table 6. Summary of linear regression results for RATE at Bank sites 2, 4 and 6. Results are presented for the mooring 891 anchor stations combined (891A+B+C), station 919A, the mooring 895 stations during cruise 88023 (895A+B), and stations 895C and 897. The intercept (a_o), slope (a_1), their standard errors (s_o, s_1), the residual standard deviation (SD) between the observations and regression model predictions, the squared correlation coefficient (r^2) and the number of observations (N) are given. The f ratio, high values of which indicate that a higher-degree regression polynomial is appropriate (BMDP 1983), is also given.

Depth Station	Dep/Ind Variable	$a_o \pm s_o$ (m/s)	$a_1 \pm s_1$	SD (m/s)	r^2	N	f Ratio
10-12 m							
891A+B+C	RCM11/AM12	.04 ±.03	.99 ±.03	.08	.93	81	4.3
895A+B	RCM11/AM12	.08 ±.02	.89 ±.02	.03	.97	83	2.2
895C	RCM11/AM12	.25 ±.05	.66 ±.06	.05	.78	32	.5
897A	RCM10/AM12	-.07 ±.08	1.14 ±.12	.08	.85	18	.6
34-43 m							
891A+B+C	RCM35/AM37	.13 ±.02	.67 ±.02	.06	.91	82	9.0
919A	RCM34/AM34	-.03 ±.04	.99 ±.09	.12	.64	65	2.1
895A+B	RCM34/AM34	.22 ±.01	.54 ±.02	.03	.92	83	5.4
895C	RCM34/AM34	.17 ±.03	.65 ±.04	.03	.88	32	.3
897A	RCM41/AM43	-.00 ±.07	.99 ±.12	.07	.81	18	.6
52-73 m							
891A+B+C	RCM57/AM55	-.03 ±.02	.78 ±.04	.07	.85	82	10.8
919A	RCM56/AM52	.20 ±.03	.24 ±.07	.08	.18	65	4.4
895A+B	RCM53/AM52	.10 ±.02	.64 ±.03	.04	.82	83	37.4
895C	RCM53/AM52	.10 ±.03	.68 ±.05	.03	.86	32	.6
897A	RCM73/AM68	.08 ±.03	.51 ±.05	.03	.85	18	.02

Table 7. Summary of linear regression results for DIRECTION at Bank sites 2, 4 and 6. Results are presented for the mooring 891 anchor stations combined (891A+B+C), station 919A, the mooring 895 stations during cruise 88023 (895A+B), and stations 895C and 897. The intercept (a_o), slope (a_1), their standard errors (s_o, s_1), the residual standard deviation (SD) between the observations and regression model predictions, the squared correlation coefficient (r^2) and the number of observations (N) are given.

Depth Station	Dep/Ind Variable	$a_o \pm s_o$ (°)	$a_1 \pm s_1$	SD (°)	r^2	N
10-12 m						
891A+B+C	RCM11/AM12	0.7 ±1.4	.993 ±.007	7.1	.996	81
895A+B	RCM11/AM12	-5.1 ±0.9	.993 ±.004	3.9	.998	83
895C	RCM11/AM12	-6.2 ±2.0	1.003 ±.010	4.7	.997	32
897A	RCM10/AM12	-4.3 ±1.8	.999 ±.009	3.6	.999	18
34-43 m						
891A+B+C	RCM35/AM37	-5.1 ±2.0	.994 ±.010	9.6	.993	82
919A	RCM34/AM34	-8.5 ±4.8	1.011 ±.021	17.5	.973	65
895A+B	RCM34/AM34	-0.2 ±1.3	.985 ±.006	5.6	.997	83
895C	RCM34/AM34	0.5 ±2.8	.986 ±.013	6.7	.995	32
897A	RCM41/AM43	-1.7 ±3.5	1.020 ±.020	7.5	.994	18
52-73 m						
891A+B+C	RCM57/AM55	1.8 ±2.2	.977 ±.010	10.1	.992	82
919A	RCM56/AM52	0.3 ±4.8	1.032 ±.021	16.8	.976	65
895A+B	RCM53/AM52	1.8 ±1.3	.991 ±.006	5.4	.997	83
895C	RCM53/AM52	-1.4 ±2.0	1.013 ±.009	4.8	.998	32
897A	RCM73/AM68	11.2 ±3.0	1.003 ±.015	5.8	.996	18

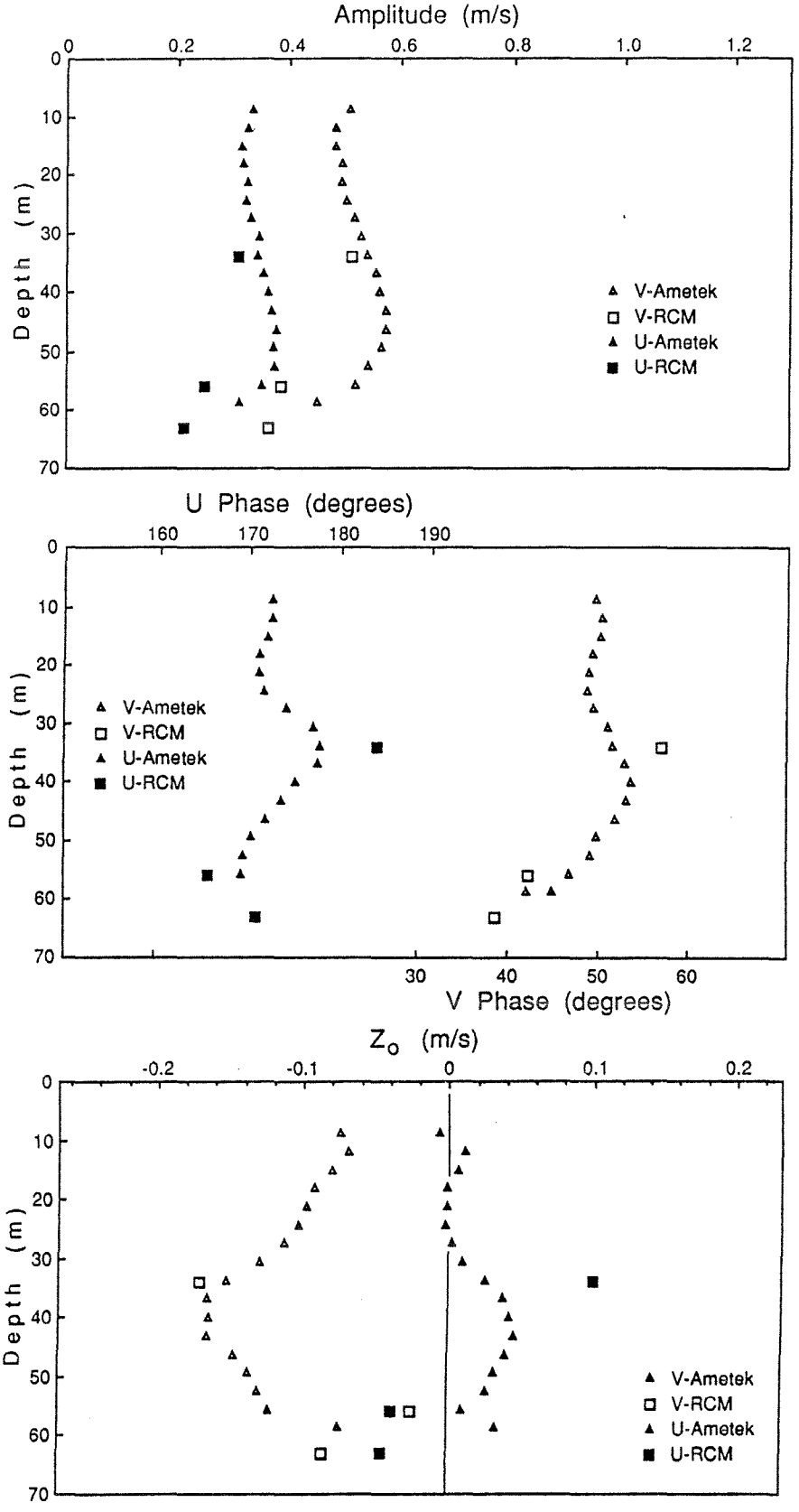

Figure 21. M_2 amplitudes and phases, and constant terms (Z_0's) for the RCM and Ametek velocity components during anchor station 919A.

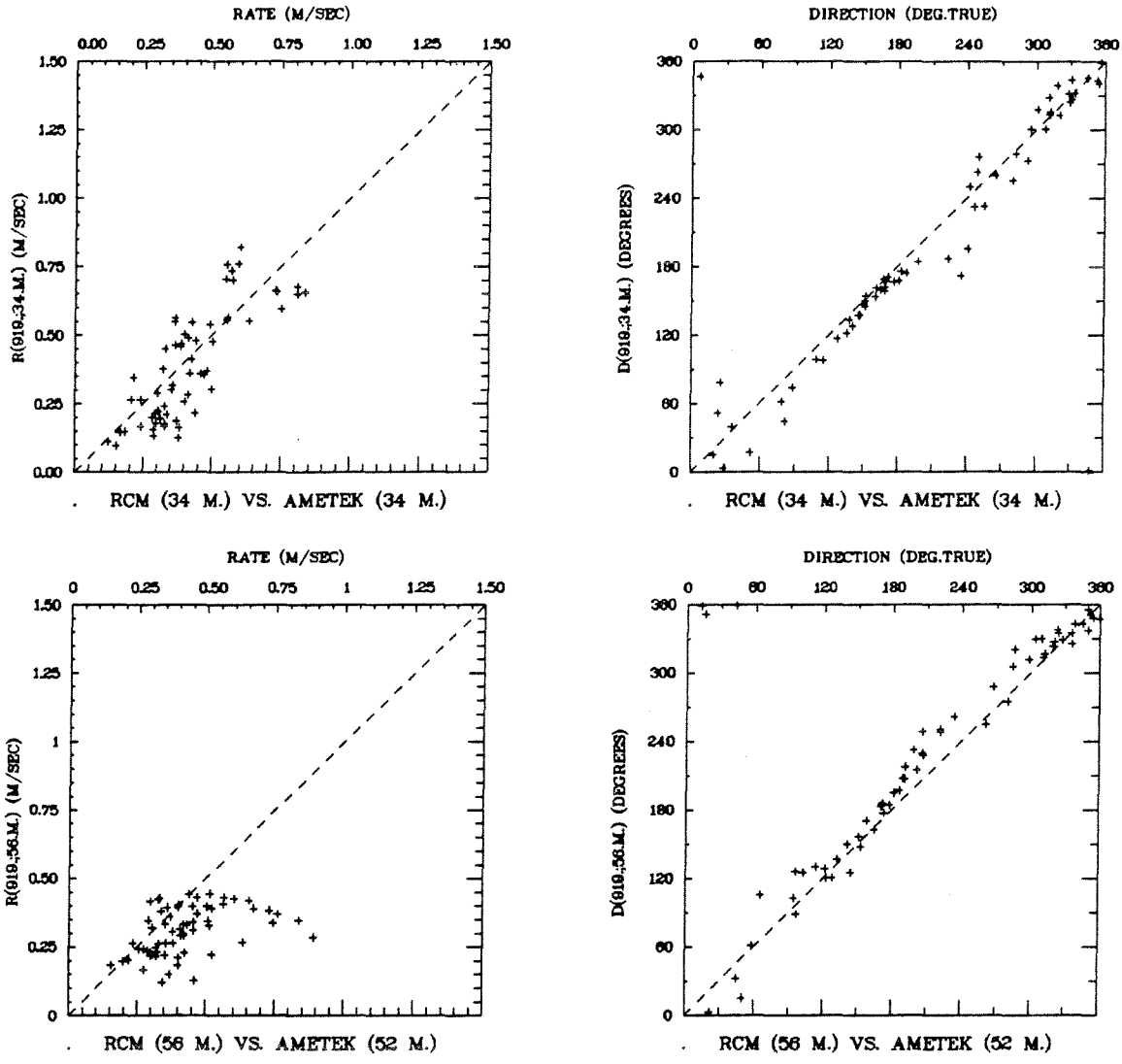

Figure 22. Rate and direction scatterplots for RCM (ordinate) versus Ametek (abscissa) data at two vertical levels during anchor station 919A.

Ametek estimates for weaker currents or when vector-averaging RCMs are used. However, the data are not adequate to draw a firm conclusion. The 56-m rate comparison is also different from that at the other moorings, with a pronounced fall-off in RCM rates at rates above 0.5 m/s and possibly increased scatter.

b. Site 4 (Mooring 895)

The southernmost mooring site on the principal line was occupied by mooring 895 from early in cruise 88023 to late in cruise 88036. The depth at this site was 63 m, and there was little stratification during the cruise surveys with the surface -to-bottom density difference less than 0.3 σ_t units. Two anchor stations (895A,B) were conducted during 88023 and one (895C) during 88036, with wind speeds 15 knots or less throughout and light seas and swell.

The intercomparison results for this site are illustrated by the tidal analysis results for station 895B, shown in Figure 23. Although the vertical structure in the amplitude and phase is reduced (as expected at this site of increased tidal mixing), the differences between the RCM and Ametek estimates show strong similarity to those at sites 2 and 3: relatively-low RCM amplitudes at mid-depth and 10 m above bottom, and good phase agreement. The residual currents show qualitative agreement but again substantial quantitative differences, with the RCM estimates generally low, particularly at 10 m above bottom.

Figure 24 shows the rate and direction scatterplots for the three 895 stations combined, while the regression results are included in Tables 6 and 7. Separate regression results are shown for the 88023 (stations 895A,B) and 88036 (station 895C) data to examine whether there is evidence for reduced RCM rates during the latter part of the mooring period associated with the biological fouling observed on the instrument upon recovery. The scatterplots indicate excellent direction agreement between the RCM and Ametek estimates, but rate differences as at sites 2 and 3: relatively-low RCM rates at mid-depth and 10 m above bottom, particularly for rates exceeding 0.6 m/s at mid-depth. In addition, there is also a suggestion of relatively-low RCM rates for high rates at the upper level. The regression results confirm these variations, and also suggest an increased deviation between the upper-level RCM and the Ametek during the last cruise, indicating a possible significant biological fouling of this instrument's rate measurement.

c. Site 6 (Mooring 897)

The final "Bank" site was site 6 where mooring 897 was deployed during cruise 88023. The nearly-uniform depth at this site was about 83 m, and there was limited stratification (surface-to-bottom density difference up to 1.0 σ_t units). Winds, seas and swell were light during the single anchor station (897A) at this site.

The scatterplots (Fig. 25) and regression results (Tables 6, 7) for this station show improved agreement at mid-depth (compared to the other Bank sites), but a similar discrepancy at the lower level. The directions are again in good agreement with the exception of a 10° offset at the lower level, and there is also a suggestion of relatively-high RCM

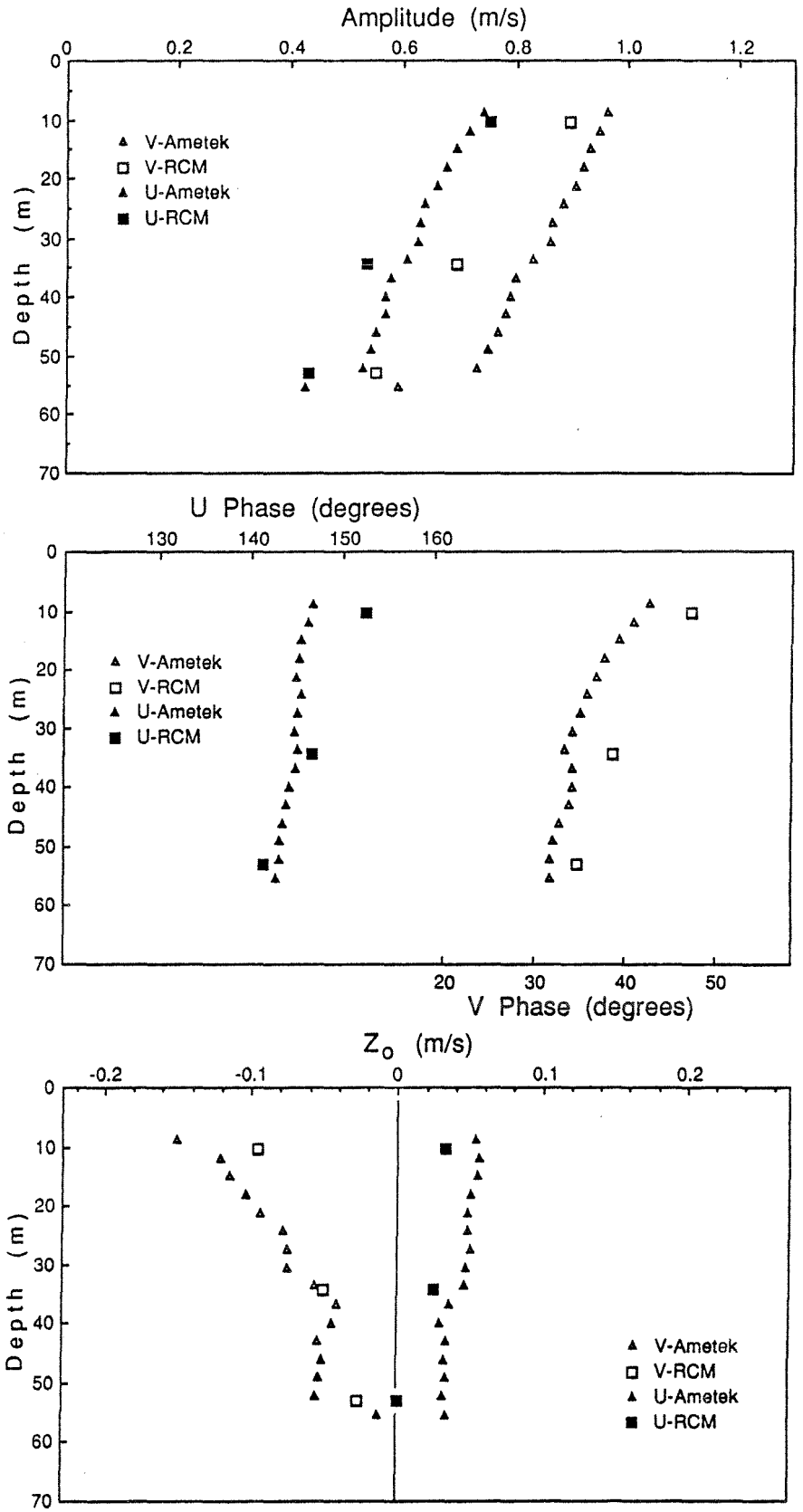

Figure 23. M_2 amplitudes and phases, and constant terms (Z_0's) for the RCM and Ametek velocity components during anchor station 895B.

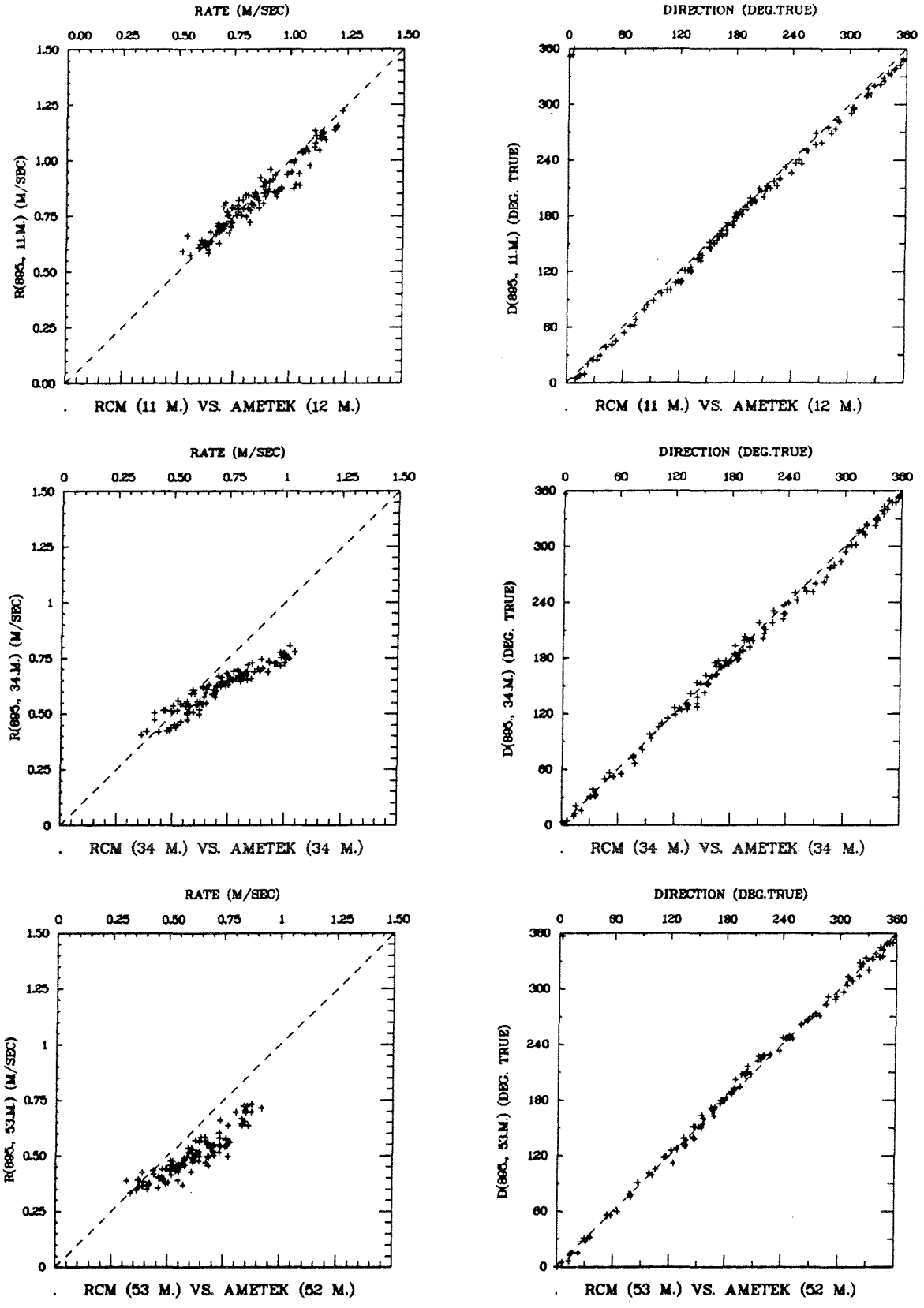

Figure 24. Rate and direction scatterplots for RCM (ordinate) versus Ametek (abscissa) data at three vertical levels during the three anchor stations at mooring 895.

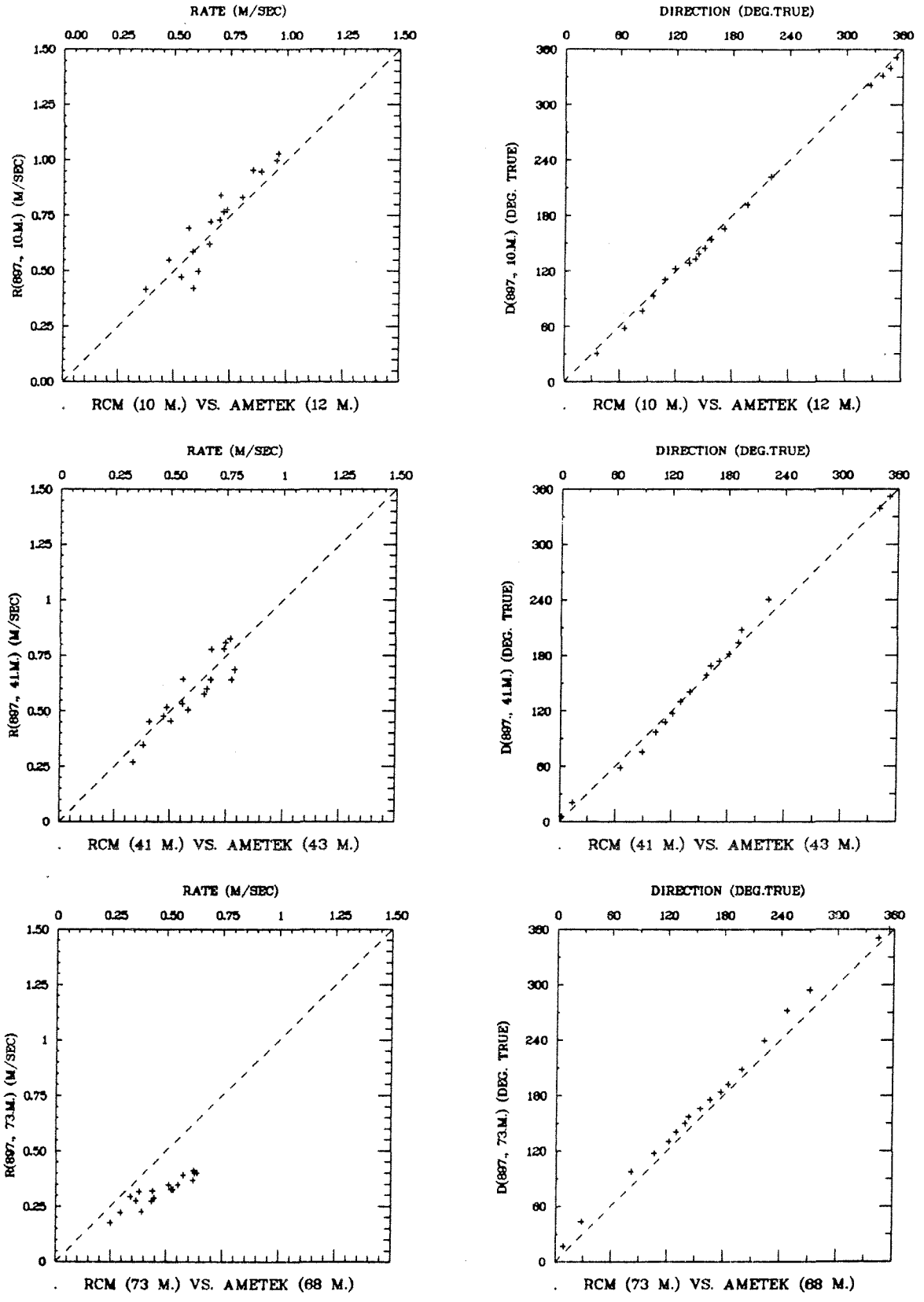

Figure 25. Rate and direction scatterplots for RCM (ordinate) versus Ametek (abscissa) data at three vertical levels during anchor station 897A.

rates at the upper level.

d. Bank-Edge Sites (Moorings 889 and 896)

The other two mooring sites (#'s 1,5) were located near the 150-m isobath on the edge of the Bank, where large cross-Bank gradients in depth, tidal current (e.g. Greenberg 1983) and residual current (e.g. Loder and Wright 1985) are expected. Two short anchor stations (889A,B) during cruise 88023 and one (889C) during 88036 were conducted at site 1, and one station (896A) at site 5. The ship was anchored in shallower water than the moorings (Tables 1,3), so that the resulting RCM and Ametek data are expected to be less suitable for a quantitative intercomparison.

Rate and direction scatterplots (not shown) for these moorings show more scatter than those for the Bank sites, although the points are generally centered near the 1:1 lines. In particular, the direction plots and regressions (Table 9) indicate that the direction estimates were generally within about 20°, while the rate scatterplots (not shown) and regressions (Table 8) show more variation with depth and station (than at the other sites).

For site 1, the rate regressions for stations 889A+B indicate approximate agreement between the RCM and Ametek estimates for the upper two levels during cruise 88023, but not for the 90-m level. In contrast, the regressions for the upper two levels in station 889C indicate poor agreement, with the regression line for the upper level being particularly different from that in stations 889A+B. The station 896A regressions show some similarities and some differences from those for station 889A+B: here the upper-level regression is poor (contrasting that at 889A+B), the lower-level regression is poor (like that at 889A+B), the 39-m regression is good, and the 71-m comparison is in intermediate agreement. It is not clear whether these discrepancies are associated with real spatial gradients in the flow, instumental problems, or biological fouling of the RCMs (in the case of 889C). Considering the quantity and quality (from an intercomparison point of view) of the data, it is also not clear that there is a degradation in any of the velocity estimates.

5. Comparison with Predicted Tidal Currents

Predictions of the barotropic component of the M_2 tidal current on Georges Bank are available from Greenberg's (1979, 1983) numerical models. Here we present a quick comparison (Table 10) between the predictions of Greenberg's (1983) model with 7-km grid resolution, and vertical averages of the observed current amplitudes and phases for selected periods at each of the mooring sites. The model predictions for these sites are obtained through a spatial interpolation scheme following that in the model solution, and rotation of the resulting tidal current variables from Greenberg's co-ordinate system to the east-north system used here. Estimates of the predicted amplitudes upon adjustment for the differing water depths between the model and observations are also presented.

The vertically-averaged observed results are obtained from unweighted averaging of the amplitudes and phases at vertical levels

Table 8. Summary of linear regression results for RATE at Bank-edge sites 1 and 5. Results are presented for the mooring 889 stations during cruise 88023 (889A+B), the mooring 889 station during cruise 88036 (889C) and station 896A. The intercept (a_o), slope (a_1), their standard errors (s_o, s_1), the residual standard deviation (SD) between the observations and regression model predictions, the squared correlation coefficient (r^2) and the number of observations (N) are given.

Depth Station	Dep/Ind Variable	$a_o \pm s_o$ (m/s)	$a_1 \pm s_1$	SD (m/s)	r^2	N
10-21 m						
889A+B	RCM21/AM21	-.02 ±.05	1.04 ±.07	.13	.86	35
889C	RCM21/AM21	.24 ±.09	.52 ±.16	.12	.32	24
896A	RCM10/AM12	.24 ±.10	.51 ±.14	.18	.46	17
39-43 m						
889A+B	RCM43/AM43	.15 ±.05	.88 ±.08	.11	.79	35
889C	RCM43/AM43	.19 ±.10	.77 ±.25	.14	.34	21
896A	RCM39/AM40	.08 ±.03	1.14 ±.05	.07	.95	25
71 m						
896A	RCM71/AM71	.12 ±.04	.83 ±.07	.08	.85	25
89-102 m						
889A+B	RCM90/AM89	.22 ±.05	.50 ±.09	.11	.46	35
896A	RCM102/AM89	.14 ±.06	.57 ±.11	.10	.53	25

Table 9. Summary of linear regression results for DIRECTION at Bank-edge sites 1 and 5. Results are presented for the mooring 889 stations during cruise 88023 (889A+B), the mooring 889 station during cruise 88036 (889C) and station 896A. The intercept (a_o), slope (a_1), their standard errors (s_o, s_1), the residual standard deviation (SD) between the observations and regression model predictions, the squared correlation coefficient (r^2) and the number of observations (N) are given.

Depth Station	Dep/Ind Variable	$a_o \pm s_o$ (°)	$a_1 \pm s_1$	SD (°)	r^2	N
10-21 m						
889A+B	RCM21/AM21	-27.5 ±4.3	1.024 ±.031	14.8	.971	35
889C	RCM21/AM21	10.6 ±6.6	1.006 ±.031	15.8	.979	24
896A	RCM10/AM12	-9.7 ±2.5	.970 ±.014	6.6	.996	25
39-43 m						
889A+B	RCM43/AM43	-6.1 ±3.4	1.006 ±.020	11.6	.987	35
889C	RCM43/AM43	-28.4 ±16.0	.933 ±.085	37.8	.863	21
896A	RCM39/AM40	-9.7 ±3.3	1.009 ±.016	7.4	.994	25
71 m						
896A	RCM71/AM71	-13.9 ±4.2	1.008 ±.020	10.2	.991	25
89-102 m						
889A+B	RCM90/AM89	-1.2 ±3.7	.971 ±.021	13.3	.984	35
896A	RCM102/AM89	11.5 ±6.1	.919 ±.028	16.9	.979	25

Table 10 Observed and predicted amplitudes and phases of the east (u) and north (v) components of the M_2 constituent of tidal current at the six mooring sites. The observed values are depth-averages of the amplitude and phase values computed for the indicated vertical levels from moored current measurements over the indicated period. The predicted values are from Greenberg's (1983) barotropic numerical model for the M_2 tide. The parenthesized predicted values are obtained by scaling the model predicted amplitudes to the observed depth at the site, assuming inverse proportionality between amplitude and depth. Phase lags are relative to the astronomical forcing at Greenwich. The 29-day analyses resolve the M_2, N_2 and S_2 constituents, while the other analyses infer the latter two constituents from the astronomical potential ratios.

Mooring No.	**Depth(m)**		**u-amp(m/s)**		**u-ph(°)**		**v-amp(m/s)**		**v-ph(°)**	
Period	**Obs**	**Pred**	**Obs**	**Pred**	**Obs**	**Pred**	**Obs**	**Pred**	**Obs**	**Pred**
Site 1:										
889(20+43+90+145m)	155	173	.43	.39	170	169	.36	.38	025	020
26/6-25/7 (29-dy)				(.44)				(.43)		
except 26/6-11/7 for 90m										
Site 2:										
912 (11+35+57m)	67	77	.45	.49	154	147	.69	.74	023	021
11/7-9/8 (29-dy)				(.56)				(.85)		
Site 3:										
920(12+34+56m)	68	63	.53	.55	143	139	.80	.80	025	023
2/6-1/7 (29-dy)				(.52)				(.76)		
Site 4:										
895(11+34+53m)	63	65	.54	.55	139	140	.67	.75	033	025
27/6-26/7 (29-dy)				(.56)				(.77)		
Site 5:										
896(39+71+102+138m)	148	145	.46	.50	159	169	.44	.46	007	027
27/6-9/7 (12-dy)				(.49)				(.45)		
Site 6:										
897(10+41+73m)	83	83	.44	.54	142	148	.59	.72	025	030
27/6-9/7 (12-dy)										

(Table 10) chosen to give as close to uniform vertical representation as is possible with the returned data. Observed results are presented for a single 29-day period at each site, except for sites 5 and 6 where only 12-day records are available. The observed amplitudes and phases for other periods generally differ from those presented here by less than 10% and 5°, respectively, except for site 1 where there are substantially larger variations at some depths. These variations are probably associated with variable baroclinic tidal currents and/or different analysis period lengths. The RDI observations (mooring 920) are used at site 3, and the RCM observations at the other sites.

The comparison indicates that the M_2 tidal currents inferred from the moored measurements during the 1988 study are generally in good agreement with the predictions of Greenberg's (1983) model, but there are quantitative differences. The observed and predicted phases have similar spatial structure, and are generally within 10°. There are slightly larger phase differences at one of the Bank-edge sites (#5) where the vertical resolution is reduced and baroclinic tides are expected to be largest (e.g. Marsden 1986). There are amplitude differences of up to about 20%, which are not significantly reduced when the the model predictions are adjusted for the depth differences. In 5 of 6 cases for RCM measurements at the Bank sites (#'s 2,4,6), the observed amplitudes are more than 0.1 m/s less than the adjusted model predictions, consistent with the RCM/Ametek intercomparison results which indicate that the RCMs underestimate rate. (Note that the apparent RCM underestimation at mid-depth and 10 m above bottom is partly cancelled by the apparent RCM overestimation at the upper level at some sites, due to the vertical averaging in the present comparison.) The amplitudes for the RDI measurements at site 3 are slightly high, but the differences are less than those within the observed amplitudes for different 29-day periods. The Bank-edge amplitudes show as good agreement as could be expected considering the expected complicated structure of the tidal current at those sites.

In short, the comparison with model predictions is consistent with the earlier suggestions that: the RCM estimates of direction are good, but of rate are degraded (in some cases); and the RDI estimates of the time-varying (both amplitude and phase) component of flow are good over most of the water column (but possibly slightly degraded above 20 m).

6. Discrepancies and Possible Explanations

a. RCM Rates

The intercomparison with the Ametek, RDI and S4 velocity estimates (e.g. Tables 4 and 6), and the comparison with model predictions (Table 10) point to significant degradation of the RCM rate measurements at some levels. To further examine the dependence of this degradation on flow rate and direction and on position, Tables 11 and 12 present statistics of the ratio of RCM rate to Ametek/S4 rate for various ranges of Ametek/S4 rate and direction for the Bank moorings.

For the upper level, it can be seen that the mean value of the rate ratio is generally within a standard deviation of 1 for all ranges of rate and direction, except for mooring 955 where the RCM rates are 3-9% higher than the S4 rates. There is also an overall tendency (35 out of

Table 11. Statistical summary of ratio of RCM rate to Ametek/S4 rate for various ranges of Ametek/S4 rate, for Bank sites. SD refers to standard deviation and N to number of observations. Also shown are the statistics for the ratio of RDI rate to RCM rate at 12 m for the 15-day intercomparison.

Depth	Variables	0-0.4 m/s			0.4-0.8 m/s			0.8-1.2 m/s			1.2-1.6 m/s		
Station		Mean	SD	N	Mean	SD	N	Mean	SD	N	Mean	SD	N
10-14 m													
891A+B+C	RCM11/AM12	1.22	.24	7	1.06	.12	23	1.02	.07	48	1.09	.06	3
893A+B+C	RCM12/AM12	1.30	-	1	1.06	.08	31	1.06	.09	42	1.01	.04	12
895A+B	RCM11/AM12	-	-	0	1.02	.04	35	.97	.03	45	.97	.02	3
895C	RCM11/AM12	-	-	0	1.01	.09	13	.94	.07	19	-	-	0
897A	RCM10/AM12	1.12	-	1	1.02	.15	12	1.07	.03	5	-	-	0
955	RCM13/S4-14	1.03	.09	271	1.06	.05	2106	1.08	.03	1603	1.09	.02	406
920/893	RDI12/RCM12	1.04	.14	10	.93	.08	306	.90	.06	308	.87	.03	147
34-43 m													
891A+B+C	RCM35/AM37	1.04	.15	12	.91	.15	33	.81	.05	33	.76	.03	4
919A	RCM34/AM34	.85	.34	35	.99	.25	27	.81	.03	3	-	-	0
893A+B+C	RCM34/AM34	1.08	.22	7	.94	.10	37	.82	.05	40	.77	.03	2
913A	RCM34/AM34	1.03	.01	2	.90	.10	17	.85	.03	9	-	-	0
895A+B	RCM34/AM34	1.11	.02	2	.89	.06	48	.78	.03	33	-	-	0
895C	RCM34/AM34	-	-	0	.96	.09	28	.84	.02	4	-	-	0
897A	RCM41/AM43	.86	.07	2	.99	.11	16	-	-	0	-	-	0
56-73 m													
891A+B+C	RCM57/AM55	.79	.27	19	.69	.12	44	.77	.08	19	-	-	0
919A	RCM56/AM52	.89	.25	31	.68	.17	32	.37	.07	2	-	-	0
893A+B+C	RCM57/AM55	.93	.19	13	.74	.14	62	.77	.04	11	-	-	0
895A+B	RCM53/AM52	1.13	.08	3	.79	.07	66	.81	.04	14	-	-	0
895C	RCM53/AM52	.98	.04	6	.85	.06	26	-	-	0	-	-	0
897A	RCM73/AM68	.75	.10	6	.65	.04	12	-	-	0	-	-	0

Table 12. Statistical summary of ratio of RCM rate to Ametek/S4 rate for four quadrants of Ametek/S4 direction, for Bank sites. SD refers to standard deviation and N to number of observations. Also shown are the statistics for the ratio of RDI rate to RCM rate for the 15-day intercomparison.

Depth	Variables	315°-045°			045°-135°			135°-225°			225°-315°		
Station		Mean	SD	N	Mean	SD	N	Mean	SD	N	Mean	SD	N
10-14 m													
891A+B+C	RCM11/AM12	1.01	.14	30	1.07	.09	16	1.06	.09	32	1.26	.11	3
893A+B+C	RCM12/AM12	1.07	.11	28	1.03	.06	13	1.05	.06	31	1.05	.11	14
895A+B	RCM11/AM12	1.01	.04	21	.98	.04	16	.97	.03	32	1.03	.04	14
895C	RCM11/AM12	1.01	.07	6	.92	.02	5	.95	.08	14	1.01	.11	7
897A	RCM10/AM12	1.01	.09	5	.99	.19	6	1.10	.07	7	-	-	0
955	RCM13/S4-14	1.06	.05	1247	1.06	.04	868	1.07	.04	1577	1.05	.07	694
920/893	RDI12/RCM12	.96	.06	226	.89	.06	160	.86	.04	265	.95	.09	120
34-43 m													
891A+B+C	RCM35/AM37	.83	.07	29	.92	.16	15	.89	.17	29	.94	.13	9
919A	RCM34/AM34	.83	.18	18	1.09	.43	7	1.11	.24	23	.63	.16	17
893A+B+C	RCM34/AM34	.86	.08	32	.94	.11	13	.88	.12	28	.95	.19	13
913A	RCM34/AM34	.93	.05	6	.80	.05	7	.89	.09	11	1.01	.05	4
895A+B	RCM34/AM34	.86	.03	22	.86	.08	15	.83	.10	32	.90	.10	14
895C	RCM34/AM34	.91	.03	7	.91	.03	6	.94	.12	12	1.01	.09	7
897A	RCM41/AM43	.90	.03	4	.95	.10	6	1.04	.12	8	-	-	0
56-73 m													
891A+B+C	RCM57/AM55	.69	.14	31	.56	.13	11	.77	.11	32	.99	.14	8
919A	RCM56/AM52	.90	.17	18	.64	.25	13	.63	.18	22	.97	.22	12
893A+B+C	RCM57/AM55	.72	.12	32	.74	.11	12	.77	.17	28	.90	.15	14
895A+B	RCM53/AM52	.81	.05	21	.83	.07	12	.78	.08	34	.86	.13	16
895C	RCM53/AM52	.86	.09	8	.92	.08	5	.85	.06	13	.89	.11	6
897A	RCM73/AM68	.68	.06	4	.71	.04	4	.62	.03	8	.85	.02	2

43 cases) for the ratio to be greater than one, such as for mooring 893 where the earlier tidal analyses (e.g. Fig. 8) indicated relatively-high RCM rates at this level. Note that the ratios for station 895C are not as suggestive of degradation as were the regression results (Table 6); apparently, the distribution of the data set over a limited rate range can lead to less-than-robust regression results.

The ratios at the mid-depth level generally show a consistent decrease with increasing rate, from values near 1 at low rates, to values near 0.8 at rates exceeding 0.8 m/s. In particular, there is remarkable consistency across moorings in the mean ratios for the latter rate ranges. No consistent dependence on direction is apparent for the mid-depth ratios.

The rate ratios at 10 m above bottom show more scatter with mooring than at the other levels, and are less than 1 for all rate and direction ranges except one. Part of this low bias may be associated with the Ametek bin generally being several metres above the RCM, but (as discussed below) this is not the dominant effect. There is some hint that the ratio is closer to 1 at low speeds and for westward flow, but there are exceptions.

Considering these results and the apparently good agreement (Figs. 13-15) between the RCM measurements at 3 m above bottom and the RDI data, there is a clear pattern of increased differences between the RCM and acoustic estimates of rate for positions away from the ends of the RCM mooring, i.e. the discrepancy appears to have an antinode (or antinodes) near the middle of the mooring and nodes at the top and bottom. In addition, there is a suggestion of increased differences at higher rates, although this is less clear at 10 m above bottom than at mid-depth. We now briefly discuss possible sources for these discrepancies.

i) Degradation of the Acoustic Measurements. The agreement between the RDI and Ametek velocities in the interior of the water column (where they should be most reliable), the consistency of their (interior) vertical structure with expectations, the unexplainable decrease of the RCM rates from 3 to 10 m above bottom, and the rate dependence of the difference between the RCM and acoustic rate measurements (more likely for a mechanical measurement than an acoustic one?) strongly indicate than the the RCM/acoustic rate discrepancies at mid-depth and 10 m above bottom arise primarily from the RCM measurement. However, as discussed in the next section, there is some degradation of the RDI measurements, particularly in the upper 20 m.

ii) Horizontal Gradients in the Velocity Field. The typical separation of 2 km between the RCM moorings and the anchor station positions raises the possibility that real spatial gradients in velocity contribute to the observed rate discrepancies. Since the discrepancies occur for the tidal velocity, the magnitude of this contribution can be estimated from the M_2 tidal currents computed from the RCM measurements at the various sites. Using the mid-depth measurements from moorings 893 and 897 for east(+x)-west gradients, and the mid-depth measurements from the first 29-day period in each of moorings 895 and 912 for north(+y)-south gradients, the following estimates are obtained: $\Delta U/\Delta x$ = .002 m/s/km, $\Delta U/\Delta y$ = -.001 m/s/km, $\Delta V/\Delta x$ = -.001 m/s/km,

$\Delta V/\Delta y$ = .004 m/s/km, $\Delta\phi_u/\Delta x$ = .1°/km, $\Delta\phi_u/\Delta y$ = .7°/km, $\Delta\phi_v/\Delta x$ = .04°/km and $\Delta\phi_v/\Delta y$ = -.3°/km where U, V, ϕ_u and ϕ_v are the amplitudes and phases of the east and north components. Clearly, for separations of a few km, gradients of this magnitude cannot account for the observed discrepancies. Closer examination (Belliveau and Loder 1990; also §6.b) of the concurrent Ametek and RDI measurements at site 3 suggests, however, that there were larger, but intermittent spatial gradients associated with internal waves. Nevertheless, it seems unlikely that the consistent discrepancies at mid-depth and 10 m above bottom at the four Bank sites reflect real structure in the current regime.

iii) Vertical Excursions of the RCMs. Some reduction of the RCM rates relative to the acoustic estimates is expected from the combination of the tilt of the mooring (and associated downward excursion of the RCMs) and the reduction (expected and generally observed) of current magnitude with depth below the surface. (Note that the acoustic estimates used in the intercomparison were generally for depths corresponding to the RCM positions in the absence of mooring tilt.) However, the small magnitude of the observed pressure variations on the upper RCMs (less than 6 and 10 db for the Bank and Bank-edge moorings, respectively), the small current changes expected and observed over these vertical distances (e.g. Fig. 8), and the different vertical structures of the observed discrepancies and those expected for mooring tilt (similar at the upper and mid-depth levels) suggest that vertical excursions of the RCM is not the major problem. Comparison of the mooring 893 RCM rates with the Ametek rates interpolated to the time-varying vertical positions of the RCMs confirms that this effect is small. In any case, the RCM measurement of smaller currents at 10 m above bottom than at 3 m cannot be explained by this effect.

iv) Tilt of the RCMs. When the tilt of the mooring line substantially exceeds the tilt allowed by the gimbal (29°), degradation of the RCM velocity measurements through jamming of the compass (expected for instrument tilts exceeding 12°) or an altered response of the rotors is of concern. Since the present discrepancy is clearly with rate, compass malfunction cannot be an explanation. Furthermore, the mooring line tilts (up to 29° for mooring 893) predicted by Hamilton's (1989) model are within the gimbal's allowance and largest for the RCMs at 3 m above bottom (where consistency between the RCM and RDI rates was apparent). Thus, it appears that excessive tilt of the RCMs is not the dominant problem.

v) Instantaneous RCM Direction Measurements. Whereas the acoustic measurements involved proper vector averaging over the 10-15 min recording interval, the RCM measurements involved some scalar averaging of rate in combination with instantaneous direction sampling: in the RCM5s, over the 30-min recording interval; in the RCM7/8s, over the 12-36 s sampling interval. The RCM/Ametek rate ratios for the RCM7/8s show improved agreement in some cases, but reduced agreement in others, and more scatter in general. Considering these observations and the expectation that the lack of vector averaging would lead to an overestimation of rate in the presence of high-frequency current fluctuations, there is little reason to expect that the discrepancies are a result of the RCM averaging procedure.

vi) RCM Rate Calibration. Other investigators (Magnell and Signorini 1986; Larouche and Deguise 1989) have recently found that the rates measured by paddle-wheel RCMs are high except at low speeds, and have suggested a calibration problem. The present observations at the upper level are qualitatively consistent with this, although there is variability in the magnitude of the discrepancies in the different experiments. It is unlikely however that a calibration problem could account for the systematic discrepancies at mid-depth and 10 m above bottom.

vii) Misalignment of RCMs. The existence of a semi-cylindrical shield (between 180 and 360° relative to the expected flow direction looking down) around the paddle-wheel rotor on the RCMs raises the possibility that the rotors are shielded if the RCM is not aligned exactly into the current. Other investigators (Woodward et al. 1988; Larouche and Deguise 1989) have suggested that this may occur for weak currents in the presence of high-frequency motion, such as from surface waves. Preliminary field tests (A.J. Hartling, BIO, personal communication, 1989) of the significance of the effect for flow speeds of 0.4-0.8 m/s indicate that rate can be underestimated by up to 19% for 15° (±5°) misalignments, and the rotor can stall for misalignments of 30° (±5°). A possible explanation for the RCM/acoustic rate discrepancies is that, under certain flow conditions, the RCMs away from the ends of the mooring were either intermittently (e.g a high-frequency fluctuation) or persistently (e.g. constantly offset) misaligned from the relative current direction, resulting in shielding of the rotors and underestimation of rate. The resulting rate underestimation should be largely independent of the extent of vector averaging. The major questions are the origin of any such misalignment and the exact magnitude of the associated degradation.

The leading candidate for the origin of RCM misalignment is a vibration of the mooring, or of particular mooring components, for current speeds above some threshold. One possibility is that a half-wavelength mooring vibration (nodes at top and bottom, antinode at mid-depth) was excited by vortex shedding from particular mooring members, similar to that described by Fofonoff (1966). Such a vibration would account for the degradation occurring only at interior positions, but seems unlikely since: (i) the present observations suggest different temporal occurrence of the mid-depth and lower-level degradations; and (ii) the expected natural period (4-9 seconds) for such a vibration should be long enough for the RCMs to remain roughly aligned with the relative water velocity.

A more likely scenario is that vortex shedding from the backup buoyancy packages (Viny floats) positioned near the interior RCMs induced local mooring-line vibrations at the Strouhal frequency (order 1 Hz), to which the RCMs were unable to adequately respond. Loder and Hamilton (1990) present a simple model for the relative water velocity associated with a mooring-line vibration normal to the current and at frequency higher than the vane response frequency. The model indicates two effects: an increase in the average speed relative to the current meter, which should be observed by a "perfect" meter; and, assuming that a paddle-wheel RCM's vane is unable to remain aligned with the fluctuating

relative velocity, a reduction in the average current speed recorded by a paddle-wheel RCM, due to rotor shielding. For a 1-Hz vibration with amplitude 0.1 m, a 1-m/s current, and the rotor shielding influence observed in Hartling's field tests, the model predicts that the second effect dominates, resulting in an average rate reduction comparable to the difference between the observed Ametek and RCM rates. Field tests in which an RCM and buoyancy package were towed behind a vessel at different speeds indicate such a vibration for speeds above 2 m/s, although the RCM remained stable and aligned with the flow (Loder and Hamilton 1990). In the case of the Georges Bank moorings, where many more Viny floats were distributed along a line under much greater tension than in the field tests, it is conceivable that resonances were set up among the various packages, resulting in an enhanced mooring-line vibration and instrument response.

A key prediction of Loder and Hamilton's (1990) simple model is that RCM rate degradation can occur without much increase in scatter in the measured directions. This is because the model assumes that the RCM remains nearly aligned with the absolute current, while the rotor shielding is induced by large direction variations in the relative water velocity. Such a limited increase in scatter for the measured directions is consistent with the Georges Bank observations. The residual standard deviations between the RCM and Ametek direction estimates for the Bank mooring sites (Tables 5, 7) are generally in the $\pm 5\text{-}10^{\circ}$ range, with more scatter at the interior levels than than at the upper level; in 7 of 7 cases, the standard deviation is larger for the mid-depth regression than for the upper-level regression for the same mooring, and in 6 of 7 cases for the regression at 10 m above bottom (than for the upper level).

b. Near-Surface Rates: RCM, RDI and Ametek

The ratios in Tables 11 and 12, and the earlier tidal analysis and statistics results suggest that, at the upper level, the RCM rates are generally high relative to the acoustic estimates and the RDI rates are generally low relative to those of the Ametek and RCM. The tidal analysis results for the RDI data (Figs. 8, 14) and, at times, the Ametek data (Fig. 19) show near-surface reductions in tidal current amplitude, while individual RDI and Ametek profiles (e.g. Figs. 4a, 5a) show that a reduction in near-surface current magnitude occurs intermittently during the tidal period.

To examine the near-surface rates further, we start with the 15-day RCM/RDI data set and show in Figure 26 time series plots of the scalar difference between the RDI and RCM rates at 12 m and the ratio of these rates, for comparison with rate (RCM), direction (RCM) and backscatter intensity (RDI) at this level. The plots show clearly that neither the rate difference nor the ratio is constant, but instead vary considerably over the semidiurnal tidal period with the difference regularly going positive (RDI > RCM) and the ratio correspondingly exceeding 1 (in addition to the dominant occurrence of negative differences and ratios less than 1). The rate and direction show strong semidiurnal variations (as expected), raising the possibility of them influencing the rate discrepancies. The backscatter intensity appears less stationary (statistically) with occasional semidiurnal variations, but also considerable variability at other frequencies including a dominant diurnal variation during days 184 - 190. The timing of this variation is

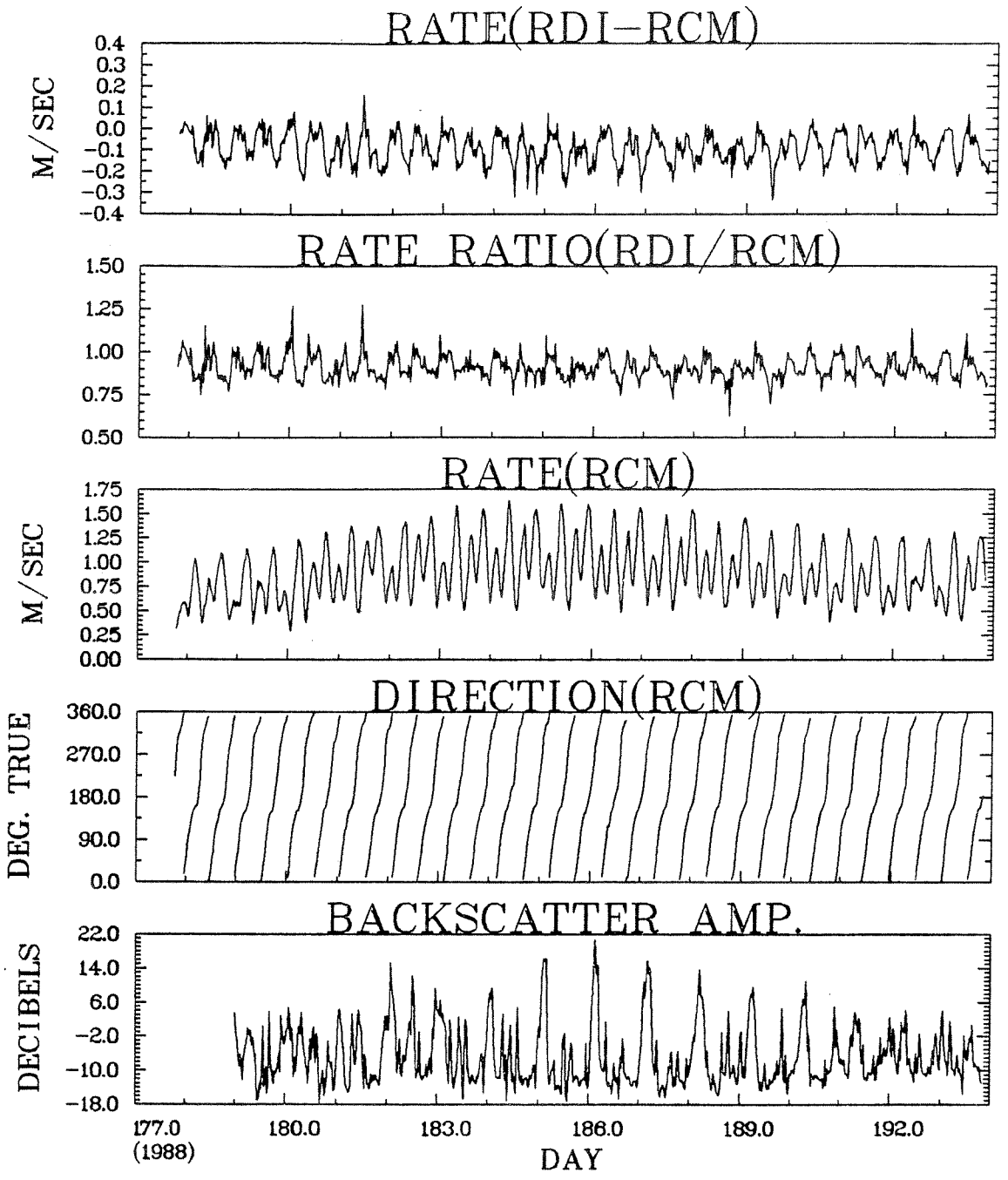

Figure 26. Time series plots of the difference between the RDI and RCM rates, the ratio of RDI rate to RCM rate, the RCM rate and direction, and the RDI backscatter intensity, all at 12 m, during the 15-day intercomparison.

suggestive of a diel vertical migration by zooplankton or larvae, perhaps moving to the surface layer at night.

The relationship among these variables is illustrated in Figure 27, which shows scatterplots of rate difference and ratio versus rate, direction and backscatter intensity. Significant correlations are apparent suggesting that the relatively-low RDI rates (or alternatively, the relatively-high RCM rates) are particularly associated with high current speeds, flow in the southeast quadrant, and low backscatter intensities. The statistics of the RDI/RCM rate ratio for various rate and direction ranges (Tables 11, 12) confirm these suggestions. Similar scatterplots (not shown here but see Belliveau and Loder 1990) indicate strong dependences of rate ratio on vertical shear and of rate and shear on current direction, such that the apparent dependences on rate may actually reflect an influence from shear.

We next examine in more detail the occurrence of near-surface rate discrepancies among the RCM, RDI and Ametek during anchor station 893B. Figure 28 shows time series plots of the rate ratios, Ametek rate and direction, temperature difference between the 12- and 64-m RCMs, and RDI backscatter intensity. The rate ratios again show considerable variability with time (including a possible semidiurnal component), with the variations in the RDI/Ametek and RCM/Ametek ratios having a striking similarity. This similarity raises the possibility of a variation in the Ametek rates being a contributor to the near-surface rate discrepancies. The rate ratio variability also shows some similarity to variations in flow speed and direction, stratification and backscatter. The RCM/Ametek ratios generally fluctuate near 1, except for values closer to 1.2 during northward flow; the RDI/Ametek ratios generally fluctuate near 0.9, except for values around 1.1 during the times of high RCM/Ametek ratio; and the RDI/RCM ratios fluctuate in the range 0.8-1.0.

These observations allow consideration of some candidate explanations:

i) RDI Degradation due to Sidelobe Reflection from a Biological Layer. The occurrence of a strong variation in near-surface backscatter intensity and visual observations (R.I. Perry, DFO St. Andrews, personal communication, 1989) of dense concentrations of amphipods near the surface in the study area lead to the hypothesis that the observed fall-off (e.g. Figs. 7,8) in RDI rate in the upper 20 m arose from sidelobe reflection from a near-surface layer of biological scatterers. However, the observed relationship of the largest rate reductions being associated with relatively-low backscatter intensities discounts this possibility.

ii) RDI Degradation due to Sidelobe Reflection from a Guard Buoy Mooring. After deployment of the RDI, a guard buoy mooring (horizontal scope of 10's of meters expected) was inadvertently placed about 100 m from the RDI position (Fig. 3). Since the relative positions of the guard buoy and the RDI are not exactly known, it is possible that the buoy and its mooring tackle and associated wake were in the path of the acoustic beams (either persistently or for particular flow directions). However, the observed relationship between rate difference and backscatter intensity, and the largest rate discrepancies being associated with southeastward flow (instead of east to northeastward flow which, on the basis of the estimated positions, should place the buoy

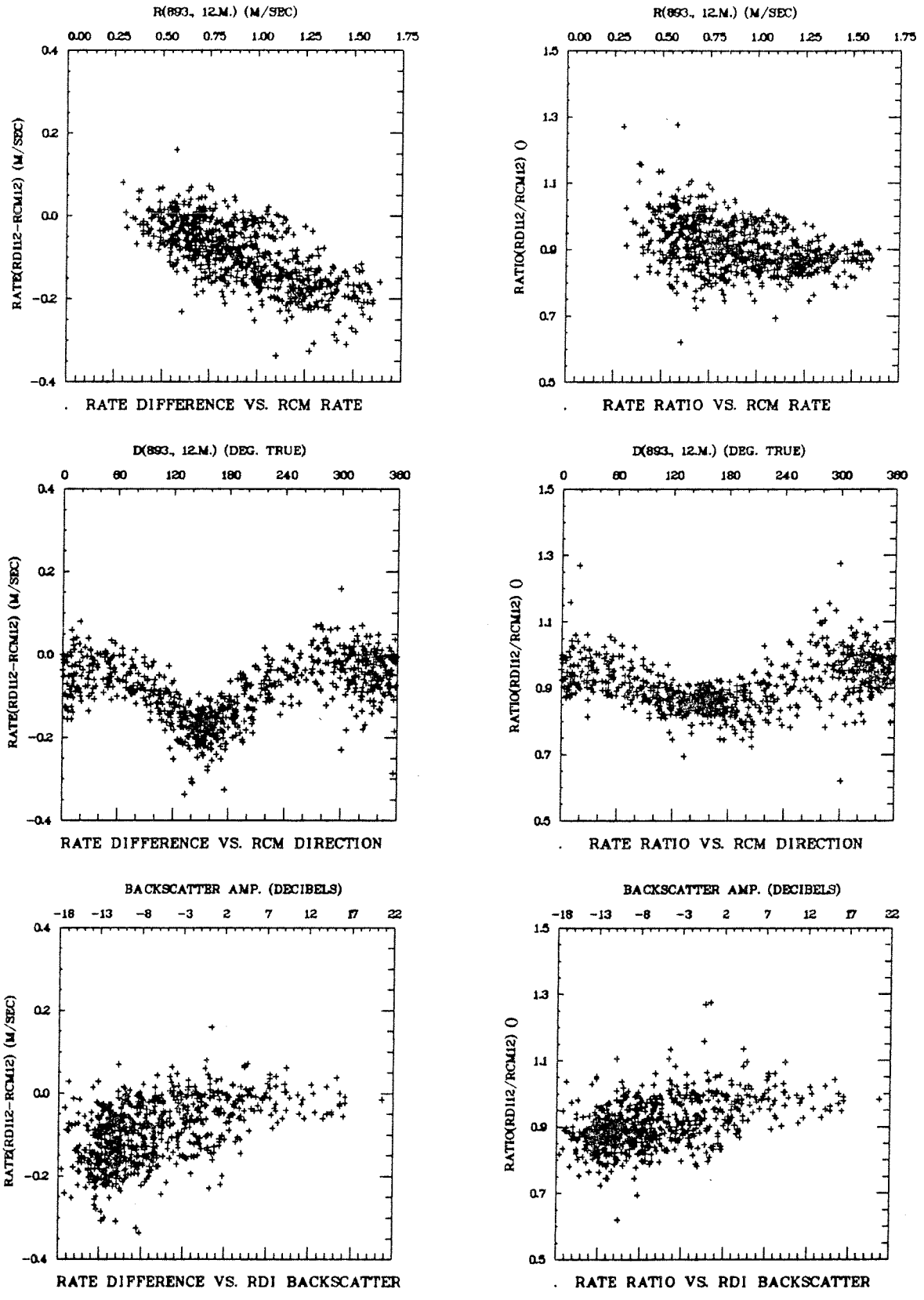

Figure 27. Scatterplots of the difference between RDI and RCM rate, and the ratio of RDI rate to RCM rate, versus RCM rate, RCM direction, and RDI backscatter intensity, all at 12 m, during the 15-day intercomparison.

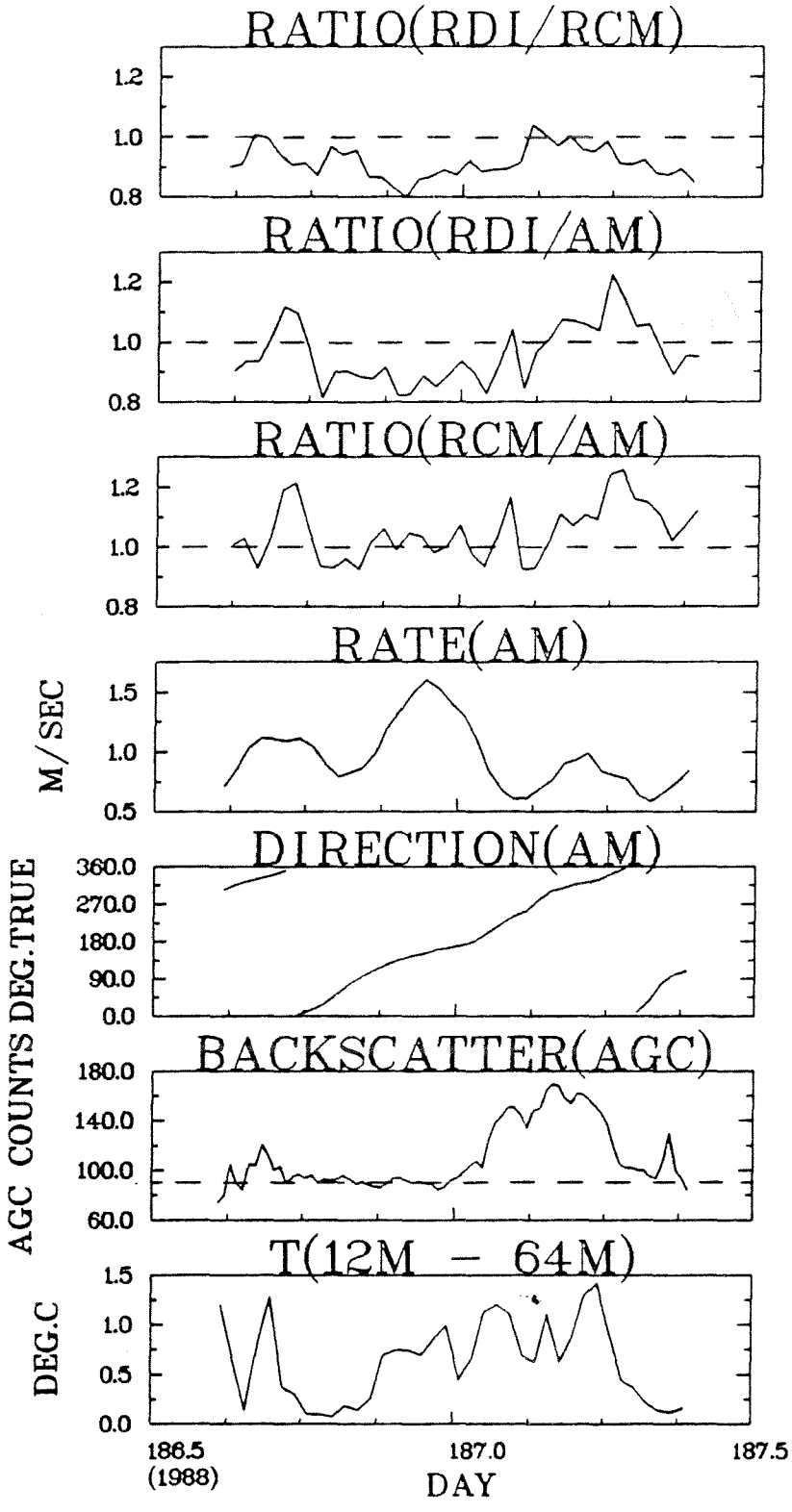

Figure 28. Time series plots of the 12-m rate ratios for RDI/RCM, RDI/Ametek and RCM/Ametek; Ametek rate and direction at 12 m; RDI backscatter intensity (AGC) at 12 m; and RCM temperature difference between 12 and 64 m, for anchor station 893B.

closest to the RDI) suggest that this was not a significant factor.

iii) Internal-Wave Signatures. Comparison of time-depth plots (Belliveau and Loder 1990) of the N-S (Ametek) current component and temperature from hourly CTD profiles during station 893B indicates that the maxima of the ratios involving Ametek rate in Figure 28 were associated with subsurface current maxima of several hours duration, which occurred while the tidal front was being advected through the mooring site. The ratio maxima arose because the near-surface current reduction observed by the Ametek was greater than that observed by the RDI and RCM (2 km away). During the other anchor stations at site 3, there also were near-surface (Ametek) current reductions during periods of stratification, but with less temporal persistence and vertical extent than during 893B. These observations point to real spatial structure in a baroclinic flow feature as a contributing factor to the differences between the Ametek and other measurements. However, since the RDI and RCM were in relatively-close agreement during the periods of near-surface (Ametek) current reduction and were located only 0.5 km apart, it is unlikely that this is the main source of the RDI/RCM discrepancy.

iv) RDI Degradation due to High Shear and Low Backscatter. Chereskin et al. (1989) have shown that the RDI velocity measurements can be biased low when there is high shear and low backscatter intensity. In particular, there can be problems when the automatic gain control (AGC) count, a measure of backscatter intensity, falls below 90. As discussed by Belliveau and Loder (1990), many of the relatively-low RDI rates in Figure 26 occurred during periods of high shear and/or low backscatter, particularly associated with southward flow when the flow speeds were highest. However, neither of these factors alone appears to explain all of the apparent RDI degradation: low RDI/RCM ratios also occurred for low shear and other flow directions, and the ratios for southward flow were always low in spite of high backscatter at times.

There are two effects associated with the AGC passing through the 90-count level which probably contribute to the relatively-low near-surface RDI rates. The first is the shutdown of Doppler tracking, which should cause increased velocity errors as the center frequency of the return signal passes out of the filter's passband or as the signal level drops into the noise floor (Chereskin et al. 1989). With tracking shut down, the expected error for the RDI settings on Georges Bank and the observed shears of order 1 cm/s/m is 6-8 cm/s (J. Gast, RD Instruments, personal communication, 1990). Secondly, RDIs with pre-1989 ROMs reduce the bandwidth of their narrow-band filters by 1/2 at the 90-count level (J. Gast, personal communication, 1990). The latter problem was exacerbated in the Georges Bank deployment by the use of short pulse lengths which led to broad transmit and return spectra. Thus, when the filters' bandwidths were reduced, the return spectrum was modified if the tracker was not centered on the signal. This would happen during times of high shear when the backscatter level was low, consistent with the observations.

In addition, the default settings for the tracking filters in pre-1989 RDI's were unable to track currents in high shears as well as more recent revisions which are specified to track shears up to 1 cm/s/m. Since shears in the range of 1-1.5 cm/s/m were common during the Georges

Bank deployment, particularly for southward flow, poor tracking during periods of high shear is a probable contributor to the relatively-low near-surface RDI rates.

To illustrate the combined influences of shear and backscatter on the RDI measurements, Figure 29 shows the mean value of the 12-m RDI/RCM rate ratio for various ranges of AGC, with the data sorted into observations corresponding to shears greater and less than 1 cm/s/m. The ratio consistently decreases with decreasing AGC count for both high and low shear, with the mean value closest to 1 for low shear and high AGC. Since the various errors resulting from poor Doppler tracking should be greatest for the bins furthest away from the instrument, we conclude that the relatively-low near-surface RDI rates arise from a variable combination of high shear and low backscatter, exacerbated by the use of short pulses.

c. S4 Rates at 37 m

The rate scatterplot (Fig. 18) for the RCM versus S4 on mooring 955 suggests a problem with the S4 measurement for certain flows above 0.6 m/s. A direction-distribution plot (not shown) of the RCM/S4 rate ratio indicates that the problem is associated with southeastward (on-Bank) flow, when the major axis of the tidal ellipse and the residual current combine to yield maximum speeds.

Further detail on this problem can be seen in time series plots (Fig. 30) of the unaveraged rates and directions, and of the S4 orientation and tilt for a typical one-day interval. The RCM and S4 rates track well, except during southeastward flow when the S4 rates are markedly "clipped" at about 0.8 m/s while the RCM rates appear clipped to a lesser extent. During this time, the S4 current direction follows a smooth tidal variation (although the S4 orientation is varying by $\pm 50^{\circ}$ on top of a tidal variation), and there is variability in the RCM direction about that of the S4, accounting for the bulge in the direction scatterplot (Fig. 18). The S4 tilts show maximum values of 27° during southeastward flow, and increased variability ($\pm\ 3^{\circ}$) during both southeastward and northwestward flow.

Although degraded and unable to resolve the high-frequency motion of itself and the water, the S4 measurements are consistent with some form of amplified relative water velocity during southeastward flow, such as mooring-line vibration. The specific cause of the S4 rate degradation is unclear, other than it appears related to mooring vibration.

d. Mean Currents

The statistics and tidal analysis results show discrepancies of order 0.05 m/s in the mean currents estimated using the different instruments. Although such current differences are small compared to the tidal current amplitudes, they exceed the differences expected on the basis of the manufacturers' specified accuracies and are very significant in relation to the typical residual current speed of 0.1 m/s. We now examine some possible explanations for these differences.

i) Direction-Dependent Degradation of Tidal Current Rate. The ratio versus direction scatterplot in Figure 27 indicates the possibility of a

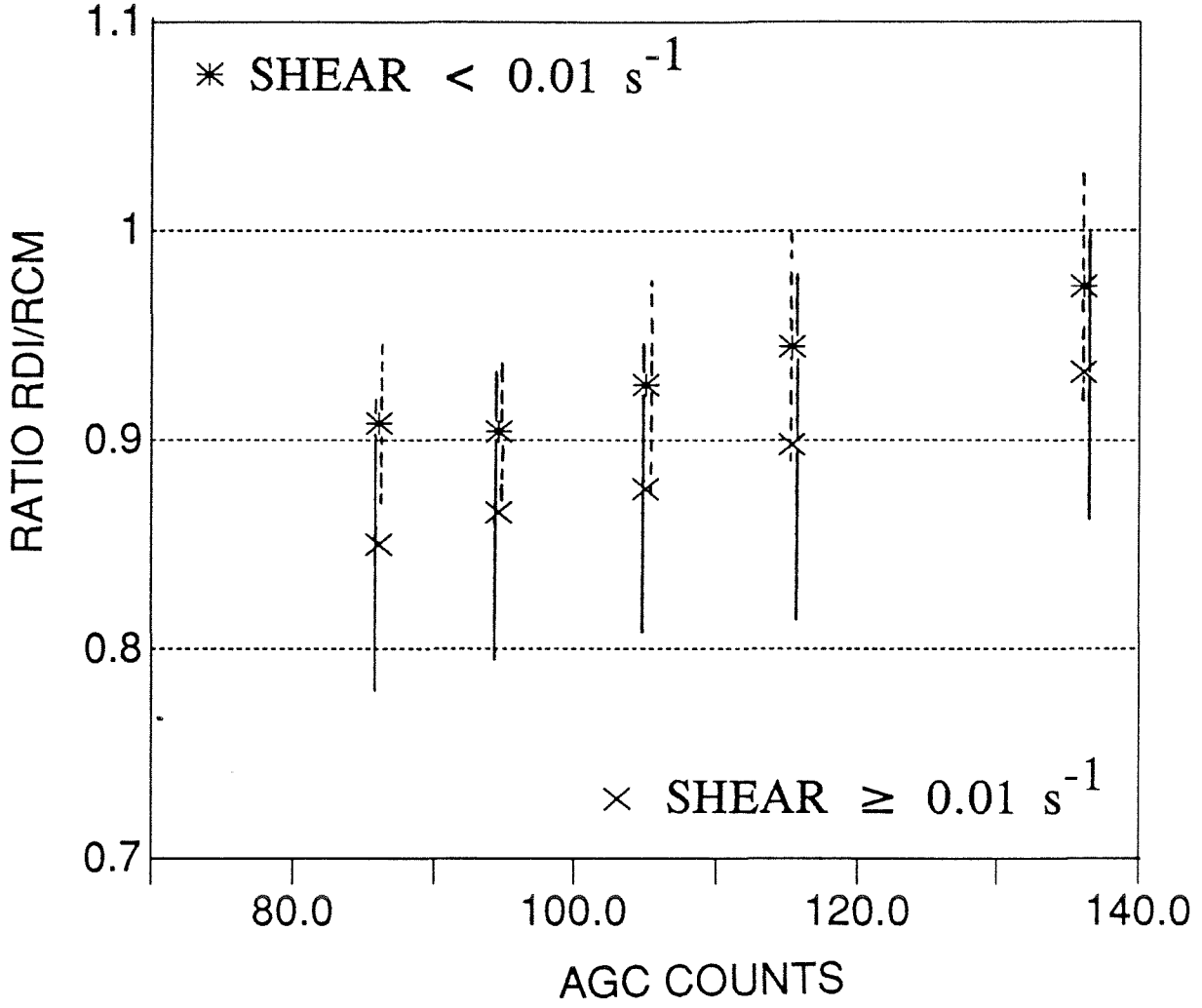

Figure 29. Means and standard deviations of the ratio of RDI rate to RCM rate at 12 m for various vertical shear and backscatter intensity (AGC) ranges. The shear is computed from the 12- and 64-m RCMs at mooring 893, and the data are grouped into shear less than and greater than 0.01 s^{-1}. The data are also grouped by AGC counts: <90, 90-100, 100-110, 110-120, and >120. Points are plotted at the mean AGC value for each group.

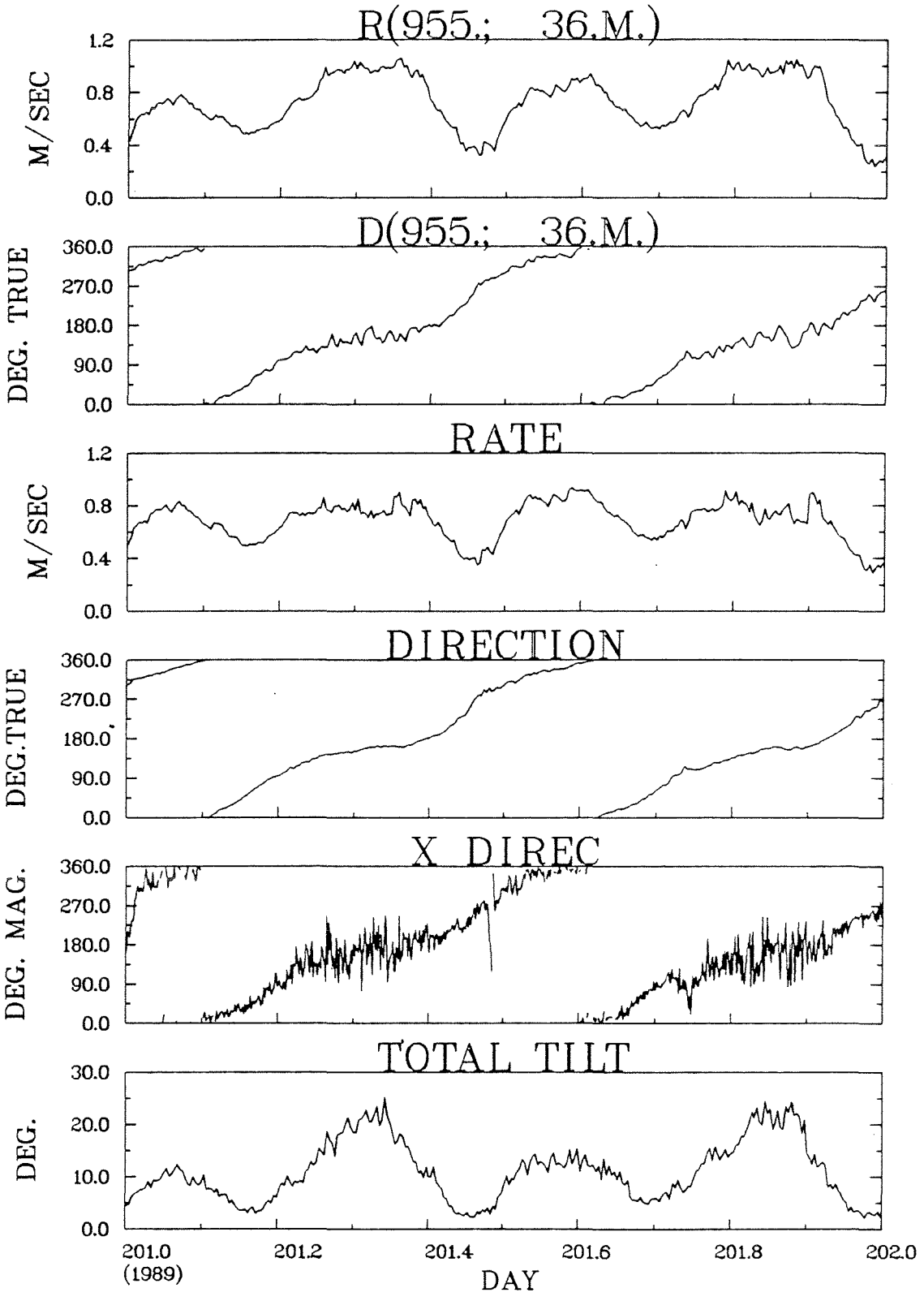

Figure 30. Time series plots of RCM rate and direction (955; 36.m.), and S4 rate, direction, instrument orientation and instrument tilt (bottom 4 panels), from the mid-depth level of mooring 955, for a typical day.

10% error in either the RCM or RDI rate measurement for southeastward flow (alternatively, the discrepancy may be due to some correlated factor such as backscatter intensity). In the presence of a dominant oscillatory flow, such a direction-dependent error in the measurement of rate can significantly bias the measured mean current. For an oscillatory flow $u(t) = u_1 \sin \omega t$, and a relative (systematic) error in rate of ϵ when $u > 0$ and 0 when $u < 0$, an absolute bias of $2\epsilon u_1/\pi$ results for the mean flow. For $\epsilon = 0.1$ and $u_1 = 1.0$ m/s (typical of Georges Bank), the bias is 0.06 m/s in the direction with larger measured velocities. Thus, this may be a significant factor to the discrepancies in measured mean current at the upper level.

ii) Rate-Dependent Degradation of Tidal Current Rate. There is a clear suggestion (Table 11) of a rate-dependent degradation of the RCM rate measurement at mid-depth, with greater relative error at high rates. In the presence of a strong background tidal current, such a measurement error can lead to enhanced relative errors in the mean current (compared to the relative error expected for the rate corresponding to the mean current). For a (mean+tidal) current $u(t) = u_o + u_1 \sin \omega t$ and a relative (systematic) rate error of $\alpha |u|$ where α is a constant (overestimate if $\alpha > 0$, underestimate if $\alpha < 0$), it can be shown that the resulting relative error ϵ' in mean current is

$$\epsilon' = -\alpha u_o \left(\frac{2}{\pi} \left(1 + \frac{u_1^2}{2u_o^2} \right) \sin^{-1}\left(-\frac{u_o}{u_1}\right) + \frac{3}{\pi} \left(\frac{u_1^2}{u_o^2} - 1 \right)^{1/2} \right).$$

Simple expressions result in two cases: (a) when $u_o = u_1$, then $\epsilon' = 3/2\ \alpha u_o$; i.e. the relative error is 50% larger than in the absence of the oscillatory current; and (b) when $2 u_o^2 \ll u_1^2$, then $\epsilon' = \left(\frac{4 u_1}{\pi u_o}\right) \alpha u_o$; i.e. the relative error is now the parenthesized factor greater than in the absence of the oscillatory flow. The significance of this effect for the Georges Bank data set can be estimated by choosing $u_1 = 10\ u_o$, in which case $\epsilon' = 12.7\ \alpha u_o$, resulting in the relative error being over an order of magnitude larger than in the purely mean-flow situation. For $u_o = 0.1$ m/s, $u_1 = 1.0$ m/s and $\alpha = -0.2$ [corresponding to relative (absolute) errors of -.02 (-.002 m/s) for $u = 0.1$ m/s and -0.2 (-0.2 m/s) for $u = 1.0$ m/s], the relative error in mean current is -0.25 with an absolute error of -0.025 m/s. Thus, this effect may contribute significantly to the observed mean-current discrepancies at mid depth and 10 m above bottom, although these models suggest that the mean current degradation would be greater for a direction-dependent current measurement degradation than for a rate-dependent one.

iii) RDI Offsets. The large vertical and error velocities measured by the RDI, and the clear offset between the mean currents obtained from the three- and four-beam solutions (e.g. Fig. 14) point to an offset problem in the RDI's Doppler trackers. In the absence of such offsets and significant instrument tilts, the Doppler counts reported by opposing

beams should be approximately equal and opposite. However, examination of the raw Doppler counts averaged over the Georges Bank deployment shows that neither pair of opposing beams had such matching Doppler counts. On the other hand, the standard deviations of the counts from opposite beams were in good agreement upon adjustment for the observed instrument tilts. This is, of course, consistent with the earlier results which indicate that the RDI measurements of the time-varying component of flow are generally accurate (below 20m) while the mean currents are biased, and indicates that the problem was not isolated to any one beam or pair of beams.

The most likely explanation for this problem is a frequency skewing of the transmitted pulse by the transducer pass band (e.g. Chereskin et al. 1989). This skewing would tend to be increased by the short (2.2-m) pulse length used in the Georges Bank deployment and, since each beam could bias the transmitted pulse differently, could result in a different offset for each beam. The offsets could also vary with depth, since the spectral shape of the transmitted pulse is not necessarily symmetrical and the symmetry of the received pulse can change with the superimposed depth-varying noise level which is likely to have different spectral properties than the transmitted pulse. As shown by Chereskin et al. (1989), these errors can be enhanced by mispositioning of the filters used in tracking the frequency center of power of the returned pulse. Furthermore, since the spectral width of the returned pulse was larger than normal in the present data set (probably associated with the short pulse length), there may be additional velocity inaccuracy associated with the autocovariance calculation. It appears then that RDI offsets associated with the small bin size and other instrument settings during the Georges Bank deployment are a major factor in the observed mean-current discrepancies.

7. Summary

The intercomparison described above has provided quantitative information on the accuracy and consistency of the various current measurements during the Georges Bank Frontal Study.

On the positive side, the instruments worked satisfactorily most of the time, the direction measurements were generally in excellent agreement, the rate measurements generally agreed within 20% (0.2 m/s errors for 1 m/s currents), and the ship-mounted ADCP (Ametek) measurements obtained at anchor appear to be reasonably accurate (other analyses, however, suggest significant errors in bottom-track velocity while steaming).

The most conclusive negative result is that Aanderaa current meters (RCMs) with paddle-wheel rotors can significantly underestimate rate in some situations. RCMs positioned near mid-depth away from the ends of the moorings consistently underestimated rate by about 20% for local flow speeds in excess of 0.8 m/s. RCMs positioned at 10 m above bottom also underestimated rate, typically by about 20%, but with less consistency than at mid-depth and a less clear dependence on flow speed. Since this degradation may exist for other RCM (paddle-wheel version) measurements at BIO and elsewhere, it is paramount that the problem's origin be identified and understood. As discussed in another report (Loder and

Hamilton 1990), the leading candidate for the origin is a high-frequency mooring-line vibration forced by vortex shedding from in-line backup-buoyancy packages, which results in shielding of the RCMs' paddle-wheel rotors. A most significant feature of this mechanism is that it can contribute to significant errors in the measurement of rate without much increase in the scatter of measured current direction (for vaned meters). Clearly, observations of high-frequency mooring and instrument motion, a model for mooring vibration, and further measurements of the degradation magnitude as a function of misalignment angle would be invaluable. The observations from the S4 positioned near-depth on the 1989 mooring indicate that the S4 performance is also affected by the mooring-line vibration, although the mechanism is unclear.

Smaller discrepancies (approximately 10%) were found among the RCM, RDI and Ametek rate estimates for the interval 10-20 m below the sea surface, with relatively-high RCM values and relatively-low RDI values. It appears that the low RDI values were primarily associated with periods of low backscatter intensity and high vertical shear, and caused by poor Doppler tracking (also see Belliveau and Loder 1990). The problem was exacerbated by the use of short pulse lengths (small bin sizes) in the Georges Bank deployment. It is expected that the use of longer pulses and recent updates in the RDI firmware would have considerably reduced the data degradation. In addition to this RDI problem, there appears to have been additional contributions to the near-surface current discrepancies from relatively-high RCM rates (supported by the RCM/S4 intercomparison), perhaps due to a calibration problem, and real spatial structure in baroclinic flow features between the Ametek anchor sites and the RCM/RDI mooring sites.

Significant discrepancies were also found among the mean-current measurements. In particular, the RDI measurements during the Georges Bank deployment include significant offsets, probably associated with some combination of frequency skewing of the acoustic pulses, mispositioning (relative to the pulse) of the tracking filters, and large spectral widths of the returned pulses. Again, it is likely that these problems would have been (at least partly) reduced with a longer pulse length. In addition, it is shown that, with a strong background tidal current, direction- or rate-dependent degradation in an instrument's rate measurement can result in enhanced relative errors in mean current. For the apparent RCM rate degradation in the Georges Bank data set, relative errors in mean current of 25-50% can result.

The intercomparison results also provide a sobering reminder that no amount of care and checking is excessive in the execution and processing of scientific measurements. In addition to the rate discrepancies discussed above and many data points rejected during quality control, the present exercise has uncovered an inadequate compass calibration (RDI), routine application of incorrect calibration coefficients in the BIO processing procedure (for paddle-wheel RCMs), and errors in an analysis program (Residual option of Tidal Analysis) in routine use at BIO (as well as a variety of mistakes by the authors).

Needless to say, measurement inaccuracies such as those identified here and others found recently in another intercomparison study (D.J.

Lawrence, BIO, personal communication, 1989) have the potential of seriously eroding the reliability and value of ocean current studies. The underestimation of high current speeds by 20% substantially alters the predicted occurrence of extreme current speeds as required in many engineering design applications. Uncertainties of 25-50% in mean current estimation, as would occur with the present measurement inconsistencies and strong high-frequency current fluctuations (as occur on the continental shelf), may exceed the interannual variability signal of importance in many climate and biological (e.g. larval drift) problems. Clearly, ongoing instrument calibration and data intercomparison should be essential components of any scientific measurement program.

8. REFERENCES

Aanderaa Instruments. 1979. Operating Manual. Recording Current Meter Models 4&5. Technical Description No. 119. Bergen, Norway.

Aanderaa Instruments. 1987. Operating Manual. Recording Current Meters Models 7&8. Technical Description No. 159. Bergen, Norway.

Belliveau, D.J. and J.W. Loder. 1990. Velocity errors associated with using short pulse lengths with 150 kHz ADCPs. Proc. Fourth IEEE Working Conference on Current Measurement (in press).

BMDP. 1983. BMDP Statistical Software. University of California Press. 734 p.

Butman, B., R.C. Beardsley, B.A. Magnell, D. Frye, J.A. Vermersch, R. Schlitz, R. Limeburner, W. R. Wright and M. A. Noble. 1982. Recent observations of the mean circulation on Georges Bank. J. Phys. Oceanogr. 12, 569-591.

Butman, B., J.W. Loder and R.C. Beardsley. 1987. The seasonal mean circulation on Georges Bank: observations and theory. p. 125-138 *In* Georges Bank, R.H. Backus (ed.), MIT press.

Chereskin, T.K., E. Firing and J.A. Gast. 1989. On identifying and screening filter skew and noise bias in acoustic Doppler current profiler measurements. J. Atmos. Oceanic Technology (in press).

Cochrane, N.A. 1985. An operational evaluation of an Ametek Straza DCP-4400 300 kHz doppler current profiler aboard C.S.S. Dawson. Can. Tech. Rep. Hydrogr. Ocean Sci. 68, iii + 52 p.

Dessureault, J.-G. and D. Belliveau. 1987. A trawl-proof housing for bottom mounted instruments. Proceedings of IEEE Oceans '87 Conference, 658-660.

Fofonoff, N.P. 1966. Oscillation modes of a deep-sea mooring. Geo-Marine Technology, Vol.2, No.9, 13-17.

Godin, G. 1972. The Analysis of Tides. University of Toronto Press, 264 p.

Greenberg, D.A. 1979. A numerical model investigation of tidal phenomena in the Bay of Fundy and Gulf of Maine. Mar. Geod. 2, 161-187.

Greenberg, D.A. 1983. Modelling the mean barotropic circulation in the Bay of Fundy and Gulf of Maine. J. Phys. Oceanogr. 13, 886-904.

Hamilton, J.M. 1989. The validation and practical applications of a subsurface mooring model. Can. Tech. Rep. Hydrogr. Ocean Sci. No. 119, iv + 45 p.

InterOcean. 1987. S4 current meter User's Manual. InterOcean Systems Inc., San Diego, California, 52 p.

Larouche, P. and J.-C. Deguise. 1989. Field intercomparison of three current meters in an environment free from high frequency motion. Continental Shelf Res. 9, 555-568.

Loder, J.W. and J.M. Hamilton. 1990. Degradation of paddle-wheel Aanderaa current measurements by mooring vibration in a strong tidal flow. Proc. Fourth IEEE Working Conference on Current Measurement (in press).

Loder, J.W. and D.G. Wright. 1985. Tidal rectification and frontal circulation on the sides of Georges Bank. J. Mar. Res. 43, 581-604.

Magnell, B.A. and S.R. Signorini. 1986. Fall 1984 Delaware Bay Acoustic Doppler Profiler Intercomparison Experiment. Proc. Third IEEE Working Conference on Current Measurement, 122-151.

Marsden, R.F. 1986. The internal tide on Georges Bank. J. Mar. Res. 44, 35-50.

Prandle, D. 1982. The vertical structure of tidal currents and other oscillatory flows. Continental Shelf Res. 1, 191-207.

RD Instruments. 1989. Acoustic Doppler current profilers. Principles of operation: a practical primer. San Diego, California, 39 p.

Saunders, P.M. 1980. Overspeeding of a Savonius Rotor. Deep-Sea Res. 27, 755-759.

Woodward, M.J., W.S. Huggett and R.E. Thomson. 1988. Near-surface moored current meter intercomparisons. Unpublished manuscript.